THERMAL STRESS PROBLEM FOR AN FGM STRIP CONTAINING PERIODIC CRACKS

A THESIS SUBMITTED TO
THE GRADUATE SCHOOL OF NATURAL AND APPLIED SCIENCES
OF
MIDDLE EAST TECHNICAL UNIVERSITY

BY

AYŞE KÖSE

IN PARTIAL FULFILLMENT OF THE REQUIREMENTS
FOR
THE DEGREE OF MASTER OF SCIENCE
IN
MECHANICAL ENGINEERING

FEBRUARY 2013

Approval of the thesis:

THERMAL STRESS PROBLEM FOR AN FGM STRIP CONTAINING PERIODIC CRACKS

submitted by **AYŞE KÖSE** in partial fulfillment of the requirements for the degree of **Master of Science in Mechanical Engineering Department, Middle East Technical University** by,

Prof. Dr. Canan ÖZGEN _____
Dean, Graduate School of **Natural and Applied Sciences**

Prof. Dr. Süha ORAL _____
Head of Department, **Mechanical Engineering**

Prof. Dr. Suat KADIOĞLU _____
Supervisor, **Mechanical Engineering Dept., METU**

Examining Committee Members:

Prof. Dr. Bülent DOYUM _____
Mechanical Engineering Dept., METU

Prof. Dr. Suat KADIOĞLU _____
Mechanical Engineering Dept., METU

Prof. Dr. Levend PARNAS _____
Engineering Sciences Dept., METU

Assoc. Prof. Dr. Serkan DAĞ _____
Mechanical Engineering Dept., METU

Prof. Dr. Bora YILDIRIM _____
Mechanical Engineering Dept., Hacettepe University

Date: 12 February 2013

I hereby declare that all information in this document has been obtained and presented in accordance with academic rules and ethical conduct. I also declare that, as required by these rules and conduct, I have fully cited and referenced all material and results that are not original to this work.

Name, Last name: Ayşe KÖSE

Signature:

ABSTRACT

THERMAL STRESS PROBLEM FOR AN FGM STRIP CONTAINING PERIODIC CRACKS

Köse, Ayşe
M.S., Department of Mechanical Engineering
Supervisor: Prof. Dr. Suat Kadıoğlu

February 2012, 93 pages

In this study the plane linear elastic problem of a functionally graded layer which contains periodic cracks is considered. The main objective of this study is to determine the thermal stress intensity factors for edge cracks. In order to find an analytic solution, Young's modulus and thermal conductivity are assumed to be varying exponentially across the thickness, whereas Poisson ratio and thermal diffusivity are taken as constant. First, one dimensional transient and steady state conduction problems are solved (heat flux being across the thickness) to determine the temperature distribution and the thermal stresses in a crack free layer. Then, the thermal stress distributions at the locations of the cracks are applied as crack surface tractions in the elasticity problem to find the stress intensity factors. By defining an appropriate auxiliary variable, elasticity problem is reduced to a singular integral equation, which is solved numerically. The influence of such parameters as the grading, crack length and crack period on the stress intensity factors is investigated.

Keywords: Functionally Graded Material (FGM), Stress Intensity Factor (SIF), Periodic Cracks, Edge Cracks, Thermal Stress

ÖZ

PERİYODİK ÇATLAK BULUNAN FONKSİYONEL OLARAK DERECELENMİŞ BİR ŞERİTİN ISIL GERİLME PROBLEMİ

Köse, Ayşe
Yüksek Lisans, Makina Mühendisliği Bölümü
Tez Yöneticisi: Prof. Dr. Suat Kadıoğlu

Şubat 2013, 93 sayfa

Bu çalışmada periyodik çatlak bulunan fonksiyonel derecelendirilmiş tabakalarda, düzlemsel lineer esneklik problemi ele alınmıştır. Bu çalışmanın esas amacı, kenar çatlaklarda ısıl gerilme şiddeti faktörünün bulunmasıdır. Analitik bir çözüm bulmak için, Poisson oranı ve ısıl dağılma sabit alınırken Young modülü ve ısıl iletkenlik katsayısının kalınlık boyunca üstel olarak değiştiği varsayılmaktadır. İlk olarak, çatlak olmayan bir tabakada sıcaklık dağılımı ve ısıl gerilmeyi bulmak için tek boyutlu geçici ve kararlı hal ısı iletimi problemleri çözülmüştür (ısı akısı kalınlık boyuncadır). Daha sonra, gerilme şiddeti faktörünü bulmak için çatlak bölgesindeki ısıl gerilme dağılımı çatlak yüzeyi basıncı olarak uygulanmıştır. Esneklik problemi, uygun bir yardımcı değişken tanımlanarak sayısal çözülebilen tekil bir integral denklemine indirgenmiştir. Derecelenme, çatlak uzunluğu ve çatlak periyodu gibi parametrelerin gerilme şiddeti faktörü üzerindeki etkileri incelenmiştir.

Anahtar Kelimeler: Fonksiyonel Olarak Derecelenmiş Malzeme, Gerilme Şiddeti Faktörü, Periyodik Çatlak, Kenar Çatlak, Isıl Gerilme

To My Family

ACKNOWLEDGMENTS

I would like to thank to my supervisor Prof. Dr. Suat Kadıoğlu for his help, guidance and suggestions during this study.

I am indebted to Prof. Dr. Bora Yıldırım for his help to verify some of the results of this study.

I also would like to thank to my committee members Prof. Dr. Bülent Doyum and Prof. Dr. Levend Parnas for their positive and helpful comments and criticisms.

Special thanks go to Hamza Gümüşcü who has the full confidence in me first.

Finally, I would like to thank to Özgür for his endless support, understanding and love.

TABLE OF CONTENTS

LIST OF TABLES

TABLES

LIST OF FIGURES

FIGURES

LIST OF SYMBOLS

FGM	: Functionally graded material
SIF	: Stress intensity factor
$\mu(x)$	: Shear modulus
μ_0	: Shear modulus at x=0
$E(x)$	: Elastic modulus
E_0	: Elastic modulus at x=0
K	: Kelvin
β	: Nonhomogeneity constant for elastic modulus
δ	: Nonhomogeneity constant for coefficient of heat conduction
ω	: Nonhomogeneity constant for coefficient of thermal expansion
ν	: Poisson's ratio
a, b	: Location of the crack tips
c	: Half of the distance between two parallel cracks
h	: Strip thickness
κ	: Kolosov constant
υ, ν	: Displacement components in x- and y- directions
U_j, V_k	: Functions that form displacement components in x- and y- directions
σ_{ij}	: Stress components ($i, j = x, y$)
A_j	: Components of U_1, and V_1
$\hat{A}_j$	: Components of A_j
$h(\rho)$	: Components of A_j
m_j	: Components of U_1
B_j	: Components of U_2 and V_2
q_j	: Components of U_2
ρ, α	: Fourier Transform variables
n_j, p_j	: Roots of the characteristic equations (j=1,.., 4)
A, B, C, D, E	: Components of n_j and m_j
L_k, M_k	: Components of σ_{xx}
$\acute{c}, \hat{c}$	: Constants
R_k, S_k	: Components of σ_{xy}
G_1	: First term of (49)
G_{11}, G_{12}	: Components of G_1
G_2	: First term of (55)
G_{21}, G_{22}	: Components of G_2
G_3	: First term of (62)
G_{31}, G_{32}	: Components of G_3
G_4	: First term of (68)
G_{41}, G_{42}	: Components of G_4
B_{jm}	: Components of U_2 and V_2
Δ, Δ_j	: Determinants for solution of A_j and B_{jm}
$g(x)$	: Unknown density function
$q(\rho)$	: Function of G_{11}, G_{21}, G_{31} and G_{41}
ρ_i	: Roots of $q(\rho)$
Γ	: A positively oriented simple closed contour in the complex plane
$I_j(t)$	: Contour Integrals (j=1,.., 4)
$F_j(\rho)$	: Function of $I_j(t)$ (j=1,.., 4)
λ_k	: Components of $I_j(t)$ (k=1,..,7)
$h_j(x,t)$	: Kernels of the singular integral equation (j=1,2)
$M(y,\rho)$	: Even part of $h_j(x,t)$
$N(y,\rho)$	: Odd part of $h_j(x,t)$

bj, ck	: Terms obtained in the asymptotic expansions of the integrands $M(y,\rho)$ and $N(y,\rho)$ (j=1,3,…,13) and (k=0,2,…,12)
a_j	: Terms obtained in the asymptotic expansion (j=-1,0,1,2)
τ	: Nondimensional time
t	: Time
ε_{ot}	: Thermal strain for the transient heat conduction problem
ε_{os}	: Thermal strain for the steady state heat conduction problem
k_0	: Heat conduction coefficient at x=0
α_0	: Thermal expansion coefficient at x=0
D	: Thermal diffusivity
$c(x)$	: Specific heat
$\rho(x)$	: Density
$\Theta(x,t)$	: Transient temperature distribution
$\Theta_{ss}(x)$	: Steady state temperature distribution
$k(b)$	: Stress intensity factor at x=b
$k^*(b)$	: Normalized stress intensity factor at x=b

CHAPTER 1

INTRODUCTION

1.1 Functionally Graded Materials

Functionally graded materials (FGMs) are materials made of two or more constituent phases that continuously vary as a function of position along certain dimension(s) from one point to another [1]. These materials are microscopically heterogeneous and consequently have property gradients which bring advantage of the properties of the individual components. Additionally, unlike traditional composites which have step-wise changing material properties, the smooth variation of composition minimizes or eliminates the mismatch between dissimilar materials. FGM is generally made from ceramic and metal. Such an FGM is better than metal in the way of resistance to wear, corrosion and large temperature gradient; while better than ceramic in the way of toughness and thermal conductivity [2].

The FGM concept was originated in Japan in 1984 during a space-plane project. The purpose was to form thermal barrier material capable of withstanding a temperature of 2000 K and a temperature gradient of 1000 K across a cross section less than 10 mm [3]. Since 1984, FGM materials have been designed for many applications where the operating conditions are severe. Thermal barrier coatings for turbine blades (electricity production), armor protection for military applications, fusion energy devices, biomedical materials including bone and dental implants, space/aerospace and automotive industries, wear and corrosion barrier applications are some of them [4].

According to [5] the FGM manufacturing process is generally divided in building the spatially inhomogeneous structure which is called gradation and transformation of this structure into bulk material which is called consolidation. Constitutive process, homogenizing and segregating are the sub processes of gradation. In constitutive processes, graded structure is built-up from precursor materials or powders. In homogenizing processes, by material transport, gradient is generated. In the last process of gradation, segregating, a macroscopically homogeneous material is converted into a graded material by material transport due to an external field. The consolidation processes which follow the gradation are usually drying and sintering or solidification.

The impeller dry blending, which is a controlled-blending process, is used for the fabrication of functionally graded materials of broad regular gradient [3]. Plasma spraying [5], chemical vapor deposition [6], powder metallurgy [7], centrifugal casting [8] and 3-D printing [9] can be listed as the other FGM fabricating techniques.

1.2 Periodic Cracks

Cracking which forms a regular array is called periodic cracking. Periodic cracks are generally observed where the local stress is high and more than one crack initiation point

exist. Periodicity can be in the plane of crack growth, normal to the direction of crack growth or combination of the two.

1.3 Literature Survey

Because of wide application areas, many scientists and engineers are interested in investigation of thermomechanical behavior of FGMs to find out the FGM's potential. A brief survey of literature is reviewed below.

Erdogan and Wu (1993) analyzed edge-cracked FGM specimens [10]. Four loading types were applied namely fixed-grip (constant strain) loading, membrane loading, bending and steady state thermal stress and mode I stress intensity factors were calculated. Erdogan and Wu (1996) also studied unconstrained FGM layer that contains an embedded or a surface crack perpendicular to its boundaries under thermal or residual stresses [11]. For an FGM layer that is under compression near and at the surface and tension in the interior region, if the surface crack is deeper than the compressive zone, the crack tip region would be subjected to a tensile stress and crack would remain partially open. This is called crack/contact problem, and was also analyzed by Erdogan and Wu [11]. Thermal stress intensity factors in a thin-walled FGM cylinder which contains a circumferential crack were studied by Dağ (1997) [12]. The thin-walled cylinder was simulated by an elastic layer on an elastic foundation. Dağ, Kadıoğlu and Yahşi (1998) examined internal and edge crack problems for an FGM layer attached to an elastic foundation under fixed grip constant strain loading, membrane loading and bending [13] and (1999) under quasi-static thermal loading [14]. Mechanical and thermal properties were assumed to be varying in thickness direction and crack was perpendicular to the surfaces [13, 14]. Lee and Erdogan (1998) considered the plane strain thermal stress problem for an interface crack in a homogeneous substrate with a graded coating [15]. The surface of the coating was exposed to a high-temperature environment while the surface of the substrate was forced-cooled. The ends of the specimen were subjected to natural convection and the surfaces of the crack were assumed to be partially insulated. Therefore, the structure was under a steady-state heat conduction with convective boundary conditions. An edge crack in a strip of a functionally graded material was studied under transient thermal loading conditions by Jin and Paulino (2001) [16]. The strip material was elastically homogeneous but thermally nonhomogeneous since it was assumed that the FGM has constant Young's modulus and Poisson's ratio but thermal properties of the material vary along the thickness direction of the strip.

Guo and Noda (2008) studied a functionally graded layered structure with a crack crossing the interface [17]. The crack was perpendicular to the surface, different layers might have different properties in the structure and the problem was solved analytically. The effects of the material and geometric parameters on SIFs were examined. They found that for the layers that have different nonhomogeneity constants when the crack tips touch the interface, SIFs reach the extremum. Same problem with an arbitrarily oriented crack crossing the interface was investigated by Guo et al. (2012) [18].

Shabana and Noda (2002) performed finite element analyses to study the behavior of a FGM structure which consists of an FGM layer sandwiched between a metal substrate and a homogeneous ceramic coating, for different geometrical parameters of the substrate and coating layers and also for different gradation forms of the FGM constituents [19]. In the study of Chi and Chung (2003), the SIFs of cracked multi-layered and FGM coatings of a coating–substrate composite were calculated by finite element method under uniform normal stress on the crack surfaces [20]. The substrate was assumed to be homogeneous

and the coating consisted of multi-layered media or sigmoid FGMs. For the multi-layered coatings, one, two, and four-layered homogeneous coatings with stepwise changing volume fractions were considered. Yıldırım, Dağ and Erdogan (2005) utilized finite element method to solve the three dimensional semi-elliptical surface crack problems in functionally graded coatings subjected to mode I mechanical or transient thermal loading [21]. Fixed-grip tension, three point bending and transient thermal loading were considered. Nami and Eskandari (2012) analyzed a three-dimensional FGM cylinder containing semi-elliptical circumferential surface crack under internal pressure by finite element method [22]. The influence of non-uniform coefficient of thermal expansion on the distribution of SIF was studied.

Since FGMs have continuously varying coefficient of thermal expansion, an eigenstrain and accordingly an eigenstress are developed in the materials when they undergo a change in temperature. By taking into account the effect of eigenstrain, Afsar and Anisuzzaman (2007) developed a method to evaluate stress intensity factors for two diametrically-opposed edge cracks emanating from the inner surface of a thick-walled FGM cylinder that is subjected to an internal pressure [23]. A thick-walled cylinder with a thin FGM coating at the inner surface was studied by Afsar and Song (2010) [24]. The effects of material distribution, cylinder wall thickness, application temperature, FGM coating thickness and the number of cracks (single or double) on SIFs were examined.

There are studies on mathematical modeling of transient heat conduction problems. Classical Fourier heat conduction law is sufficient for many practical engineering applications. However, this theory cannot accurately explain conduction of heat caused by highly-varying thermal loading, and in structures at temperatures close to absolute zero. Therefore, non-Fourier heat conduction theories have been developed to explain heat conduction in solids better. One of the non-Fourier theories is hyperbolic heat conduction theory. Babaei and Chen (2008) used this theory to analyze the temperature field in a functionally graded hollow sphere [25] and (2010) in a functionally graded hollow cylinder [26]. Transient hyperbolic heat conduction problem in thick-walled FGM cylinders and spheres with exponentially-varying properties was considered by Keles and Conker (2011) [27]. Temperature and heat flux distributions were given for different nonhomogeneity parameters. Hu and Chen (2012) calculated SIFs for a crack parallel to the free surface in a homogeneous strip under temperature impact loading by using hyperbolic heat conduction equation [28]. Transient thermal fracture problem corresponding to non-Fourier heat conduction theory in a brittle homogeneous semi-infinite medium with a surface crack was studied by Chang and Wang (2012) [29].

Solutions to periodic crack problems in functionally graded materials have started to appear in the literature since 1990's. Erdogan and Öztürk (1995) considered periodic cracking of a functionally graded coating bonded to a homogeneous substrate under anti-plane loading [30]. Wang and Mai (2005) investigated a periodic array of cracks in an infinite FGM under mechanical and/or thermal loading [31]. Effect of the material non-homogeneity on the crack tip stress intensity factors (SIFs) is discussed. Wang and Mai also (2006) considered the same problem under transient mechanical loading. The effects of material nonhomogeneity constants and crack spacing on SIF was examined under in-plane normal (mode I) and shear (mode II) loading conditions both at transient state and steady state [32]. Both single crack and a periodic array of interface cracking between an FGM and elastic substrate are analyzed under anti-plane shear loads by Ding and Li (2008) [33]. Jin and Feng (2008) studied the thermal fracture resistance of a functionally graded coating with an array of periodic edge cracks [34] and (2009) fracture behaviour of a FGM plate containing parallel surface cracks with alternating lengths subjected to a thermal shock [35]. In both problems since the constituents have similar Young's moduli; it is assumed that the FGM in those studies have graded thermal properties but constant elastic properties [34, 35].

The most relevant article to the subject of this study and the method followed belongs to Yıldırım, Kutlu and Kadıoğlu (2011). The plane elasticity problem of a functionally graded semi-infinite plane, containing periodic imbedded or edge cracks perpendicular to the free surface is considered [36]. Crack surface tractions which simulate in-plane mechanical or thermal loadings are applied to the crack. It is assumed that Young's modulus, conduction coefficient, coefficient of thermal expansion are exponentially varying functions of the depth coordinate while Poisson's ratio and thermal diffusivity are constant. In the formulation Fourier integrals, which represents a strip solution, and Fourier series, which represents the solution of a periodic half plane, are used. A Cauchy type singular integral equation is obtained. By using numerical methods, stress intensity factor is calculated. An extensive survey of literature regarding periodic crack problems in FGMs can be found in this article.

1.4 Scope of the Study

The scope of this study is to examine the effect of some geometric and material parameters on the stress intensity factors in an FGM strip containing periodic cracks. The material property gradation in the strip is represented in shear modulus along the thickness direction in an exponential form and the cracks lie perpendicular to the boundaries.

CHAPTER 2

FORMULATION OF THE PROBLEM

2.1 Description of the Problem

The geometry of the plane elasticity problem of periodic cracks in a functionally graded strip is given in Fig. 2.1. The material property gradation of the FGM strip is in x-direction.

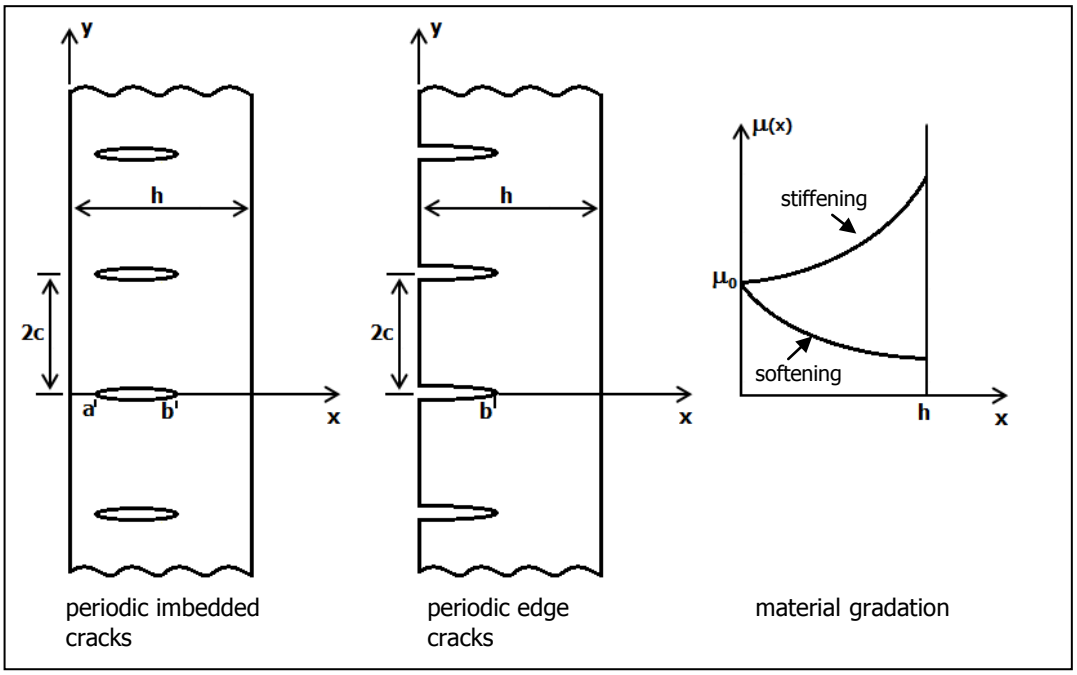

Figure 2.1 Geometry of the problem

2.2 Governing Equations and Their Solutions

Shear modulus varies along x-direction as an exponential function since the strip is functionally graded.

$$\mu(x) = \mu_0 \times e^{\beta x} \tag{1}$$

where β is the nonhomogeneity constant and μ_0 is the modulus of rigidity at x=0.

Poisson's ratio, ν, is assumed to be constant. Kolosov constant, κ, which is defined as $\kappa = 3 - 4\nu$ for plane strain and $\kappa = \frac{3-\nu}{1+\nu}$ for plane stress is used to unify plane strain and plane stress formulations.

By using Hookes Law, stress can be expressed in terms of the displacements as follows:

$$\sigma_{xx}(x,y) = \frac{\mu(x)}{\kappa-1}[(\kappa+1)\frac{\partial u}{\partial x} + (3-\kappa)\frac{\partial v}{\partial y}] \ , \tag{2.a}$$

$$\sigma_{yy}(x,y) = \frac{\mu(x)}{\kappa-1}[(\kappa+1)\frac{\partial v}{\partial y} + (3-\kappa)\frac{\partial u}{\partial x}] \ , \tag{2.b}$$

$$\sigma_{xy}(x,y) = \mu(x)[\frac{\partial u}{\partial y} + \frac{\partial v}{\partial x}] \ . \tag{2.c}$$

In the absence of body forces, the equations of equilibrium can be written as

$$\frac{\partial \sigma_{xx}}{\partial x} + \frac{\partial \sigma_{xy}}{\partial y} = 0 \ , \tag{3.a}$$

$$\frac{\partial \sigma_{xy}}{\partial x} + \frac{\partial \sigma_{yy}}{\partial y} = 0. \tag{3.b}$$

Substituting stress-displacement Eqs. (2) into the equilibrium Eqs. (3), governing equations in terms of displacements can be found as

$$(\kappa+1)\frac{\partial^2 u}{\partial x^2} + (\kappa-1)\frac{\partial^2 u}{\partial y^2} + 2\frac{\partial^2 v}{\partial x \partial y} + \beta(\kappa+1)\frac{\partial u}{\partial x} + \beta(3-\kappa)\frac{\partial v}{\partial y} = 0, \tag{4.a}$$

$$(\kappa-1)\frac{\partial^2 v}{\partial x^2} + (\kappa+1)\frac{\partial^2 v}{\partial y^2} + 2\frac{\partial^2 u}{\partial x \partial y} + \beta(\kappa-1)\frac{\partial u}{\partial y} + \beta(\kappa-1)\frac{\partial v}{\partial x} = 0. \tag{4.b}$$

Assumed form of solution which has the capacity to satisfy the governing Eqs. (4) and the boundary conditions is as follows [37]:

$$u(x,y) = \frac{1}{2\pi}\int_{-\infty}^{\infty} U_1(y,\rho)e^{-ix\rho}d\rho + \sum_{n=0}^{\infty} U_2(x,\alpha_n)cos(y\alpha_n) \ , \tag{5.a}$$

$$v(x,y) = \frac{1}{2\pi}\int_{-\infty}^{\infty} V_1(y,\rho)e^{-ix\rho}d\rho + \sum_{n=0}^{\infty} V_2(x,\alpha_n)sin(y\alpha_n) \ , \tag{5.b}$$

where

$$\alpha_n = \frac{n\pi}{c} \ . \tag{5.c}$$

In Eqs. (5.a) and (5.b), the first term in the summation represents the Fourier transform along the crack. The second term is a Fourier series along the boundary. It can solve periodic strip problem with no crack.

Two systems of O.D.E.'s can be found for U_1, V_1, U_2 and V_2 by substituting Eqs. (5) into governing Eqs. (4).

$$(\kappa-1)\frac{d^2}{dy^2}U_1(y,\rho) - (\kappa+1)(\rho^2 + i\beta\rho)U_1(y,\rho) + (\beta(3-\kappa) - 2i\rho)\frac{d}{dy}V_1(y,\rho) = 0 \tag{6.a}$$

$$(\beta(\kappa-1) - 2i\rho)\frac{d}{dy}U_1(y,\rho) + (\kappa+1)\frac{d^2}{dy^2}V_1(y,\rho) - (\kappa-1)(\rho^2 + i\beta\rho)V_1(y,\rho) = 0 \tag{6.b}$$

$$(\kappa+1)\frac{d^2}{dx^2}U_2(x,\alpha_n)+\beta(\kappa+1)\frac{d}{dx}U_2(x,\alpha_n)-(\kappa-1){\alpha_n}^2U_2(x,\alpha_n)+2\alpha_n\frac{d}{dx}V_2(x,\alpha_n)+\beta(3-\kappa)\alpha_nV_2(x,\alpha_n)=0 \quad (6.c)$$

$$-2\alpha_n\frac{d}{dx}U_2(x,\alpha_n)-\beta(\kappa-1)\alpha_nU_2(x,\alpha_n)+(\kappa-1)\frac{d^2}{dx^2}V_2(x,\alpha_n)+\beta(\kappa-1)\frac{d}{dx}V_2(x,\alpha_n)-(\kappa+1){\alpha_n}^2V_2(x,\alpha_n)=0 \quad (6.d)$$

By using an operator notation $D=\frac{d}{dy}$ and $D^2=\frac{d^2}{dy^2}$, Eqs. (6.a) and (6.b) can be written in matrix form as follows:

$$\begin{bmatrix}(\kappa-1)D^2-(\kappa+1)\rho(\rho+i\beta) & (\beta(3-\kappa)-2i\rho)D\\ (\beta(\kappa-1)-2i\rho)D & (\kappa+1)D^2-(\kappa-1)\rho(\rho+i\beta)\end{bmatrix}\cdot\begin{bmatrix}U_1(y,\rho)\\ V_1(y,\rho)\end{bmatrix}=\begin{bmatrix}0\\0\end{bmatrix}. \quad (7)$$

Since U_1 and V_1 are not 0, determinant of the coefficient matrix of Eq. (7), Δ, should be 0.

$$\Delta=(\kappa^2-1)D^4-[2\rho(i\beta+\rho)(\kappa^2-1)+\beta^2(\kappa-1)(3-\kappa)]D^2+(\kappa^2-1)\rho^2(\rho^2+2i\rho\beta-\beta^2) \quad (8)$$

U_1 and V_1 are assumed to be in the form e^{ny}. By substituting the solution into the Eq. (8), the following equation is obtained.

$$[(\kappa^2-1)n^4-[2\rho(i\beta+\rho)(\kappa^2-1)+\beta^2(\kappa-1)(3-\kappa)]n^2+(\kappa^2-1)\rho^2(\rho^2+2i\rho\beta-\beta^2)]e^{ny}=0 \quad (9)$$

The roots of the Eq. (9) are

$$n_1=-\frac{1}{2}\beta\sqrt{\frac{3-\kappa}{\kappa+1}}-\frac{1}{2}\sqrt{4\rho(\rho+i\beta)+\beta^2\frac{3-\kappa}{\kappa+1}}\ , \quad (10.a)$$

$$n_2=\frac{1}{2}\beta\sqrt{\frac{3-\kappa}{\kappa+1}}-\frac{1}{2}\sqrt{4\rho(\rho+i\beta)+\beta^2\frac{3-\kappa}{\kappa+1}}\ , \quad (10.b)$$

$$n_3=-\frac{1}{2}\beta\sqrt{\frac{3-\kappa}{\kappa+1}}+\frac{1}{2}\sqrt{4\rho(\rho+i\beta)+\beta^2\frac{3-\kappa}{\kappa+1}}\ , \quad (10.c)$$

$$n_4=\frac{1}{2}\beta\sqrt{\frac{3-\kappa}{\kappa+1}}+\frac{1}{2}\sqrt{4\rho(\rho+i\beta)+\beta^2\frac{3-\kappa}{\kappa+1}}\ . \quad (10.d)$$

Accordingly the solution for displacements U_1 and V_1 can be written as

$$U_1=m_1A_1(\rho)e^{n_1y}+m_2A_2(\rho)e^{n_2y}+m_3A_3(\rho)e^{n_3y}+m_4A_4(\rho)e^{n_4y}\ , \quad (11.a)$$

$$V_1=A_1(\rho)e^{n_1y}+A_2(\rho)e^{n_2y}+A_3(\rho)e^{n_3y}+A_4(\rho)e^{n_4y}\ . \quad (11.b)$$

Substituting the expressions of U_1 and V_1 into the Eq. (6.b), following equation can be found.

$$(\beta(\kappa-1)-2i\rho)[m_1n_1A_1(\rho)e^{n_1y}+m_2n_2A_2(\rho)e^{n_2y}+m_3n_3A_3(\rho)e^{n_3y}+m_4n_4A_4(\rho)e^{n_4y}]+(\kappa+1)[{n_1}^2A_1(\rho)e^{n_1y}+{n_2}^2A_2(\rho)e^{n_2y}+{n_3}^2A_3(\rho)e^{n_3y}+{n_4}^2A_4(\rho)e^{n_4y}]-(\kappa-1)(\rho^2+i\beta\rho)[A_1(\rho)e^{n_1y}+A_2(\rho)e^{n_2y}+A_3(\rho)e^{n_3y}+A_4(\rho)e^{n_4y}]=0 \quad (12)$$

Knowing that the coefficients of A_j are zero, m_j ($j=1,..,4$) can be found as:

$$m_j = \frac{(\kappa-1)\rho(\rho+i\beta)-(\kappa+1){n_j}^2}{(\beta(\kappa-1)-2i\rho)n_j} \quad , \quad (j=1,..,4) \tag{13}$$

Similarly, the equation system for U_2 and V_2 can be obtained as follows:

$$\begin{bmatrix} (\kappa+1)D^2+\beta(\kappa+1)D-(\kappa-1){\alpha_n}^2 & 2\alpha_n D+\beta(3-\kappa)\alpha_n \\ -2\alpha_n D-\beta(\kappa-1)\alpha_n & (\kappa-1)D^2+\beta(\kappa-1)D-(\kappa+1){\alpha_n}^2 \end{bmatrix} \begin{bmatrix} U_2(x,\alpha_n) \\ V_2(x,\alpha_n) \end{bmatrix} = \begin{bmatrix} 0 \\ 0 \end{bmatrix} \tag{14}$$

where $D = \frac{d}{dx}$.

Since U_2 and V_2 are not 0, determinant of the coefficient matrix of Eq. (14), Δ, should be 0.

$$\Delta = D^4 + 2\beta D^3 + (\beta^2 - 2{\alpha_n}^2)D^2 - 2\beta{\alpha_n}^2 D + {\alpha_n}^4 + \beta^2{\alpha_n}^2\frac{3-\kappa}{\kappa+1} \tag{15}$$

U_2 and V_2 are assumed to be in the form e^{px}. By substituting the solution into the Eq. (15), the following equation is obtained.

$$\left[p^4 + 2\beta p^3 + (\beta^2 - 2{\alpha_n}^2)p^2 - 2\beta{\alpha_n}^2 p + {\alpha_n}^4 + \beta^2{\alpha_n}^2\frac{3-\kappa}{\kappa+1}\right]e^{px} = 0 \tag{16}$$

The roots of Eq. (16) are

$$p_1 = -\frac{\beta}{2} - \frac{1}{2}\sqrt{\beta^2 + 4\alpha^2 + i4\alpha\beta\sqrt{\frac{3-\kappa}{\kappa+1}}} \quad , \tag{17.a}$$

$$p_2 = -\frac{\beta}{2} - \frac{1}{2}\sqrt{\beta^2 + 4\alpha^2 - i4\alpha\beta\sqrt{\frac{3-\kappa}{\kappa+1}}} \quad , \tag{17.b}$$

$$p_3 = -\frac{\beta}{2} + \frac{1}{2}\sqrt{\beta^2 + 4\alpha^2 + i4\alpha\beta\sqrt{\frac{3-\kappa}{\kappa+1}}} \quad , \tag{17.c}$$

$$p_4 = -\frac{\beta}{2} + \frac{1}{2}\sqrt{\beta^2 + 4\alpha^2 - i4\alpha\beta\sqrt{\frac{3-\kappa}{\kappa+1}}} \quad . \tag{17.d}$$

Then the solution for displacements U_2 and V_2 can be written as:

$$U_2 = q_1 B_{1n}(\alpha_n)e^{p_1 x} + q_2 B_{2n}(\alpha_n)e^{p_2 x} + q_3 B_{3n}(\alpha_n)e^{p_3 x} + q_4 B_{4n}(\alpha_n)e^{p_4 x} \tag{18.a}$$

$$V_2 = B_{1n}(\alpha_n)e^{p_1 x} + B_{2n}(\alpha_n)e^{p_2 x} + B_{3n}(\alpha_n)e^{p_3 x} + B_{4n}(\alpha\alpha_n)e^{p_4 x} \tag{18.b}$$

Substituting the expressions of U_2 and V_2 into the Eq. (6.d), following equation can be found.

$$(-2\alpha_n)[q_1p_1B_{1n}(\alpha_n)e^{p_1x}+q_2p_2B_{2n}(\alpha_n)e^{p_2x}+q_3p_3B_{3n}(\alpha_n)e^{p_3x}+q_4p_4B_{4n}(\alpha_n)e^{p_4x}]-$$
$$\beta\alpha_n(\kappa-1)[q_1B_{1n}(\alpha_n)e^{p_1x}+q_2B_{2n}(\alpha_n)e^{p_2x}+q_3B_{3n}(\alpha_n)e^{p_3x}+q_4B_{4n}(\alpha_n)e^{p_4x}]+$$
$$(\kappa-1)[{p_1}^2B_{1n}(\alpha_n)e^{p_1x}+{p_2}^2B_{2n}(\alpha_n)e^{p_2x}+{p_3}^2B_{3n}(\alpha_n)e^{p_3x}+{p_4}^2B_{4n}(\alpha_n)e^{p_4x}]+$$
$$\beta(\kappa-1)[p_1B_{1n}(\alpha_n)e^{p_1x}+p_2B_{2n}(\alpha_n)e^{p_2x}+p_3B_{3n}(\alpha_n)e^{p_3x}+p_4B_{4n}(\alpha_n)e^{p_4x}]-$$
$${\alpha_n}^2(\kappa+1)[B_{1n}(\alpha_n)e^{p_1x}+B_{2n}(\alpha_n)e^{p_2x}+B_{3n}(\alpha_n)e^{p_3x}+B_{4n}(\alpha_n)e^{p_4x}]=0 \quad (19)$$

Knowing that the coefficients of B_j are zero, $q_j(j=1,..,4)$ can be found as:

$$q_j=\frac{p_j(\kappa-1)(p_j+\beta)-{\alpha_n}^2(\kappa+1)}{\alpha_n(2p_j+\beta(\kappa-1))} \quad (20)$$

Substituting U_1, V_1, U_2 and V_2 into the Eqs. (5.a) and (5.b), the solution which has the capacity to satisfy the boundary conditions of the problem of periodic cracks in strip can be written as:

$$u(x,y)=\frac{1}{2\pi}\int_{-\infty}^{\infty}\sum_{j=1}^{4}m_j(\rho)A_j(\rho)e^{n_jy-ix\rho}\,d\rho+\sum_{n=0}^{\infty}\sum_{j=1}^{4}q_j(\alpha_n)B_{jn}(\alpha_n)e^{p_jx}cos(y\alpha_n), \quad (21.a)$$

$$v(x,y)=\frac{1}{2\pi}\int_{-\infty}^{\infty}\sum_{j=1}^{4}A_j(\rho)e^{n_jy-ix\rho}\,d\rho+\sum_{n=0}^{\infty}\sum_{j=1}^{4}B_{jn}(\alpha_n)e^{p_jx}sin(y\alpha_n)\ . \quad (21.b)$$

The expressions for stresses can be obtained by using Hooke's Law as follows

$$\sigma_{xx}(x,y)=\frac{\mu(x)}{\kappa-1}\Big[\frac{1}{2\pi}\int_{-\infty}^{\infty}\sum_{j=1}^{4}\big[(3-\kappa)n_j(\rho)-i\rho(\kappa+1)m_j(\rho)\big]A_j(\rho)e^{n_jy-ix\rho}d\rho+$$
$$\sum_{n=0}^{\infty}\sum_{j=1}^{4}\big[(\kappa+1)p_j(\alpha_n)q_j(\alpha_n)+(3-\kappa)\alpha_n\big]B_{jn}(\alpha_n)e^{p_jx}cos(y\alpha_n)\big]\ , \quad (22.a)$$

$$\sigma_{yy}(x,y)=\frac{\mu(x)}{\kappa-1}\Big[\frac{1}{2\pi}\int_{-\infty}^{\infty}\sum_{j=1}^{4}\big[(\kappa+1)n_j(\rho)-i\rho(3-\kappa)m_j(\rho)\big]A_j(\rho)e^{n_jy-ix\rho}d\rho+$$
$$\sum_{n=0}^{\infty}\sum_{j=1}^{4}\big[(3-\kappa)p_j(\alpha_n)q_j(\alpha_n)+(\kappa+1)\alpha_n\big]B_{jn}(\alpha_n)e^{p_jx}cos(y\alpha_n)\big]\ , \quad (22.b)$$

$$\sigma_{xy}(x,y)=\mu(x)[\frac{1}{2\pi}\int_{-\infty}^{\infty}\sum_{j=1}^{4}\big[m_j(\rho)n_j(\rho)-i\rho\big]A_j(\rho)e^{n_jy-ix\rho}d\rho+$$
$$\sum_{n=0}^{\infty}\sum_{j=1}^{4}\big[p_j(\alpha_n)-(\alpha_n)q_j(\alpha_n)\big]B_{jn}(\alpha_n)e^{p_jx}sin(y\alpha_n)]\ . \quad (22.c)$$

There are four unknowns namely A_1, A_2, A_3 and A_4 in integral groups and four unknowns namely B_{1n}, B_{2n}, B_{3n} and B_{4n} in series groups in Eqs. (22.a-c). They are supposed to be determined by using boundary conditions.

2.3 Application of Boundary Conditions

Boundary conditions of the problem are shown in Fig. 2.2 below. The domain of the elastic solution is shaded. Note that a similar unit cell has been used, for example, in [34] and [37].

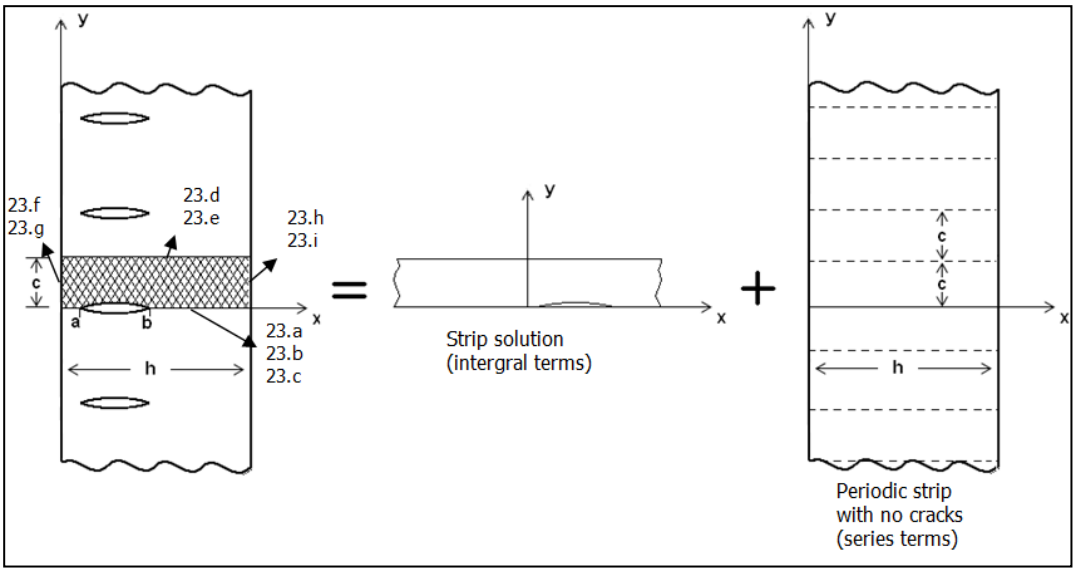

Figure 2.2 Representation of boundary conditions

By taking a=0 the problem becomes periodic edge crack problem.

The FGM strip containing periodic cracks as represented by the shaded region in Fig. 2.2 is subjected to the following boundary conditions:

$v(x,0) = 0$ $\quad 0<x<a$ and $b<x<h$, (23.a)

$\sigma_{yy}(x,0) = -p(x)$ $\quad a<x<b$, (23.b)

$\sigma_{xy}(x,0) = 0$ $\quad 0<x<h$, (23.c)

$\sigma_{xy}(x,c) = 0$ $\quad 0<x<h$, (23.d)

$v(x,c) = 0$ $\quad 0<x<h$, (23.e)

$\sigma_{xx}(0,y) = 0$ $\quad 0<y<c$, (23.f)

$\sigma_{xy}(0,y) = 0$ $\quad 0<y<c$, (23.g)

$\sigma_{xx}(h,y) = 0$ $\quad 0<y<c$, (23.h)

$\sigma_{xy}(h,y) = 0$ $\quad 0<y<c$. (23.i)

Of the conditions above, (23.a-e) are due to symmetry and (23.f-i) are the free surface conditions. Conditions (23.a) and (23.b) are the mixed boundary conditions.

The derivative of crack surface displacement is going to be used as the auxiliary unknown in terms of which other unknowns will be expressed.

Defining

$$g(x) = \frac{\partial}{\partial x}\big(v(x,0)\big)\,, \qquad 0 < x < h, \tag{24}$$

And using Eq. (24) and the equation of $v(x,y)$ (21.b), following can be obtained:

$$g(x) = \frac{1}{2\pi}\int_{-\infty}^{\infty} -i\rho[A_1(\rho) + A_2(\rho) + A_3(\rho) + A_4(\rho)]\, e^{-ix\rho} d\rho \tag{25.a}$$

Note that series term in the derivative of $v(x,y)$ disappears since $sin(0) = 0$.

Applying inverse Fourier transform, right hand side of the Eq. (25.a):

$$F^{-1}\left\{\frac{1}{2\pi}\int_{-\infty}^{\infty} -i\rho[A_1(\rho) + A_2(\rho) + A_3(\rho) + A_4(\rho)]\, e^{-ix\rho} d\rho\right\} = \frac{-i\rho}{2\pi}[A_1(\rho) + A_2(\rho) + A_3(\rho) + A_4(\rho)]\,,$$

left hand side:

$$F^{-1}\{g(x)\} = \frac{1}{2\pi}\int_{-\infty}^{\infty} g(x)\, e^{i\rho x} dx\ ,$$

and equating the sides, one can obtain

$$\frac{1}{2\pi}\int_{-\infty}^{\infty} g(x)\, e^{i\rho x} dx = \frac{-i\rho}{2\pi}[A_1(\rho) + A_2(\rho) + A_3(\rho) + A_4(\rho)]\ , \tag{25.b}$$

which is simplified to

$$A_1(\rho) + A_2(\rho) + A_3(\rho) + A_4(\rho) = \frac{i}{\rho}\int_{-\infty}^{\infty} g(x)\, e^{i\rho x} dx\ . \tag{25.c}$$

Knowing from the boundary condition (23.a), $v(x,0)$ and accordingly $g(x)$ are nonzero only between a and b, the integral limits in the Eq. (25.c) can be modified as:

$$A_1(\rho) + A_2(\rho) + A_3(\rho) + A_4(\rho) = \frac{i}{\rho}\int_{a}^{b} g(x)\, e^{i\rho x} dx \tag{26.a}$$

Applying the boundary condition (23.c) to Eq. (22.c), the series term drops out because of $sin(y\alpha_n)$ term and the following expression is obtained.

$$\sigma_{xy}(x,0) = \mu(x)\frac{1}{2\pi}\int_{-\infty}^{\infty}\sum_{j=1}^{4}\big[m_j(\rho)n_j(\rho) - i\rho\big]A_j(\rho)e^{-ix\rho} d\rho = 0 \tag{26.b}$$

Since $\mu(x) \neq 0$,

$$\frac{1}{2\pi}\int_{-\infty}^{\infty}\sum_{j=1}^{4}\big[m_j(\rho)n_j(\rho) - i\rho\big]A_j(\rho)e^{-ix\rho} d\rho = 0 \tag{26.c}$$

Applying inverse Fourier transform to the Eq. (26.c),

$$\sum_{j=1}^{4}\big[m_j(\rho)n_j(\rho) - i\rho\big]A_j(\rho) = 0\ . \tag{26.d}$$

Applying the boundary condition (23.d) the series term disappears because of $sin(y\alpha_n)$ term again, and one can obtain

$$\sum_{j=1}^{4}[m_j(\rho)n_j(\rho) - i\rho]A_j(\rho)e^{n_j c} = 0 \ . \tag{26.e}$$

Applying the boundary condition (23.e) and inverse Fourier transform,

$$A_1(\rho)e^{n_1 c} + A_2(\rho)e^{n_2 c} + A_3(\rho)e^{n_3 c} + A_4(\rho)e^{n_4 c} = 0 \tag{26.f}$$

Eqs. (26.a,d,e,f) can be expressed in matrix form as follows,

$$\begin{bmatrix} 1 & 1 & 1 & 1 \\ m_1n_1 - i\rho & m_2n_2 - i\rho & m_3n_3 - i\rho & m_4n_4 - i\rho \\ e^{n_1c}(m_1n_1 - i\rho) & e^{n_2c}(m_2n_2 - i\rho) & e^{n_3c}(m_3n_3 - i\rho) & e^{n_4c}(m_4n_4 - i\rho) \\ e^{n_1c} & e^{n_2c} & e^{n_3c} & e^{n_4c} \end{bmatrix} \begin{bmatrix} A_1 \\ A_2 \\ A_3 \\ A_4 \end{bmatrix} = \begin{bmatrix} 1 \\ 0 \\ 0 \\ 0 \end{bmatrix} f(\rho) \ , \tag{27}$$

where

$$f(\rho) = \frac{i}{\rho}\int_a^b e^{it\rho} g(t)dt \ . \tag{28}$$

Applying Cramer's Rule, A_k can be written as:

$$A_j = f(\rho)\frac{\Delta_j}{\Delta} \qquad (j=1,.., 4). \tag{29}$$

In the expression of A_j (29), Δ which is given in Eq. (30) is the determinant of the 4x4 matrix in equation system (27), and Δ_j are obtained by replacing the j_{th} column of the 4x4 matrix with the unit vector on the right hand side of the equation system.

$$\begin{aligned} \Delta = &\left[e^{(n_1+n_2)c} + e^{(n_3+n_4)c}\right](m_1n_1 - m_2n_2)(m_4n_4 - m_3n_3) + \\ &\left[e^{(n_1+n_3)c} + e^{(n_2+n_4)c}\right](m_1n_1 - m_3n_3)(m_2n_2 - m_4n_4) + \\ &\left[e^{(n_1+n_4)c} + e^{(n_2+n_3)c}\right](m_1n_1 - m_4n_4)(m_3n_3 - m_2n_2) \end{aligned} \tag{30}$$

Defining

$$A = \frac{1}{2}\beta\sqrt{\frac{3-\kappa}{\kappa+1}} \ , \tag{31.a}$$

$$B = \frac{1}{2}\sqrt{4\rho(\rho + i\beta) + \beta^2\frac{3-\kappa}{\kappa+1}} \ , \tag{31.b}$$

$$C = (\kappa - 1)\rho(\rho + i\beta) \ , \tag{31.c}$$

$$D = \kappa + 1 \ , \tag{31.d}$$

$$E = \beta(\kappa - 1) - 2i\rho \ , \tag{31.e}$$

n_j and m_j can be written as follows:

$$n_1 = -A - B \ , \tag{32.a}$$

$$n_2 = A - B \ , \tag{32.b}$$

$$n_3 = -A + B \ , \tag{32.c}$$

$$n_4 = A + B \ , \tag{32.d}$$

and

$$m_j = \frac{C - Dn_j{}^2}{En_j} \ , \qquad (j=1,.., 4). \tag{32.e}$$

Eq. (30) can be simplified by substituting the Eqs. (31) and (32) as:

$$\Delta = \{[e^{-2Bc} + e^{2Bc}] - [e^{-2Ac} + e^{2Ac}]\}(\frac{4ABD}{E})^2 \ , \tag{33.a}$$

or writing in terms of hyperbolic function

$$\Delta = 2\{cosh\, 2Bc - cosh\, 2Ac\}(\frac{4ABD}{E})^2 \ . \tag{33.b}$$

To determine Δ_1 , first column of the 4x4 matrix is replaced with the unit vector on the right hand side of equation system (27).

$$\Delta_1 = det \begin{bmatrix} 1 & 1 & 1 & 1 \\ 0 & m_2n_2 - i\rho & m_3n_3 - i\rho & m_4n_4 - i\rho \\ 0 & e^{n_2c}(m_2n_2 - i\rho) & e^{n_3c}(m_3n_3 - i\rho) & e^{n_4c}(m_4n_4 - i\rho) \\ 0 & e^{n_2c} & e^{n_3c} & e^{n_4c} \end{bmatrix} \tag{34.a}$$

Substituting Eqs. (31) and (32) into the expansion of Δ_1 and simplifying following expression is obtained:

$$\Delta_1 = (m_2n_2 - i\rho)(e^{2Ac} - e^{2Bc})(\frac{4ABD}{E}) \tag{34.b}$$

To determine Δ_2 , second column of the 4x4 matrix is replaced with the unit vector on the right hand side of equation system (27).

$$\Delta_2 = det \begin{bmatrix} 1 & 1 & 1 & 1 \\ m_1n_1 - i\rho & 0 & m_3n_3 - i\rho & m_4n_4 - i\rho \\ e^{n_1c}(m_1n_1 - i\rho) & 0 & e^{n_3c}(m_3n_3 - i\rho) & e^{n_4c}(m_4n_4 - i\rho) \\ e^{n_1c} & 0 & e^{n_3c} & e^{n_4c} \end{bmatrix} \tag{35.a}$$

Substituting Eqs. (31) and (32) into the expansion of Δ_2 and simplifying following expression is obtained:

$$\Delta_2 = (m_1n_1 - i\rho)(e^{-2Ac} - e^{2Bc})(\frac{4ABD}{E}) \tag{35.b}$$

To determine Δ_3 , third column of the 4x4 matrix is replaced with the unit vector on the right hand side of equation system (27).

$$\Delta_3 = det\begin{bmatrix} 1 & 1 & 1 & 1 \\ m_1n_1 - i\rho & m_2n_2 - i\rho & 0 & m_4n_4 - i\rho \\ e^{n_1c}(m_1n_1 - i\rho) & e^{n_2c}(m_2n_2 - i\rho) & 0 & e^{n_4c}(m_4n_4 - i\rho) \\ e^{n_1c} & e^{n_2c} & 0 & e^{n_4c} \end{bmatrix} \tag{36.a}$$

Substituting Eqs. (31) and (32) into the expansion of Δ_3 and simplifying following expression is obtained:

$$\Delta_3 = (m_1n_1 - i\rho)(e^{2Ac} - e^{-2Bc})(\frac{4ABD}{E}) \tag{36.b}$$

To determine Δ_4 , fourth column of the 4x4 matrix is replaced with the unit vector on the right hand side of equation system (27).

$$\Delta_4 = det\begin{bmatrix} 1 & 1 & 1 & 1 \\ m_1n_1 - i\rho & m_2n_2 - i\rho & m_3n_3 - i\rho & 0 \\ e^{n_1c}(m_1n_1 - i\rho) & e^{n_2c}(m_2n_2 - i\rho) & e^{n_3c}(m_3n_3 - i\rho) & 0 \\ e^{n_1c} & e^{n_2c} & e^{n_3c} & 0 \end{bmatrix} \tag{37.a}$$

Substituting Eqs. (31) and (32) into the expansion of Δ_4 and simplifying following expression is obtained:

$$\Delta_4 = (m_2n_2 - i\rho)(e^{-2Bc} - e^{-2Ac})(\frac{4ABD}{E}) \tag{37.b}$$

Substituting Δ and Δ_k $(k=1,.., 4)$ into Eq. (29) one by one, A_k $(k=1,.., 4)$ are calculated as follows:

$$A_1 = \frac{\Delta_1}{\Delta} f(g) = \frac{(m_2n_2 - i\rho)(e^{2Ac} - e^{2Bc})(\frac{4ABD}{E})}{2\{cosh\ 2Bc - cosh\ 2Ac\}(\frac{4ABD}{E})^2} \frac{i}{\rho} \int_a^b e^{itg} g(t)dt \tag{38.a}$$

Knowing from Eqs. (32.a-e)

$$m_2n_2 - m_1n_1 = \frac{4ABD}{E} .$$

Then, one can find

$$A_1 = \frac{(e^{2Ac} - e^{2Bc})}{2\{\cosh 2Ac - \cosh 2Bc\}} \frac{(m_2n_2 - i\rho)}{(m_2n_2 - m_1n_1)} \frac{i}{\rho} \int_a^b e^{itg} g(t)dt . \tag{38.b}$$

Similarly

$$A_2 = \frac{\Delta_2}{\Delta} f(g) = \frac{(m_1n_1 - i\rho)(e^{-2Ac} - e^{2Bc})(\frac{4ABD}{E})}{2\{\cosh 2Bc - \cosh 2Ac\}(\frac{4ABD}{E})^2} \frac{i}{\rho} \int_a^b e^{itg} g(t)dt , \tag{39.a}$$

$$A_2 = \frac{(e^{2Bc} - e^{-2Ac})}{2\{\cosh 2Ac - \cosh 2Bc\}} \frac{(m_1n_1 - i\rho)}{(m_2n_2 - m_1n_1)} \frac{i}{\rho} \int_a^b e^{itg} g(t)dt , \tag{39.b}$$

$$A_3 = \frac{\Delta_3}{\Delta} f(g) = \frac{(m_1 n_1 - i\rho)(e^{2Ac} - e^{-2Bc})(\frac{4ABD}{E})}{2\{\cosh 2Bc - \cosh 2Ac\}(\frac{4ABD}{E})^2} \frac{i}{\rho} \int_a^b e^{itg} g(t) dt \ , \tag{40.a}$$

$$A_3 = \frac{(e^{-2Bc} - e^{2Ac})}{2\{\cosh 2Ac - \cosh 2Bc\}} \frac{(m_1 n_1 - i\rho)}{(m_2 n_2 - m_1 n_1)} \frac{i}{\rho} \int_a^b e^{itg} g(t) dt \ , \tag{40.b}$$

$$A_4 = \frac{\Delta_4}{\Delta} f(g) = \frac{(m_2 n_2 - i\rho)(e^{-2Bc} - e^{-2Ac})(\frac{4ABD}{E})}{2\{\cosh 2Bc - \cosh 2Ac\}(\frac{4ABD}{E})^2} \frac{i}{\rho} \int_a^b e^{itg} g(t) dt \ , \tag{41.a}$$

$$A_4 = \frac{(e^{-2Ac} - e^{-2Bc})}{2\{\cosh 2Ac - \cosh 2Bc\}} \frac{(m_2 n_2 - i\rho)}{(m_2 n_2 - m_1 n_1)} \frac{i}{\rho} \int_a^b e^{itg} g(t) dt \ . \tag{41.b}$$

Defining

$$h(\rho) = \frac{1}{2\{\cosh 2Ac - \cosh 2Bc\}} \frac{1}{(m_2 n_2 - m_1 n_1)} \frac{i}{\rho} \int_a^b e^{itg} g(t) dt \ , \tag{42}$$

A_k *(k=1,.., 4)* are can be written as follows:

$$A_1 = (e^{2Ac} - e^{2Bc})(m_2 n_2 - i\rho) h(\rho) = \hat{A}_1 h(\rho) \ , \tag{43.a}$$

$$A_2 = -(e^{-2Ac} - e^{2Bc})(m_1 n_1 - i\rho) h(\rho) = \hat{A}_2 h(\rho) \ , \tag{43.b}$$

$$A_3 = -(e^{2Ac} - e^{-2Bc})(m_1 n_1 - i\rho) h(\rho) = \hat{A}_3 h(\rho) \ , \tag{43.c}$$

$$A_4 = (e^{-2Ac} - e^{-2Bc})(m_2 n_2 - i\rho) h(\rho) = \hat{A}_4 h(\rho) \ . \tag{43.d}$$

Here $\hat{A}_k$ terms are implied in Eqs. (43.a-d). After determining A_1, A_2, A_3 and A_4 one can turn to the question of finding $B_{1n}(\alpha_n)$, $B_{2n}(\alpha_n)$, $B_{3n}(\alpha_n)$ and $B_{4n}(\alpha_n)$.

Applying boundary condition (23.f) to the Eq. (22.a),

$$\sigma_{xx}(0, y) = \frac{\mu(0)}{\kappa - 1} \Big[\frac{1}{2\pi} \int_{-\infty}^{\infty} \sum_{j=1}^{4} \big[(3-\kappa) n_j(\rho) - i\rho(\kappa+1) m_j(\rho) \big] A_j(\rho) e^{n_j y} d\rho + \sum_{n=0}^{\infty} \sum_{j=1}^{4} \big[(\kappa+1) p_j(\alpha_n) q_j(\alpha_n) + (3-\kappa)\alpha_n \big] B_{jn}(\alpha_n) cos(y\alpha_n) \Big] = 0 \ . \tag{44}$$

Defining

$$L_j = (3-\kappa) n_j(\rho) - i\rho(\kappa+1) m_j(\rho) \ , \quad (j=1,..,4) \tag{45.a}$$

$$M_j = (\kappa+1) p_j(\alpha_n) q_j(\alpha_n) + (3-\kappa)\alpha_n \ , \quad (j=1,..,4) \tag{45.b}$$

and knowing that

$$\frac{\mu(0)}{\kappa - 1} \neq 0 \ ,$$

Eq. (44) can be reduced to the following form

$$\frac{1}{2\pi} \int_{-\infty}^{\infty} \sum_{j=1}^{4} L_j A_j e^{n_j y} d\rho + \sum_{n=0}^{\infty} \sum_{j=1}^{4} M_j B_{jn} cos(y\alpha_n) = 0 \ . \tag{46}$$

Recalling the orthogonality relationship for cosine function

$$\int_0^c \cos\frac{\pi y n}{c}\cos\frac{\pi y m}{c}\,dy = \begin{cases} c\,, & n=m=0 \\ \frac{c}{2}\,, & n=m\neq 0 \\ 0\,, & n\neq m \end{cases} \tag{47}$$

one can multiply both sides of equation with $cos(y\alpha_m)dy$ and integrate y∈(0,c), then obtain

$$\frac{1}{2\pi}\int_{-\infty}^{\infty}\sum_{j=1}^{4} L_j A_j\left(\int_0^c e^{n_j y} cos(y\alpha_m)dy\right) d\rho + \sum_{n=0}^{\infty}\sum_{j=1}^{4} M_j B_{jn}\int_0^c cos(y\alpha_n)cos(y\alpha_m)dy = 0. \tag{48}$$

In above equation while the inner integral in the first term can be taken, the integral in the second term vanishes except in the case of n=m. Then Eq. (48) can be written as follows

$$\frac{1}{2\pi}\int_{-\infty}^{\infty}\sum_{j=1}^{4} L_j A_j\left(\frac{c^2 n_j(-1+(-1)^m e^{c n_j})}{c^2 {n_j}^2+m^2\pi^2}\right)d\rho + \sum_{j=1}^{4} M_j B_{jm}\hat{c}_m = 0\ ,\ (m=0,1,2...) \tag{49}$$

where

$$\hat{c}_m = \begin{cases} c, & m=0 \\ c/2\,, & m\neq 0 \end{cases}. \tag{50}$$

The first term of the Eq. (49) is named G_1.

$$G_1 = \frac{1}{2\pi}\int_{-\infty}^{\infty}\sum_{j=1}^{4} L_j A_j\left(\frac{c^2 n_j(-1+(-1)^m e^{c n_j})}{c^2 {n_j}^2+m^2\pi^2}\right)d\rho \tag{51}$$

Applying boundary condition (23.h) to the Eq. (22.a),

$$\sigma_{xx}(h,y) = \frac{\mu(h)}{\kappa-1}\left[\frac{1}{2\pi}\int_{-\infty}^{\infty}\sum_{j=1}^{4}\left[(3-\kappa)n_j(\rho) - i\rho(\kappa+1)m_j(\rho)\right]A_j(\rho)e^{n_j y - ih\rho}d\rho + \sum_{n=0}^{\infty}\sum_{j=1}^{4}\left[(\kappa+1)p_j(\alpha_n)q_j(\alpha_n) + (3-\kappa)\alpha_n\right]B_{jn}(\alpha_n)e^{p_j h}cos(y\alpha_n)\right] = 0 \tag{52}$$

Using the definition of L_j and M_j in Eq. (45), and knowing that

$$\frac{\mu(h)}{\kappa-1} \neq 0\ ,$$

Eq. (52) is reduced to the following form

$$\frac{1}{2\pi}\int_{-\infty}^{\infty}\sum_{j=1}^{4} L_j A_j e^{n_j y - ih\rho}d\rho + \sum_{n=0}^{\infty}\sum_{j=1}^{4} M_j B_{jn} e^{p_j h} cos(y\alpha_n) = 0\ . \tag{53}$$

Using the orthogonality relationship for cosine function (47), one can multiply both sides of equation with $cos(y\alpha_m)dy$ and integrate y∈(0,c), then obtain

$$\frac{1}{2\pi}\int_{-\infty}^{\infty}\sum_{j=1}^{4} L_j A_j\left(\int_0^c e^{n_j y} cos(y\alpha_m)dy\right)e^{-ih\rho}\,d\rho + \sum_{n=0}^{\infty}\sum_{j=1}^{4} M_j B_{jn} e^{p_j h}\int_0^c cos(y\alpha_n)cos(y\alpha_m)dy = 0\ . \tag{54}$$

In Eq. (54) while the inner integral in the first term can be taken, the integral in the second term vanishes except in the case of n=m. Then Eq. (54) can be written as follows

$$\frac{1}{2\pi}\int_{-\infty}^{\infty}\sum_{j=1}^{4}L_jA_j\left(\frac{c^2n_j(-1+(-1)^m e^{cn_j})}{c^2{n_j}^2+m^2\pi^2}\right)e^{-ih\rho}d\rho+\sum_{j=1}^{4}M_jB_{jm}e^{p_jh}\,\hat{c}_m=0,\ \ (m=0,1,2...) \tag{55}$$

where $\hat{c}_m$ is defined in Eq. (50).

The first term of the Eq. (55) is named G_2.

$$G_2=\frac{1}{2\pi}\int_{-\infty}^{\infty}\sum_{j=1}^{4}L_jA_j\left(\frac{c^2n_j(-1+(-1)^m e^{cn_j})}{c^2{n_j}^2+m^2\pi^2}\right)e^{-ih\rho}d\rho \tag{56}$$

Applying boundary condition (23.g) to the Eq. (22.c),

$$\sigma_{xy}(0,y)=\mu(0)\left[\frac{1}{2\pi}\int_{-\infty}^{\infty}\sum_{j=1}^{4}\left[m_j(\rho)n_j(\rho)-i\rho\right]A_j(\rho)e^{n_jy}d\rho+\right.$$
$$\left.\sum_{n=0}^{\infty}\sum_{j=1}^{4}\left[p_j(\alpha_n)-\alpha_nq_j(\alpha_n)\right]B_{jn}(\alpha_n)sin(y\alpha_n)\right]=0\ . \tag{57}$$

Defining

$$R_j=m_j(\rho)n_j(\rho)-i\rho\quad,\quad (j=1,...,4) \tag{58.a}$$

$$S_j=p_j(\alpha_n)-\alpha_nq_j(\alpha_n)\quad,\quad (j=1,...,4) \tag{58.b}$$

and knowing that

$\mu(0)\neq 0$,

Eq. (57) can be reduced to the following form

$$\frac{1}{2\pi}\int_{-\infty}^{\infty}\sum_{j=1}^{4}R_jA_je^{n_jy}d\rho+\sum_{n=0}^{\infty}\sum_{j=1}^{4}S_jB_{jn}sin(y\alpha_n)=0\ . \tag{59}$$

Recalling the orthogonality relationship for sine function

$$\int_0^c\sin\frac{\pi yn}{c}\sin\frac{\pi ym}{c}dy=\begin{cases}0\ ,\ \ n=m=0\\ \frac{c}{2}\ ,\ \ n=m\neq 0\\ 0\ ,\ \ n\neq m\end{cases} \tag{60}$$

one can multiply both sides of equation with $sin(y\alpha_m)dy$ and integrate y∈(0,c), then obtain

$$\frac{1}{2\pi}\int_{-\infty}^{\infty}\sum_{j=1}^{4}R_jA_j\left(\int_0^c sin(y\alpha_m)\,e^{n_jy}dy\right)d\rho+\sum_{n=0}^{\infty}\sum_{j=1}^{4}S_jB_{jn}\int_0^c sin(y\alpha_m)\,sin(y\alpha_n)dy=0\ . \tag{61}$$

In above equation while the inner integral in the first term can be taken, the integral in the second term vanishes except in the case of n=m≠0. Then Eq. (61) can be written as follows

$$\frac{1}{2\pi}\int_{-\infty}^{\infty}\sum_{j=1}^{4}R_jA_j\left(\frac{m\pi}{c}\frac{(1-(-1)^m e^{cn_j})}{(\frac{m\pi}{c})^2+{n_j}^2}\right)d\rho+\sum_{j=1}^{4}S_jB_{jm}c'_m=0\ ,\ \ (m=0,1,2...) \tag{62}$$

where

$$c'_m=\begin{cases}0\ ,\ \ m=0\\ c/2\ ,\ \ m\neq 0\end{cases}\ . \tag{63}$$

The first term of the Eq. (62) is named G_3.

$$G_3 = \frac{1}{2\pi}\int_{-\infty}^{\infty}\sum_{j=1}^{4} R_j A_j \left(\frac{m\pi}{c}\frac{(1-(-1)^m e^{cn_j})}{(\frac{m\pi}{c})^2+n_j{}^2}\right)d\rho \tag{64}$$

Applying boundary condition (23.i) to the Eq. (22.c),

$$\sigma_{xy}(h,y) = \mu(h)\left[\frac{1}{2\pi}\int_{-\infty}^{\infty}\sum_{j=1}^{4}\left[m_j(\rho)n_j(\rho) - i\rho\right]A_j(\rho)e^{n_j y - ih\rho}d\rho + \sum_{n=0}^{\infty}\sum_{j=1}^{4}\left[p_j(\alpha_n) - (\alpha_n)q_j(\alpha_n)\right]B_{jn}(\alpha_n)e^{p_j h}sin(y\alpha_n)\right] = 0 \tag{65}$$

Using the definition of R_j and S_j in Eq. (58), and knowing that

$\mu(h) \neq 0$,

Eq. (65) can be reduced to the following form

$$\frac{1}{2\pi}\int_{-\infty}^{\infty}\sum_{j=1}^{4} R_j A_j e^{n_j y - ih\rho}d\rho + \sum_{n=0}^{\infty}\sum_{j=1}^{4} S_j B_{jn} e^{p_j h} sin(y\alpha_n) = 0 \ . \tag{66}$$

Using the orthogonality relationship for sine function (60), one can multiply both sides of equation with $sin(y\alpha_m)dy$ and integrate y∈(0,c), then obtain

$$\frac{1}{2\pi}\int_{-\infty}^{\infty}\sum_{j=1}^{4} R_j A_j e^{-ih\rho}\left(\int_0^c sin(y\alpha_m)\, e^{n_j y}dy\right)d\rho + \sum_{n=0}^{\infty}\sum_{j=1}^{4} S_j B_{jn} e^{p_j h}\int_0^c sin(y\alpha_m)\, sin(y\alpha_n)dy = 0 \tag{67}$$

In above equation while the inner integral in the first term can be taken, the integral in the second term vanishes except in the case of n=m≠0. Then Eq. (67) can be written as follows

$$\frac{1}{2\pi}\int_{-\infty}^{\infty}\sum_{j=1}^{4} R_j A_j \left(\frac{m\pi}{c}\frac{(1-(-1)^m e^{cn_j})}{(\frac{m\pi}{c})^2+n_j{}^2}\right)e^{-ih\rho}d\rho + \sum_{j=1}^{4} S_j B_{jm} e^{p_j h} c'_m = 0 \text{ , } (m=0,1,2...) \tag{68}$$

where c'_m is defined in Eq. (63).

The first term of the e Eq. (68) is named G_4.

$$G_4 = \frac{1}{2\pi}\int_{-\infty}^{\infty}\sum_{j=1}^{4} R_j A_j \left(\frac{m\pi}{c}\frac{(1-(-1)^m e^{cn_j})}{(\frac{m\pi}{c})^2+n_j{}^2}\right)e^{-ih\rho}d\rho \tag{69}$$

Eqs. (49), (55), (62) and (69) can be written respectively as follows:

$$G_1 + \sum_{j=1}^{4} M_j B_{jm}\hat{c}_m = 0 \ , \tag{70.a}$$

$$G_2 + \sum_{j=1}^{4} M_j B_{jm} e^{p_j h}\hat{c}_m = 0 \ , \tag{70.b}$$

$$G_3 + \sum_{j=1}^{4} S_j B_{jm} c'_m = 0 \ , \tag{70.c}$$

$$G_4 + \sum_{j=1}^{4} S_j B_{jm} e^{p_j h} c'_m = 0 \ . \tag{70.d}$$

An equation system where $B_{1m}(\alpha_m)$, $B_{2m}(\alpha_m)$, $B_{3m}(\alpha_m)$ and $B_{4m}(\alpha_m)$ can be solved is obtained.

$$\begin{bmatrix} M_1\hat{c}_m & M_2\hat{c}_m & M_3\hat{c}_m & M_4\hat{c}_m \\ M_1e^{p_1h}\hat{c}_m & M_2e^{p_2h}\hat{c}_m & M_3e^{p_3h}\hat{c}_m & M_4e^{p_4h}\hat{c}_m \\ S_1c'_m & S_2c'_m & S_3c'_m & S_4c'_m \\ S_1e^{p_1h}c'_m & S_2e^{p_2h}c'_m & S_3e^{p_3h}c'_m & S_4e^{p_4h}c'_m \end{bmatrix} \begin{bmatrix} B_{1m} \\ B_{2m} \\ B_{3m} \\ B_{4m} \end{bmatrix} = \begin{bmatrix} -G_1 \\ -G_2 \\ -G_3 \\ -G_4 \end{bmatrix} \tag{71}$$

Applying Cramer's Rule:

$$\Delta = \begin{vmatrix} M_1\hat{c}_m & M_2\hat{c}_m & M_3\hat{c}_m & M_4\hat{c}_m \\ M_1e^{p_1h}\hat{c}_m & M_2e^{p_2h}\hat{c}_m & M_3e^{p_3h}\hat{c}_m & M_4e^{p_4h}\hat{c}_m \\ S_1c'_m & S_2c'_m & S_3c'_m & S_4c'_m \\ S_1e^{p_1h}c'_m & S_2e^{p_2h}c'_m & S_3e^{p_3h}c'_m & S_4e^{p_4h}c'_m \end{vmatrix}, \tag{72.a}$$

$$\begin{aligned} \Delta = \{ & (M_1M_2S_3S_4 + M_3M_4S_1S_2)\left[e^{h(p_2+p_4)} + e^{h(p_1+p_3)} - e^{h(p_2+p_3)} - e^{h(p_1+p_4)}\right] + \\ & (M_1M_3S_2S_4 + M_2M_4S_1S_3)\left[e^{h(p_2+p_3)} + e^{h(p_1+p_4)} - e^{h(p_3+p_4)} - e^{h(p_1+p_2)}\right] + \\ & (M_1M_4S_2S_3 + M_2M_3S_1S_4)\left[e^{h(p_3+p_4)} + e^{h(p_1+p_2)} - e^{h(p_2+p_4)} - e^{h(p_1+p_3)}\right]\}\hat{c}_m{}^2c'_m{}^2 \quad , \end{aligned} \tag{72.b}$$

$$\Delta_1 = \begin{vmatrix} -G_1 & M_2\hat{c}_m & M_3\hat{c}_m & M_4\hat{c}_m \\ -G_2 & M_2e^{p_2h}\hat{c}_m & M_3e^{p_3h}\hat{c}_m & M_4e^{p_4h}\hat{c}_m \\ -G_3 & S_2c'_m & S_3c'_m & S_4c'_m \\ -G_4 & S_2e^{p_2h}c'_m & S_3e^{p_3h}c'_m & S_4e^{p_4h}c'_m \end{vmatrix}, \tag{73.a}$$

$$\begin{aligned} \Delta_1 = \{ & (G_1M_2S_3S_4c'_m + G_3M_3M_4S_2\hat{c}_m)\left[e^{h(p_2+p_3)} - e^{h(p_2+p_4)}\right] + \\ & (G_1M_3S_2S_4c'_m + G_3M_2M_4S_3\hat{c}_m)\left[e^{h(p_3+p_4)} - e^{h(p_2+p_3)}\right] + \\ & (G_1M_4S_2S_3c'_m + G_3M_2M_3S_4\hat{c}_m)\left[e^{h(p_2+p_4)} - e^{h(p_3+p_4)}\right] + \\ & (G_2M_2S_3S_4c'_m + G_4M_3M_4S_2\hat{c}_m)[e^{hp_4} - e^{hp_3}] + \\ & (G_2M_3S_2S_4c'_m + G_4M_2M_4S_3\hat{c}_m)[e^{hp_2} - e^{hp_4}] + \\ & (G_2M_4S_2S_3c'_m + G_4M_2M_3S_4\hat{c}_m)[e^{hp_3} - e^{hp_2}]\}\hat{c}_mc'_m \quad , \end{aligned} \tag{73.b}$$

$$\Delta_2 = \begin{vmatrix} M_1\hat{c}_m & -G_1 & M_3\hat{c}_m & M_4\hat{c}_m \\ M_1e^{p_1h}\hat{c}_m & -G_2 & M_3e^{p_3h}\hat{c}_m & M_4e^{p_4h}\hat{c}_m \\ S_1c'_m & -G_3 & S_3c'_m & S_4c'_m \\ S_1e^{p_1h}c'_m & -G_4 & S_3e^{p_3h}c'_m & S_4e^{p_4h}c'_m \end{vmatrix}, \tag{74.a}$$

$$\begin{aligned} \Delta_2 = \{ & (G_1M_4S_1S_3c'_m + G_3M_1M_3S_4\hat{c}_m)\left[e^{h(p_3+p_4)} - e^{h(p_1+p_4)}\right] + \\ & (G_1M_3S_1S_4c'_m + G_3M_1M_4S_3\hat{c}_m)\left[e^{h(p_1+p_3)} - e^{h(p_3+p_4)}\right] + \\ & (G_1M_1S_3S_4c'_m + G_3M_3M_4S_1\hat{c}_m)\left[e^{h(p_1+p_4)} - e^{h(p_1+p_3)}\right] + \\ & (G_2M_1S_3S_4c'_m + G_4M_3M_4S_1\hat{c}_m)[e^{hp_3} - e^{hp_4}] + \\ & (G_2M_4S_1S_3c'_m + G_4M_1M_3S_4\hat{c}_m)[e^{hp_1} - e^{hp_3}] + \\ & (G_2M_3S_1S_4c'_m + G_4M_1M_4S_3\hat{c}_m)[e^{hp_4} - e^{hp_1}]\}\hat{c}_mc'_m \quad , \end{aligned} \tag{74.b}$$

$$\Delta_3 = \begin{vmatrix} M_1\hat{c}_m & M_2\hat{c}_m & -G_1 & M_4\hat{c}_m \\ M_1e^{p_1h}\hat{c}_m & M_2e^{p_2h}\hat{c}_m & -G_2 & M_4e^{p_4h}\hat{c}_m \\ S_1c'_m & S_2c'_m & -G_3 & S_4c'_m \\ S_1e^{p_1h}c'_m & S_2e^{p_2h}c'_m & -G_4 & S_4e^{p_4h}c'_m \end{vmatrix}, \tag{75.a}$$

$$\Delta_3 = \{(G_1M_4S_1S_2c'_m + G_3M_1M_2S_4\hat{c}_m)\left[e^{h(p_1+p_4)} - e^{h(p_2+p_4)}\right] +$$
$$(G_1M_2S_1S_4c'_m + G_3M_1M_4S_2\hat{c}_m)\left[e^{h(p_2+p_4)} - e^{h(p_1+p_2)}\right] +$$
$$(G_1M_1S_2S_4c'_m + G_3M_2M_4S_1\hat{c}_m)\left[e^{h(p_1+p_2)} - e^{h(p_1+p_4)}\right] +$$
$$(G_2M_4S_1S_2c'_m + G_4M_1M_2S_4\hat{c}_m)[e^{hp_2} - e^{hp_1}] +$$
$$(G_2M_1S_2S_4c'_m + G_4M_2M_4S_1\hat{c}_m)[e^{hp_4} - e^{hp_2}] +$$
$$(G_2M_2S_1S_4c'_m + G_4M_1M_4S_2\hat{c}_m)[e^{hp_1} - e^{hp_4}]\}\hat{c}_m c'_m \quad , \tag{75.b}$$

$$\Delta_4 = \begin{vmatrix} M_1\hat{c}_m & M_2\hat{c}_m & M_3\hat{c}_m & -G_1 \\ M_1e^{p_1h}\hat{c}_m & M_2e^{p_2h}\hat{c}_m & M_3e^{p_3h}\hat{c}_m & -G_2 \\ S_1c'_m & S_2c'_m & S_3c'_m & -G_3 \\ S_1e^{p_1h}c'_m & S_2e^{p_2h}c'_m & S_3e^{p_3h}c'_m & -G_4 \end{vmatrix} , \tag{76.a}$$

$$\Delta_4 = \{(G_1M_3S_1S_2c'_m + G_3M_1M_2S_3\hat{c}_m)\left[e^{h(p_2+p_3)} - e^{h(p_1+p_3)}\right] +$$
$$(G_1M_2S_1S_3c'_m + G_3M_1M_3S_2\hat{c}_m)\left[e^{h(p_1+p_2)} - e^{h(p_2+p_3)}\right] +$$
$$(G_1M_1S_2S_3c'_m + G_3M_2M_3S_1\hat{c}_m)\left[e^{h(p_1+p_3)} - e^{h(p_1+p_2)}\right] +$$
$$(G_2M_3S_1S_2c'_m + G_4M_1M_2S_3\hat{c}_m)[e^{hp_1} - e^{hp_2}] +$$
$$(G_2M_2S_1S_3c'_m + G_4M_1M_3S_2\hat{c}_m)[e^{hp_3} - e^{hp_1}] +$$
$$(G_2M_1S_2S_3c'_m + G_4M_2M_3S_1\hat{c}_m)[e^{hp_2} - e^{hp_3}]\}\hat{c}_m c'_m \quad . \tag{76.b}$$

Then one can find $B_{1m}(\alpha_m)$, $B_{2m}(\alpha_m)$, $B_{3m}(\alpha_m)$ and $B_{4m}(\alpha_m)$ by using Eqs. (73-76.b):

$$B_{1m} = \frac{\Delta_1}{\Delta} , \tag{77.a}$$

$$B_{2m} = \frac{\Delta_2}{\Delta} , \tag{77.b}$$

$$B_{3m} = \frac{\Delta_3}{\Delta} , \tag{77.c}$$

$$B_{4m} = \frac{\Delta_4}{\Delta} . \tag{77.d}$$

To complete the solution for B_{1m}, B_{2m}, B_{3m} and B_{4m}; G_1, G_2, G_3 *and* G_4 should be obtained in terms of the unknown density function *g(t).*

G_1 can be simplified as shown below:

$$G_1 = \frac{1}{2\pi}\int_{-\infty}^{\infty}\sum_{j=1}^{4} L_jA_j\left(\frac{n_j(-1+(-1)^m e^{cn_j})}{n_j{}^2+\frac{m^2\pi^2}{c^2}}\right)d\rho \quad ,$$

where $\frac{m\pi}{c} = \alpha_m$.

Then G_1 can be separated as

$$G_1 = -\frac{1}{2\pi}\int_{-\infty}^{\infty}\sum_{j=1}^{4}\frac{L_jA_jn_j}{n_j{}^2+\alpha_m{}^2}d\rho + \frac{1}{2\pi}(-1)^m\int_{-\infty}^{\infty}\sum_{j=1}^{4}\frac{L_jA_jn_je^{cn_j}}{n_j{}^2+\alpha_m{}^2}d\rho \ . \tag{78}$$

In Eq. (78), first term is called G_{11} and second term is called G_{12}. Using Eq. (43) G_{11} and G_{12} can be written as:

$$G_{11} = -\frac{1}{2\pi}\int_{-\infty}^{\infty} h(\rho)\sum_{j=1}^{4}\frac{L_j\hat{A}_j n_j}{{n_j}^2+{\alpha_m}^2}d\rho \ , \tag{79.a}$$

$$G_{12} = \frac{1}{2\pi}(-1)^m\int_{-\infty}^{\infty} h(\rho)\sum_{j=1}^{4}\frac{L_j\hat{A}_j n_j e^{cn_j}}{{n_j}^2+{\alpha_m}^2}d\rho \ . \tag{79.b}$$

To calculate G_{11}; L_j, $\hat{A}_j$ and n_j are substituted. Then by using Maple the summation part is obtained as:

$$\sum_{j=1}^{4}\frac{L_j\hat{A}_j n_j}{{n_j}^2+{\alpha_m}^2} = \frac{64AB\rho^2{\alpha_m}^2(\kappa-1)(\cosh 2Ac-\cosh 2Bc))}{q(\rho)(\beta(\kappa-1)-2i\rho)} \ , \tag{80}$$

where

$$q(\rho) = \rho^4 + 2i\rho^3\beta - \rho^2\beta^2 + \alpha^2(\beta^2\frac{3-\kappa}{\kappa+1} + \alpha^2 + 2\rho^2 + 2i\beta\rho) \ . \tag{81}$$

Substituting $h(\rho)$ and simplifying, one can find:

$$G_{11} = -\frac{4i(\kappa-1){\alpha_m}^2}{\pi(\kappa+1)}\int_a^b g(t)\int_{-\infty}^{\infty} e^{it\rho}\frac{\rho}{q(\rho)}d\rho\, dt. \tag{82}$$

Then G_{11} can be expressed as

$$G_{11} = -\frac{4i(\kappa-1){\alpha_m}^2}{\pi(\kappa+1)}\int_a^b g(t)I_1(t)dt \ , \tag{83}$$

where

$$I_1(t) = \int_{-\infty}^{\infty} e^{it\rho}\frac{\rho}{q(\rho)}d\rho = \int_{-\infty}^{\infty} F_1(\rho)\, d\rho \ , \tag{84}$$

and

$$F_1(\rho) = e^{it\rho}\frac{\rho}{q(\rho)} \ . \tag{85}$$

The integral $I_1(t)$ can be evaluated using Residue Theorem which states that if Γ is a closed curve and if $f(z)$ is analytic within and on Γ except at a finite number of singular points z_j in the interior of Γ, then

$$\oint_\Gamma f(z)dz = 2\pi i\sum_k Res\ f(z)|_{z_k} \ . \tag{86}$$

Residue Theorem gives an easy way of evaluating integrals which would be hard by conventional methods.

$$\oint_\Gamma F_1(\rho)d\rho = 2\pi i(\sum_{k=1}^{n}(Residue\ of\ F_1(\rho) inside\ \Gamma)) \tag{87}$$

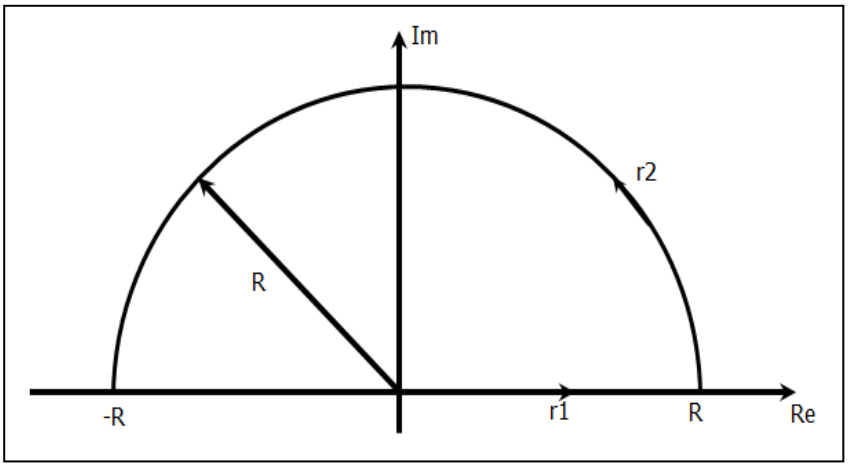

Figure 2.3 Upper contour for evaluation of the integral

Using the upper contour above,

$$\int_{\Gamma} F_1(\rho)d\rho = \lim_{R\to\infty}\int_{\Gamma_1} F_1(\rho)d\rho + \lim_{R\to\infty}\int_{\Gamma_2} F_1(\rho)d\rho \tag{88}$$

where $I_1(t) = \lim_{R\to\infty}\int_{\Gamma_1} F_1(\rho)d\rho = \lim_{R\to\infty}\int_{-R}^{R} F_1(\rho)d\rho = \int_{-\infty}^{\infty} F_1(\rho)d\rho$ will be found.

It can be shown that the second term in the summation in Eq. (88) is 0. $Re^{i\theta}$is substituted instead of ρ.

$$\lim_{R\to\infty}\int_{\Gamma_2} F_1(\rho)d\rho = \lim_{R\to\infty}\int_0^{\pi} F_1\left(Re^{i\theta}\right)iRe^{i\theta}d\theta \tag{89}$$

The integral would vanish in the limit as $R\to\infty$, since the integrand in (89) contains *"R^2"* in the numerator while it contains *"R^4"*in the denominator.

Using Eq. (87),

$$\int_{-\infty}^{\infty} F_1(\rho)d\rho = 2\pi i(\sum Residue\ of\ F_1(\rho) in\ upper\ half\ plane) \tag{90}$$

Roots of the denominator of $F_1(\rho)$ are the singular points in contour. Roots of $q(\rho)$ are found by Maple as:

$$\rho_1 = -\frac{\beta i}{2} - \frac{i}{2}\sqrt{\beta^2 + 4\alpha^2 - 4i\alpha\beta\sqrt{\frac{3-\kappa}{\kappa+1}}}, \tag{91.a}$$

$$\rho_2 = -\frac{\beta i}{2} + \frac{i}{2}\sqrt{\beta^2 + 4\alpha^2 - 4i\alpha\beta\sqrt{\frac{3-\kappa}{\kappa+1}}}, \tag{91.b}$$

$$\rho_3 = -\frac{\beta i}{2} - \frac{i}{2}\sqrt{\beta^2 + 4\alpha^2 + 4i\alpha\beta\sqrt{\frac{3-\kappa}{\kappa+1}}}, \tag{91.c}$$

$$\rho_4 = -\frac{\beta i}{2} + \frac{i}{2}\sqrt{\beta^2 + 4\alpha^2 + 4i\alpha\beta\sqrt{\frac{3-\kappa}{\kappa+1}}}. \tag{91.d}$$

Since ρ_2 and ρ_4 are in the upper half plane, residues at these roots will be used.

$$I_1(t) = 2\pi i\big(Res\ F_1(\rho_2) + Res\ F_1(\rho_4)\big) \tag{92}$$

$I_1(t)$ can be found by Maple (Appendix A) as:

$$I_1(t) = \frac{2\pi}{\lambda_1}\left[\lambda_4\left(1-\frac{\beta}{\lambda_2}\right) - \lambda_5\left(1-\frac{\beta}{\lambda_3}\right)\right] \tag{93}$$

where

$$\lambda_1 = 4\alpha_m\beta\sqrt{\frac{3-\kappa}{\kappa+1}}\ , \tag{94.a}$$

$$\lambda_2 = \sqrt{4{\alpha_m}^2 + \beta^2 - i\lambda_1}\ , \tag{94.b}$$

$$\lambda_3 = \sqrt{4{\alpha_m}^2 + \beta^2 + i\lambda_1}\ , \tag{94.c}$$

$$\lambda_4 = e^{(\beta-\lambda_2)\frac{t}{2}}\ , \tag{94.d}$$

$$\lambda_5 = e^{(\beta-\lambda_3)\frac{t}{2}}\ . \tag{94.e}$$

Substituting (93) into (83),

$$G_{11} = -\frac{8i(\kappa-1){\alpha_m}^2}{\lambda_1(\kappa+1)}\int_a^b g(t)\left[\lambda_4\left(1-\frac{\beta}{\lambda_2}\right) - \lambda_5\left(1-\frac{\beta}{\lambda_3}\right)\right]dt\ . \tag{95}$$

To calculate G_{12}; L_j, $\hat{A}_j$ and n_j are substituted into (79.b). By using Maple, G_{12} is found as zero. Then

$$G_1 = G_{11} = -\frac{8i(\kappa-1){\alpha_m}^2}{\lambda_1(\kappa+1)}\int_a^b g(t)\left[\lambda_4\left(1-\frac{\beta}{\lambda_2}\right) - \lambda_5\left(1-\frac{\beta}{\lambda_3}\right)\right]dt\ . \tag{96}$$

Remembering Eq. (56), G_2 can be simplified as shown below:

$$G_2 = \frac{1}{2\pi}\int_{-\infty}^{\infty}\sum_{j=1}^{4} L_jA_j\left(\frac{n_j(-1+(-1)^m e^{cn_j})}{{n_j}^2+\frac{m^2\pi^2}{c^2}}e^{-ih\rho}\right)d\rho\ . \tag{97}$$

Then G_2 can be separated as

$$G_2 = -\frac{1}{2\pi}\int_{-\infty}^{\infty}\sum_{j=1}^{4}\frac{L_jA_jn_j}{{n_j}^2+{\alpha_m}^2}e^{-ih\rho}d\rho + \frac{1}{2\pi}(-1)^m\int_{-\infty}^{\infty}\sum_{j=1}^{4}\frac{L_jA_jn_je^{cn_j}}{{n_j}^2+{\alpha_m}^2}e^{-ih\rho}d\rho\ . \tag{98}$$

In Eq. (98), first term is called G_{21} and second term is called G_{22}. Using Eq. (43) G_{11} and G_{12} can be written as:

$$G_{21} = -\frac{1}{2\pi}\int_{-\infty}^{\infty}h(\rho)\sum_{j=1}^{4}\frac{L_j\hat{A}_jn_j}{{n_j}^2+{\alpha_m}^2}e^{-ih\rho}d\rho\ , \tag{99.a}$$

$$G_{22} = \frac{1}{2\pi}(-1)^m\int_{-\infty}^{\infty}h(\rho)\sum_{j=1}^{4}\frac{L_j\hat{A}_jn_je^{cn_j}}{{n_j}^2+{\alpha_m}^2}e^{-ih\rho}d\rho\ . \tag{99.b}$$

To calculate G_{21}; L_j, $\hat{A}_j$ and n_j are substituted. Then by using Maple the summation part is obtained as:

$$\sum_{j=1}^{4} \frac{L_j \hat{A}_j n_j}{(n_j{}^2+\alpha_m{}^2)e^{ih\rho}} = \frac{64AB\rho^2\alpha_m{}^2(\kappa-1)(\cosh 2Ac-\cosh 2Bc))}{q(\rho)(\beta(\kappa-1)-2i\rho)e^{ih\rho}} , \tag{100}$$

Substituting $h(\rho)$ and simplifying, one can find:

$$G_{21} = -\frac{4i(\kappa-1)\alpha_m{}^2}{\pi(\kappa+1)} \int_a^b g(t) \int_{-\infty}^{\infty} e^{it\rho} \frac{\rho}{q(\rho)e^{ih\rho}} d\rho \, dt. \tag{101}$$

Then G_{21} can be expressed as

$$G_{21} = -\frac{4i(\kappa-1)\alpha_m{}^2}{\pi(\kappa+1)} \int_a^b g(t) I_2(t) dt , \tag{102}$$

where

$$I_2(t) = \int_{-\infty}^{\infty} e^{it\rho} \frac{\rho}{q(\rho)e^{ih\rho}} d\rho = \int_{-\infty}^{\infty} F_2(\rho)\, d\rho , \tag{103}$$

and

$$F_2(\rho) = e^{it\rho} \frac{\rho}{q(\rho)e^{ih\rho}} . \tag{104}$$

$I_2(t)$ can be found by using Residue Theorem, but this time using the lower contour.

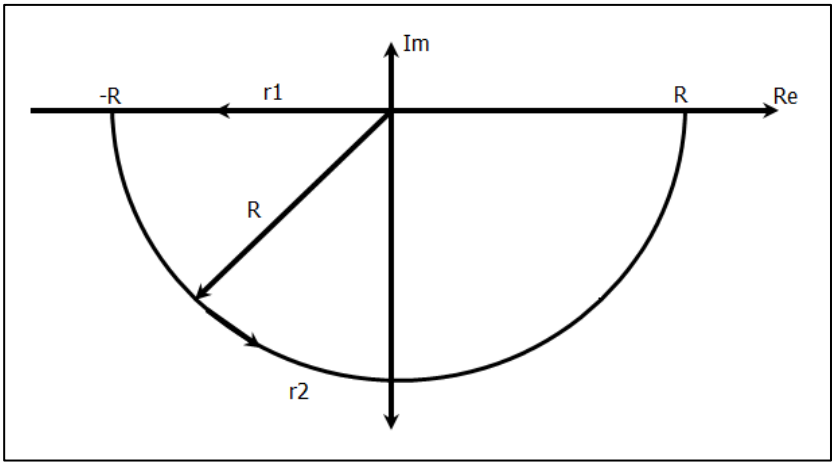

Figure 2.4 Lower contour for evaluation of the integral

$$\int_\Gamma F_2(\rho)d\rho = \lim_{R\to\infty} \int_{\Gamma_1} F_2(\rho)d\rho + \lim_{R\to\infty} \int_{\Gamma_2} F_2(\rho)d\rho \tag{105}$$

where $I_2(t) = -\lim_{R\to\infty} \int_{\Gamma_1} F_2(\rho)d\rho = -\lim_{R\to\infty} \int_R^{-R} F_2(\rho)d\rho = \int_{-\infty}^{\infty} F_2(\rho)d\rho$ will be found.

The second term in the summation in Eq. (105) is 0. When $Re^{i\theta}$ is substituted instead of ρ, similar to (89), the integrand contains *"R^2"* in the numerator while it contains *"R^4"* in the denominator. Therefore, the integral would vanish in the limit as $R \to \infty$.
Then,

$$\int_{-\infty}^{\infty} F_2(\rho)d\rho = -2\pi i(\sum Residue\ of\ F_2(\rho) in\ lower\ half\ plane) \tag{106}$$

Roots of $q(\rho)$ have already been found in (91.a-d).

$$I_2(t) = -2\pi i\big(Res\ F_2(\rho_1) + Res\ F_2(\rho_3)\big) \tag{107}$$

Remembering (94.a-d) and defining

$$\lambda_6 = e^{(\beta+\lambda_2)\left(\frac{t-h}{2}\right)}\ , \tag{108.a}$$

$$\lambda_7 = e^{(\beta+\lambda_3)\left(\frac{t-h}{2}\right)}\ , \tag{108.b}$$

$I_2(t)$ can be found by Maple (Appendix A) as:

$$I_2(t) = -\frac{2\pi}{\lambda_1}\left[\lambda_6\left(1+\frac{\beta}{\lambda_2}\right) - \lambda_7\left(1+\frac{\beta}{\lambda_3}\right)\right]. \tag{109}$$

Substituting (109) into (102)

$$G_{21} = \frac{8i(\kappa-1)\alpha_m{}^2}{\lambda_1(\kappa+1)}\int_a^b g(t)\left[\lambda_6\left(1+\frac{\beta}{\lambda_2}\right) - \lambda_7\left(1+\frac{\beta}{\lambda_3}\right)\right]dt\ . \tag{110}$$

By using Maple, G_{22} is found as zero. Therefore,

$$G_2 = G_{21} = \frac{8i(\kappa-1)\alpha_m{}^2}{\lambda_1(\kappa+1)}\int_a^b g(t)\left[\lambda_6\left(1+\frac{\beta}{\lambda_2}\right) - \lambda_7\left(1+\frac{\beta}{\lambda_3}\right)\right]dt\ . \tag{111}$$

Remembering equation (64), G_3 can be simplified as shown below:

$$G_3 = \frac{1}{2\pi}\int_{-\infty}^{\infty}\alpha_m\sum_{j=1}^{4}R_jA_j\left(\frac{(1-(-1)^m e^{cn_j})}{\alpha_m{}^2+n_j{}^2}\right)d\rho\ . \tag{112}$$

Then G_3 can be separated as

$$G_3 = \frac{1}{2\pi}\int_{-\infty}^{\infty}\alpha_m\sum_{j=1}^{4}R_jA_j\left(\frac{1}{\alpha_m{}^2+n_j{}^2}\right)d\rho - \frac{1}{2\pi}\int_{-\infty}^{\infty}\alpha_m(-1)^m\sum_{j=1}^{4}R_jA_j\left(\frac{e^{cn_j}}{\alpha_m{}^2+n_j{}^2}\right)d\rho\ . \tag{113}$$

In Eq. (113), first term is called G_{31} and second term is called G_{32}. Using Eq. (43) G_{31} and G_{32} can be written as:

$$G_{31} = \frac{1}{2\pi}\int_{-\infty}^{\infty}\alpha_m h(\rho)\sum_{j=1}^{4}\frac{R_j\hat{A}_j}{(\alpha_m)^2+n_j{}^2}d\rho\ , \tag{114.a}$$

$$G_{32} = -\frac{1}{2\pi}\int_{-\infty}^{\infty}\alpha_m(-1)^m h(\rho)\sum_{j=1}^{4}\frac{R_j\hat{A}_j e^{cn_j}}{(\alpha_m)^2+n_j{}^2}d\rho\ . \tag{114.b}$$

To calculate G_{31}; R_j, $\hat{A}_j$ and n_j are substituted. Then by using Maple the summation part is obtained as:

$$\sum_{j=1}^{4}\frac{R_j\hat{A}_j}{\alpha_m{}^2+n_j{}^2} = \frac{64AB\rho^2(\beta-i\rho)(\cosh 2Ac-\cosh 2Bc)}{q(\rho)(\beta(\kappa-1)-2i\rho)} \tag{115}$$

Substituting $h(\rho)$ and simplifying, one can find:

$$G_{31} = \frac{4i\alpha_m}{\pi(\kappa+1)}\int_a^b g(t)\int_{-\infty}^{\infty}e^{it\rho}\frac{(\beta-i\rho)\rho}{q(\rho)}d\rho dt\ . \tag{116}$$

Then G_{31} can be expressed as

$$G_{31} = \frac{4i\alpha_m}{\pi(\kappa+1)} \int_a^b g(t)\, I_3(t) dt \ , \tag{117}$$

where

$$I_3(t) = \int_{-\infty}^{\infty} e^{it\rho} \frac{(\beta - i\rho)\rho}{q(\rho)} d\rho = \int_{-\infty}^{\infty} F_3(\rho)\, d\rho \ , \tag{118}$$

and

$$F_3(\rho) = e^{it\rho} \frac{(\beta - i\rho)\rho}{q(\rho)} \ . \tag{119}$$

$I_3\,(t)$ can be found by using Residue Theorem and using the upper contour similar to $I_1(t)$.

$$\int_\Gamma F_3(\rho) d\rho = \lim_{R\to\infty} \int_{\Gamma_1} F_3(\rho) d\rho + \lim_{R\to\infty} \int_{\Gamma_2} F_3(\rho) d\rho \tag{120}$$

where $I_3(t) = \lim_{R\to\infty} \int_{\Gamma_1} F_3(\rho) d\rho = \lim_{R\to\infty} \int_{-R}^{R} F_3(\rho) d\rho = \int_{-\infty}^{\infty} F_3(\rho) d\rho$ will be found.

The second term in the summation in Eq. (120) is 0. When $Re^{i\theta}$ is substituted instead of ρ, the integrand contains *"R^3"* in the numerator while it contains *"R^4"* in the denominator. Therefore, the integral would vanish in the limit as $R \to \infty$.
Then,

$$\int_{-\infty}^{\infty} F_3(\rho) d\rho \ = 2\pi i (\sum Residue\ of\ F_3(\rho) in\ upper\ half\ plane) \tag{121}$$

Roots of $q(\rho)$ have already been found in (91.a-d)

$$I_3(t) = 2\pi i \big(Res\ F_3(\rho_2) + Res\ F_3(\rho_4) \big) \tag{122}$$

Remembering (94.a-d), $I_3(t)$ can be found by Maple (Appendix A) as:

$$I_3(t) = \frac{\pi i}{\lambda_1} \Big[-\frac{\lambda_4}{\lambda_2} (\lambda_1 + 4i{\alpha_m}^2) + \frac{\lambda_5}{\lambda_3} (-\lambda_1 + 4i{\alpha_m}^2) \Big] \tag{123}$$

Substituting (123) into (117)

$$G_{31} = \frac{-4\alpha_m}{\lambda_1(\kappa+1)} \int_a^b g(t) \Big[-\frac{\lambda_4}{\lambda_2} (\lambda_1 + 4i{\alpha_m}^2) + \frac{\lambda_5}{\lambda_3} (-\lambda_1 + 4i{\alpha_m}^2 \Big] dt \tag{124}$$

By using Maple, G_{32} is found as zero. Therefore,

$$G_3 = G_{31} = \frac{-4\alpha_m}{\lambda_1(\kappa+1)} \int_a^b g(t) \Big[-\frac{\lambda_4}{\lambda_2} (\lambda_1 + 4i{\alpha_m}^2) + \frac{\lambda_5}{\lambda_3} (-\lambda_1 + 4i{\alpha_m}^2 \Big] dt \tag{125}$$

Remembering Eq. (69), G_4 can be simplified as shown below:

$$G_4 = \frac{1}{2\pi} \int_{-\infty}^{\infty} \alpha_m \sum_{j=1}^{4} R_j A_j \Big(\frac{(1-(-1)^m e^{cn_j})}{(\alpha_m)^2 + {n_j}^2} \Big) e^{-ih\rho} d\rho \tag{126}$$

Then G_4 can be separated as

$$G_4 = \frac{1}{2\pi}\int_{-\infty}^{\infty} \alpha_m \sum_{j=1}^{4} R_j A_j \left(\frac{1}{(\alpha_m)^2+n_j{}^2}\right) e^{-ih\rho} d\rho - \frac{1}{2\pi}\int_{-\infty}^{\infty} \alpha_m (-1)^m \sum_{j=1}^{4} R_j A_j \left(\frac{e^{cn_j}}{(\alpha_m)^2+n_j{}^2}\right) e^{-ih\rho} d\rho \tag{127}$$

In Eq. (127), first term is called G_{41} and second term is called G_{42}. Using Eq. (43) G_{41} and G_{42} can be written as:

$$G_{41} = \frac{1}{2\pi}\int_{-\infty}^{\infty} \alpha_m h(\rho) \sum_{j=1}^{4} \frac{R_j \hat{A}_j}{\alpha_m{}^2+n_j{}^2} e^{-ih\rho} d\rho \ , \tag{128.a}$$

$$G_{42} = -\frac{1}{2\pi}\int_{-\infty}^{\infty} \alpha_m (-1)^m h(\rho) \sum_{j=1}^{4} \frac{R_j \hat{A}_j e^{cn_j}}{\alpha_m{}^2+n_j{}^2} e^{-ih\rho} d\rho \ . \tag{128.b}$$

To calculate G_{41}; R_j, $\hat{A}_j$ and n_j are substituted. Then by using Maple the summation part is obtained as:

$$\sum_{j=1}^{4} \frac{R_j \hat{A}_j}{(\alpha_m{}^2+n_j{}^2)e^{ih\rho}} = \frac{64AB\rho^2(\beta-i\rho)(\cosh 2Ac - \cosh 2Bc)}{q(\rho)(\beta(\kappa-1)-2i\rho)e^{ih\rho}} \tag{129}$$

$$G_{41} = \frac{4i\alpha_m}{\pi(\kappa+1)}\int_a^b g(t) \int_{-\infty}^{\infty} e^{it\rho} \frac{(\beta-i\rho)\rho}{q(\rho)e^{ih\rho}} d\rho dt \ . \tag{130}$$

Then G_{41} can be expressed as

$$G_{41} = \frac{4i\alpha_m}{\pi(\kappa+1)}\int_a^b g(t)\, I_4(t) dt \ , \tag{131}$$

where

$$I_4(t) = \int_{-\infty}^{\infty} e^{it\rho} \frac{(\beta-i\rho)\rho}{q(\rho)e^{ih\rho}} d\rho = \int_{-\infty}^{\infty} F_4(\rho)\, d\rho \ , \tag{132}$$

and

$$F_4(\rho) = e^{it\rho} \frac{(\beta-i\rho)\rho}{q(\rho)e^{ih\rho}} \ . \tag{133}$$

$I_4(t)$ can be found by using Residue Theorem and using the lower contour similar to $I_2(t)$.

$$\int_\Gamma F_4(\rho) d\rho = \lim_{R\to\infty} \int_{\Gamma_1} F_4(\rho) d\rho + \lim_{R\to\infty} \int_{\Gamma_2} F_4(\rho) d\rho \tag{134}$$

where $I_4(t) = -\lim_{R\to\infty} \int_{\Gamma_1} F_4(\rho) d\rho = -\lim_{R\to\infty} \int_R^{-R} F_4(\rho) d\rho = \int_{-\infty}^{\infty} F_4(\rho) d\rho$ will be found.

The second term in the summation in Eq. (134) is 0. When $Re^{i\theta}$ is substituted instead of ρ, the integrand contains *"R^3"* in the numerator while it contains *"R^4"* in the denominator. Therefore, the integral would vanish in the limit as $R \to \infty$.

Then,

$$\int_{-\infty}^{\infty} F_4(\rho) d\rho = -2\pi i (\sum Residue\ of\ F_4(\rho) in\ lower\ half\ plane) \tag{135}$$

Roots of $q(\rho)$ have already been found in (91.a-d).

$$I_4(t) = -2\pi i\big(Res\ F_4(\rho_1) + Res\ F_4(\rho_3)\big) \tag{136}$$

Remembering (94.a-b) and (108.a-b), $I_4(t)$ can be found by Maple (Appendix A) as:

$$I_4(t) = -\frac{\pi i}{\lambda_1}\left[\frac{\lambda_6}{\lambda_2}(\lambda_1 + 4i\alpha_m{}^2) - \frac{\lambda_7}{\lambda_3}(-\lambda_1 + 4i\alpha_m{}^2)\right] \tag{137}$$

Substituting (137) into (131)

$$G_{41} = \frac{4\alpha_m}{\lambda_1(\kappa+1)}\int_a^b g(t)\left[\frac{\lambda_6}{\lambda_2}(\lambda_1 + 4i\alpha_m{}^2) - \frac{\lambda_7}{\lambda_3}(-\lambda_1 + 4i\alpha_m{}^2)\right]dt \tag{138}$$

By using Maple, G_{42} is found as zero. Therefore,

$$G_4 = G_{41} = \frac{4\alpha_m}{\lambda_1(\kappa+1)}\int_a^b g(t)\left[\frac{\lambda_6}{\lambda_2}(\lambda_1 + 4i\alpha_m{}^2) - \frac{\lambda_7}{\lambda_3}(-\lambda_1 + 4i\alpha_m{}^2)\right]dt \tag{139}$$

Following equations can be expressed

$$G_1 = \int_a^b g(t)\,\hat{G}_1 dt \tag{140.a}$$

$$G_2 = \int_a^b g(t)\,\hat{G}_2 dt \tag{140.b}$$

$$G_3 = \int_a^b g(t)\,\hat{G}_3 dt \tag{140.c}$$

$$G_4 = \int_a^b g(t)\,\hat{G}_4 dt \tag{140.d}$$

where

$$\hat{G}_1 = \frac{8i(\kappa-1)\alpha_m{}^2}{\lambda_1(\kappa+1)}\left[\lambda_4\left(-1 + \frac{\beta}{\lambda_2}\right) + \lambda_5\left(1 - \frac{\beta}{\lambda_3}\right)\right] \tag{141.a}$$

$$\hat{G}_2 = \frac{8i(\kappa-1)\alpha_m{}^2}{\lambda_1(\kappa+1)}\left[\lambda_6\left(1 + \frac{\beta}{\lambda_2}\right) - \lambda_7\left(1 + \frac{\beta}{\lambda_3}\right)\right] \tag{141.b}$$

$$\hat{G}_3 = \frac{4\alpha_m}{\lambda_1(\kappa+1)}\left[\frac{\lambda_4}{\lambda_2}(\lambda_1 + 4i\alpha_m{}^2) - \frac{\lambda_5}{\lambda_3}(-\lambda_1 + 4i\alpha_m{}^2\right] \tag{141.c}$$

$$\hat{G}_4 = \frac{4\alpha_m}{\lambda_1(\kappa+1)}\left[\frac{\lambda_6}{\lambda_2}(\lambda_1 + 4i\alpha_m{}^2) - \frac{\lambda_7}{\lambda_3}(-\lambda_1 + 4i\alpha_m{}^2)\right] \tag{141.d}$$

Equations of $\hat{G}_j$ (141.a-d) have α_m as a multiplier. When $m = 0$, $\alpha_m = 0$ and accordingly $\hat{G}_j = 0$ and $\hat{B}_j = 0$. Therefore, the Fourier series start from one. Remembering Eqs. (50) and (63), $\hat{c}_m = c'_m = \frac{c}{2}$.

B_{1m} , B_{2m} , B_{3m} and B_{4m} can be written as follows:

$$B_{1m} = \int_a^b g(t)\,\hat{B}_{1m} dt \tag{142.a}$$

$$B_{2m} = \int_a^b g(t)\,\hat{B}_{2m} dt \tag{142.b}$$

$$B_{3m} = \int_a^b g(t)\,\hat{B}_{3m} dt \tag{142.c}$$

$$B_{4m} = \int_a^b g(t)\,\hat{B}_{4m} dt \tag{142.d}$$

where

$$\hat{B}_{1m} = \frac{\hat{\Delta}_1}{\hat{\Delta}} \tag{143.a}$$

$$\hat{B}_{2m} = \frac{\hat{\Delta}_2}{\hat{\Delta}} \tag{143.b}$$

$$\hat{B}_{3m} = \frac{\hat{\Delta}_3}{\hat{\Delta}} \tag{143.c}$$

$$\hat{B}_{4m} = \frac{\hat{\Delta}_4}{\hat{\Delta}} \tag{143.d}$$

and

$$\begin{aligned}\hat{\Delta}= \frac{c}{2}\,\{&(M_1M_2S_3S_4 + M_3M_4S_1S_2)\left[e^{h(p_2+p_4)} + e^{h(p_1+p_3)} - e^{h(p_2+p_3)} - e^{h(p_1+p_4)}\right] + \\ &(M_1M_3S_2S_4 + M_2M_4S_1S_3)\left[e^{h(p_2+p_3)} + e^{h(p_1+p_4)} - e^{h(p_3+p_4)} - e^{h(p_1+p_2)}\right] + \\ &(M_1M_4S_2S_3 + M_2M_3S_1S_4)\left[e^{h(p_3+p_4)} + e^{h(p_1+p_2)} - e^{h(p_2+p_4)} - e^{h(p_1+p_3)}\right]\}\end{aligned} \tag{144.a}$$

$$\begin{aligned}\hat{\Delta}_1= &\left(\hat{G}_1M_2S_3S_4 + \hat{G}_3M_3M_4S_2\right)\left[e^{h(p_2+p_3)} - e^{h(p_2+p_4)}\right] + \\ &\left(\hat{G}_1M_3S_2S_4 + \hat{G}_3M_2M_4S_3\right)\left[e^{h(p_3+p_4)} - e^{h(p_2+p_3)}\right] + \\ &\left(\hat{G}_1M_4S_2S_3 + \hat{G}_3M_2M_3S_4\right)\left[e^{h(p_2+p_4)} - e^{h(p_3+p_4)}\right] + \\ &\left(\hat{G}_2M_2S_3S_4 + \hat{G}_4M_3M_4S_2\right)[e^{hp_4} - e^{hp_3}] + \\ &\left(\hat{G}_2M_3S_2S_4 + \hat{G}_4M_2M_4S_3\right)[e^{hp_2} - e^{hp_4}] + \\ &\left(\hat{G}_2M_4S_2S_3 + \hat{G}_4M_2M_3S_4\right)[e^{hp_3} - e^{hp_2}]\end{aligned} \tag{144.b}$$

$$\begin{aligned}\hat{\Delta}_2= &\left(\hat{G}_1M_4S_1S_3 + \hat{G}_3M_1M_3S_4\right)\left[e^{h(p_3+p_4)} - e^{h(p_1+p_4)}\right] + \\ &\left(\hat{G}_1M_3S_1S_4 + \hat{G}_3M_1M_4S_3\right)\left[e^{h(p_1+p_3)} - e^{h(p_3+p_4)}\right] + \\ &\left(\hat{G}_1M_1S_3S_4 + \hat{G}_3M_3M_4S_1\right)\left[e^{h(p_1+p_4)} - e^{h(p_1+p_3)}\right] + \\ &\left(\hat{G}_2M_1S_3S_4 + \hat{G}_4M_3M_4S_1\right)[e^{hp_3} - e^{hp_4}] + \\ &\left(\hat{G}_2M_4S_1S_3 + \hat{G}_4M_1M_3S_4\right)[e^{hp_1} - e^{hp_3}] + \\ &\left(\hat{G}_2M_3S_1S_4 + \hat{G}_4M_1M_4S_3\right)[e^{hp_4} - e^{hp_1}]\end{aligned} \tag{144.c}$$

$$\begin{aligned}\hat{\Delta}_3= &\left(\hat{G}_1M_4S_1S_2 + \hat{G}_3M_1M_2S_4\right)\left[e^{h(p_1+p_4)} - e^{h(p_2+p_4)}\right] + \\ &\left(\hat{G}_1M_2S_1S_4 + \hat{G}_3M_1M_4S_2\right)\left[e^{h(p_2+p_4)} - e^{h(p_1+p_2)}\right] + \\ &\left(\hat{G}_1M_1S_2S_4 + \hat{G}_3M_2M_4S_1\right)\left[e^{h(p_1+p_2)} - e^{h(p_1+p_4)}\right] + \\ &\left(\hat{G}_2M_4S_1S_2 + \hat{G}_4M_1M_2S_4\right)[e^{hp_2} - e^{hp_1}] + \\ &\left(\hat{G}_2M_1S_2S_4 + \hat{G}_4M_2M_4S_1\right)[e^{hp_4} - e^{hp_2}] + \\ &\left(\hat{G}_2M_2S_1S_4 + \hat{G}_4M_1M_4S_2\right)[e^{hp_1} - e^{hp_4}]\end{aligned} \tag{144.d}$$

$$\begin{aligned}\hat{\Delta}_4= &\left(\hat{G}_1M_3S_1S_2 + \hat{G}_3M_1M_2S_3\right)\left[e^{h(p_2+p_3)} - e^{h(p_1+p_3)}\right] + \\ &\left(\hat{G}_1M_2S_1S_3 + \hat{G}_3M_1M_3S_2\right)\left[e^{h(p_1+p_2)} - e^{h(p_2+p_3)}\right] + \\ &\left(\hat{G}_1M_1S_2S_3 + \hat{G}_3M_2M_3S_1\right)\left[e^{h(p_1+p_3)} - e^{h(p_1+p_2)}\right] + \\ &\left(\hat{G}_2M_3S_1S_2 + \hat{G}_4M_1M_2S_3\right)[e^{hp_1} - e^{hp_2}] + \\ &\left(\hat{G}_2M_2S_1S_3 + \hat{G}_4M_1M_3S_2\right)[e^{hp_3} - e^{hp_1}] + \\ &\left(\hat{G}_2M_1S_2S_3 + \hat{G}_4M_2M_3S_1\right)[e^{hp_2} - e^{hp_3}]\end{aligned} \tag{144.e}$$

At this point, the only remaining unknown is the auxiliary function *g(t)*. By applying the so far unused boundary condition (23.b) along with Eqs. (22.b), (43.a-d) and (142.a-d) a singular integral equation is obtained.

2.4 Derivation of the Singular Integral Equation

The last boundary condition (23.b) is repeated below.

$\sigma_{yy}(x,0) = -p(x) \qquad 0<x<b$

Substituting Eq. (22.b) into (23.b) along with (43.a-d) and (142.a-d), the following singular integral equation is obtained where the only unknown is *g(t)*.

$$\int_a^b \big(h_1(x,t) + h_2(x,t)\big) g(t)dt = -\frac{p(x)(\kappa-1)}{\mu(x)} \tag{145}$$

In (145),

$$h_1(x,t) = \lim_{y\to 0}\left\{\frac{1}{2\pi}\int_{-\infty}^{\infty} K_1(y,\rho)e^{i\rho(t-x)}d\rho\right\} \tag{146}$$

$$K_1(y,\rho) = \frac{i[K_{11}(y,\rho)-K_{12}(y,\rho)-K_{13}(y,\rho)+K_{14}(y,\rho)]}{2\rho\left(\frac{4ABD}{E}\right)(\cosh(2Ac)-\cosh(2Bc))} \tag{147}$$

$$K_{11}(y,\rho) = \big((\kappa+1)n_1(\rho) - i\rho(3-\kappa)m_1(\rho)\big)(m_2n_2 - i\rho)e^{n_1y}(e^{2Ac} - e^{2Bc}) \tag{148.a}$$

$$K_{12}(y,\rho) = \big((\kappa+1)n_2(\rho) - i\rho(3-\kappa)m_2(\rho)\big)(m_1n_1 - i\rho)e^{n_2y}(e^{-2Ac} - e^{2Bc}) \tag{148.b}$$

$$K_{13}(y,\rho) = \big((\kappa+1)n_3(\rho) - i\rho(3-\kappa)m_3(\rho)\big)(m_1n_1 - i\rho)e^{n_3y}(e^{2Ac} - e^{-2Bc}) \tag{148.c}$$

$$K_{14}(y,\rho) = \big((\kappa+1)n_4(\rho) - i\rho(3-\kappa)m_4(\rho)\big)(m_2n_2 - i\rho)e^{n_4y}(e^{-2Ac} - e^{-2Bc}) \tag{148.d}$$

$$h_2(x,t) = \lim_{y\to 0}\{\textstyle\sum_{n=1}^{\infty} K_2(x,t,\alpha_n)\cos(\alpha_n,y)\} \tag{149}$$

$$K_2(x,t,\alpha_n) = \textstyle\sum_{j=1}^{4}\big[(3-\kappa)p_j(\alpha_n)q_j(\alpha_n) + (\kappa+1)\alpha_n\big]\hat{B}_{jm}(\alpha_n)e^{p_jx} \tag{150}$$

In this study, the integral equation (145) will only be solved for edge crack problem by setting *a=0* since this case is more realistic than the imbedded crack problem. First, singular behavior of kernels $h_1(x, t)$ and $h_2(x, t)$ should be determined. This is done by making an asymptotic analysis such that the behavior of kernel K_1 should be determined as $\rho \to \infty$ and the behavior of kernel K_2 should be determined as $\alpha_n \to \infty$. Then the asymptotic terms can be added and subtracted as follows:

$$\int K_1 d\rho = \int (K_1 - K_1{}^{\infty}) d\rho + \int K_1{}^{\infty} d\rho \ , \tag{151.a}$$

$$\sum K_2 = \sum (K_2 - K_2{}^{\infty}) + \sum K_2{}^{\infty} \ . \tag{151.b}$$

By doing so, the first terms can be evaluated numerically whereas the second terms can be obtained in closed form. Furthermore, the second term of Eq. (151.a) gives the singular behavior of the integral equation.

The asymptotic analysis which has been done in [12] is valid for $K_1(y,\rho)$. In the forthcoming sections main steps of the asymptotic analysis are given.

First the limits of integration $h_1(x, t)$, (146), are modified such that the integral is taken in (0, ∞) rather than (-∞, ∞).

Knowing that, $e^{i\rho(t-x)} = cos\big(\rho(t-x)\big) + isin(\rho(t-x))$, (146) can be expressed as

$$h_1(x,t) = \lim_{y\to 0} \left\{ \frac{1}{2\pi} \int_0^{\infty} M(y,\rho) \cos\big(\rho(t-x)\big)\, d\rho + \frac{1}{2\pi} \int_0^{\infty} N(y,\rho) \sin\big(\rho(t-x)\big)\, d\rho \right\} , \tag{152}$$

where

$$M(y,\rho) = K_1(y,\rho) + K_1(y,-\rho), \tag{153}$$

and

$$N(y,\rho) = i(K_1(y,\rho) - K_1(y,-\rho)). \tag{154}$$

Numerator of (147) can be called $R(\rho)$,

$$i[K_{11}(y,\rho) - K_{12}(y,\rho) - K_{13}(y,\rho) + K_{14}(y,\rho)] = R(\rho). \tag{155}$$

Defining,

$$T1(\rho) = ((\kappa+1)n_1(\rho) - i\rho(3-\kappa)m_1(\rho))(m_2 n_2 - i\rho) \ , \tag{156}$$

and

$$T2(\rho) = ((\kappa+1)n_2(\rho) - i\rho(3-\kappa)m_2(\rho))(m_1 n_1 - i\rho) \ , \tag{157}$$

(148.a-d) can be rewritten as following and $R(\rho)$ can be simplified.

$$K_{11}(y,\rho) = T1(\rho) e^{n_1 y}(e^{2Ac} - e^{2Bc}) \ , \tag{158.a}$$

$$K_{12}(y,\rho) = T2(\rho) e^{n_2 y}(e^{-2Ac} - e^{2Bc}) \ , \tag{158.b}$$

$$K_{13}(y,\rho) = -T2(\rho) e^{n_3 y}(e^{2Ac} - e^{-2Bc}) \ , \tag{158.c}$$

$$K_{14}(y,\rho) = -T1(\rho) e^{n_4 y}(e^{-2Ac} - e^{-2Bc}) \ , \tag{158.d}$$

$$\begin{aligned} R(\rho) = i[&T1(\rho) e^{n_1 y}(e^{2Ac} - e^{2Bc}) - T2(\rho) e^{n_2 y}(e^{-2Ac} - e^{2Bc}) \\ &+ T2(\rho) e^{n_3 y}(e^{2Ac} - e^{-2Bc}) - T1(\rho) e^{n_4 y}(e^{-2Ac} - e^{-2Bc})] \ . \end{aligned} \tag{159.a}$$

Using the relation given in (32.a-d), $R(\rho)$ can be rearranged as following.

$$R(\rho) = i[T1(\rho)(e^{n_1 y+2Ac} - e^{n_1 y+2Bc} - e^{-n_1 y-2Ac} + e^{-n_1 y-2Bc}) \\ -T2(\rho)(e^{n_2 y-2Ac} - e^{n_2 y+2Bc} - e^{-n_2 y+2Ac} + e^{-n_2 y-2Bc})] \ . \tag{159.b}$$

Inserting $R(\rho)$, $K_1(y,\rho)$ can be written as,

$$K_1(y,\rho) = \frac{R(\rho)}{2\rho\left(\frac{4ABD}{E}\right)(\cosh(2Ac)-\cosh(2Bc))} \ . \tag{160}$$

Using Eqs. (33.a-b), Eq. (160) can be expressed as,

$$K_1(y,\rho) = \frac{R(\rho)}{\rho\left(\frac{4ABD}{E}\right)(\mathrm{e}^{2Ac}+e^{-2Ac}-\mathrm{e}^{2Bc}-e^{-2Bc})} \ . \tag{161}$$

Expanding $R(\rho)$,

$$K_1(y,\rho) = \frac{iT1(\rho)(e^{n_1 y+2Ac}-e^{n_1 y+2Bc}-e^{-n_1 y-2Ac}+e^{-n_1 y-2Bc})}{\rho\left(\frac{4ABD}{E}\right)(\mathrm{e}^{2Ac}+e^{-2Ac}-\mathrm{e}^{2Bc}-e^{-2Bc})} \\ -\frac{iT2(\rho)(e^{n_2 y-2Ac}-e^{n_2 y+2Bc}-e^{-n_2 y+2Ac}+e^{-n_2 y-2Bc})}{\rho\left(\frac{4ABD}{E}\right)(\mathrm{e}^{2Ac}+e^{-2Ac}-\mathrm{e}^{2Bc}-e^{-2Bc})} \tag{162}$$

Defining,

$$T3(\rho) = \rho\left(\frac{4ABD}{E}\right) \tag{163.a}$$

$$T1T3(\rho) = \frac{iT1(\rho)}{T3(\rho)} \tag{163.b}$$

$$T2T3(\rho) = \frac{iT2(\rho)}{T3(\rho)} \tag{163.c}$$

Substituting (163.a-c), $K_1(y,\rho)$ can be written as,

$$K_1(y,\rho) = T1T3(\rho)\frac{(e^{n_1 y+2Ac}-e^{n_1 y+2Bc}-e^{-n_1 y-2Ac}+e^{-n_1 y-2Bc})}{(\mathrm{e}^{2Ac}+e^{-2Ac}-\mathrm{e}^{2Bc}-e^{-2Bc})} \\ -T2T3(\rho)\frac{(e^{n_2 y-2Ac}-e^{n_2 y+2Bc}-e^{-n_2 y+2Ac}+e^{-n_2 y-2Bc})}{(\mathrm{e}^{2Ac}+e^{-2Ac}-\mathrm{e}^{2Bc}-e^{-2Bc})} \tag{164}$$

Exponential terms in (164) are reduced to,

$$\frac{e^{n_1 y+2Ac}-e^{n_1 y+2Bc}-e^{-n_1 y-2Ac}+e^{-n_1 y-2Bc}}{\mathrm{e}^{2Ac}+e^{-2Ac}-\mathrm{e}^{2Bc}-e^{-2Bc}} = \frac{e^{B(2c-y)}e^{-Ay}}{e^{2Bc}} = e^{-By-Ay} \ , \tag{165.a}$$

and

$$\frac{e^{n_2 y-2Ac}-e^{n_2 y+2Bc}-e^{-n_2 y+2Ac}+e^{-n_2 y-2Bc}}{\mathrm{e}^{2Ac}+e^{-2Ac}-\mathrm{e}^{2Bc}-e^{-2Bc}} = \frac{e^{B(2c-y)}e^{Ay}}{e^{2Bc}} = e^{-By+Ay} \ . \tag{165.b}$$

Finally, $K_1(y,\rho)$ can be expressed as,

$$K_1(y,\rho) = T1T3(\rho)e^{-B(\rho)y-Ay} - T2T3(\rho)e^{-B(\rho)y+Ay} \ . \tag{166}$$

Similarly $K_1(y,-\rho)$ can be expressed as,

$$K_1(y,-\rho) = T1T3(-\rho)e^{-B(-\rho)y-Ay} - T2T3(-\rho)e^{-B(-\rho)y+Ay} \ . \tag{167}$$

When asymptotic analysis is applied to B as $\rho \to \infty$ the following results can be obtained

$$B^{\infty}(\rho) \cong -\rho - \frac{i\beta}{2} \ , \tag{168.a}$$

and

$$B^{\infty}(-\rho) \cong -\rho + \frac{i\beta}{2} \ . \tag{168.b}$$

Therefore,

$$M^{\infty}(y,\rho) \cong T1T3^{\infty}(\rho)e^{-\rho y-\frac{i\beta y}{2}-Ay} - T2T3^{\infty}(\rho)e^{-\rho y-\frac{i\beta y}{2}+Ay}$$
$$+T1T3^{\infty}(-\rho)e^{-\rho y+\frac{i\beta y}{2}-Ay} - T2T3^{\infty}(-\rho)e^{-\rho y+\frac{i\beta y}{2}+Ay} \tag{169.a}$$

Exponential terms can be simplified to $e^{-\rho y}$ when $\rho \to \infty$.

$$M^{\infty}(y,\rho) \cong [T1T3^{\infty}(\rho) - T2T3^{\infty}(\rho) + T1T3^{\infty}(-\rho) - T2T3^{\infty}(-\rho)]e^{-\rho y} \tag{169.b}$$

$$M^{\infty}(y,\rho) \cong \left(\frac{b_1}{\rho} + \frac{b_3}{\rho^3} + \frac{b_5}{\rho^5} + \frac{b_7}{\rho^7} + \frac{b_9}{\rho^9} + \frac{b_{11}}{\rho^{11}} + O(\frac{1}{\rho^{13}})\right) e^{-\rho y} \tag{169.c}$$

$$N^{\infty}(y,\rho) \cong i\left[T1T3^{\infty}(\rho)e^{-\rho y-\frac{i\beta y}{2}-Ay} - T2T3^{\infty}(\rho)e^{-\rho y-\frac{i\beta y}{2}+Ay}\right.$$
$$\left.-T1T3^{\infty}(-\rho)e^{-\rho y+\frac{i\beta y}{2}-Ay} + T2T3^{\infty}(-\rho)e^{-\rho y+\frac{i\beta y}{2}+Ay}\right] \tag{170.a}$$

Similarly,

$$N^{\infty}(y,\rho) \cong i[T1T3^{\infty}(\rho) - T2T3^{\infty}(\rho) - T1T3^{\infty}(-\rho) + T2T3^{\infty}(-\rho)]e^{-\rho y} \tag{170.b}$$

$$N^{\infty}(y,\rho) \cong \left(c_0 + \frac{c_2}{\rho^2} + \frac{c_4}{\rho^4} + \frac{c_6}{\rho^6} + \frac{c_8}{\rho^8} + \frac{c_{10}}{\rho^{10}} + \frac{c_{12}}{\rho^{12}} + O(\frac{1}{\rho^{14}})\right) e^{-\rho y} \tag{170.c}$$

$O(\frac{1}{\rho^{13}})$ and $O(\frac{1}{\rho^{14}})$ denote the terms of the order ρ^{-13} and ρ^{-14} respectively. The leading terms of $M(y,\rho)$ and $N(y,\rho)$ are expressed as follows.

$$b_1 = \frac{4\beta(\kappa-1)}{\kappa+1} \tag{171.a}$$

$$c_0 = \frac{8(\kappa-1)}{\kappa+1} \tag{171.b}$$

The other terms in the asymptotic expansion are given in Appendix C. First, c_0 will be extracted from $h_1(x,t)$ to obtain the Cauchy singularity. Therefore, $h_1(x,t)$ will be written in the following form.

$$h_1(x,t) = \lim_{y\to 0}\left\{\frac{1}{2\pi}\int_0^{\infty} M(y,\rho)\cos\big(\rho(t-x)\big)\,d\rho\right.$$
$$+\frac{1}{2\pi}\int_0^{\infty}(N(y,\rho) - e^{-\rho y}c_0)\sin\big(\rho(t-x)\big)\,d\rho$$
$$\left.+\frac{1}{2\pi}\lim_{y\to 0}\int_0^{\infty} e^{-\rho y}c_0\sin\big(\rho(t-x)\big)\,d\rho\right\} \tag{172}$$

Last term in (172) can be evaluated as follows.

$$\frac{1}{2\pi}\int_0^\infty e^{-\rho y} c_0 \sin\big(\rho(t-x)\big)\, d\rho = \frac{c_0}{2\pi}\frac{t-x}{y^2+(t-x)^2} \tag{173}$$

As $y \to 0$ right hand side of Eq. (173) becomes $\frac{c_0}{2\pi}\frac{1}{t-x}$ which is the Cauchy Singularity. By taking the limit Eq. (172) reduces to:

$$\begin{aligned} h_1(x,t) = {} & \frac{c_0}{2\pi}\frac{1}{t-x} + \frac{1}{2\pi}\int_0^\infty (N(0,\rho)-c_0)\sin\big(\rho(t-x)\big)\, d\rho \\ & + \frac{1}{2\pi}\int_0^\infty M(0,\rho)\cos\big(\rho(t-x)\big)\, d\rho \end{aligned} \tag{174}$$

2nd and 3rd terms of (174) are reorganized such that the limits of the integrals are from 0 to F, G and from F, G to ∞. Then approximate values obtained from asymptotic analysis are subtracted and added.

$$\begin{aligned} h_1(x,t) = {} & \frac{c_0}{2\pi}\frac{1}{t-x} + \frac{1}{2\pi}\int_0^F (N(0,\rho)-c_0)\sin\big(\rho(t-x)\big)\, d\rho \\ & + \frac{1}{2\pi}\int_F^\infty \left(N(0,\rho)-c_0-\frac{c_2}{\rho^2}-\frac{c_4}{\rho^4}-\frac{c_6}{\rho^6}-\frac{c_8}{\rho^8}-\frac{c_{10}}{\rho^{10}}-\frac{c_{12}}{\rho^{12}}\right)\sin\big(\rho(t-x)\big)\, d\rho \\ & + \frac{1}{2\pi}\int_F^\infty \left(\frac{c_2}{\rho^2}+\frac{c_4}{\rho^4}+\frac{c_6}{\rho^6}+\frac{c_8}{\rho^8}+\frac{c_{10}}{\rho^{10}}+\frac{c_{12}}{\rho^{12}}\right)\sin\big(\rho(t-x)\big)\, d\rho \\ & + \frac{1}{2\pi}\int_0^G M(0,\rho)\cos\big(\rho(t-x)\big)\, d\rho \\ & + \frac{1}{2\pi}\int_G^\infty \left(M(0,\rho)-\frac{b_1}{\rho}-\frac{b_3}{\rho^3}-\frac{b_5}{\rho^5}-\frac{b_7}{\rho^7}-\frac{b_9}{\rho^9}-\frac{b_{11}}{\rho^{11}}\right)\cos\big(\rho(t-x)\big)\, d\rho \\ & + \frac{1}{2\pi}\int_G^\infty \left(\frac{b_1}{\rho}+\frac{b_3}{\rho^3}+\frac{b_5}{\rho^5}+\frac{b_7}{\rho^7}+\frac{b_9}{\rho^9}+\frac{b_{11}}{\rho^{11}}\right)\cos\big(\rho(t-x)\big)\, d\rho \end{aligned} \tag{175}$$

For sufficiently large F and G, 3rd and 6th terms of (175) are small enough to be neglected.

$$\frac{1}{2\pi}\int_F^\infty \left(N(0,\rho)-c_0-\frac{c_2}{\rho^2}-\frac{c_4}{\rho^4}-\frac{c_6}{\rho^6}-\frac{c_8}{\rho^8}-\frac{c_{10}}{\rho^{10}}-\frac{c_{12}}{\rho^{12}}\right)\sin\big(\rho(t-x)\big)\, d\rho \approx 0 \tag{176}$$

$$\frac{1}{2\pi}\int_G^\infty \left(M(0,\rho)-\frac{b_1}{\rho}-\frac{b_3}{\rho^3}-\frac{b_5}{\rho^5}-\frac{b_7}{\rho^7}-\frac{b_9}{\rho^9}-\frac{b_{11}}{\rho^{11}}\right)\cos\big(\rho(t-x)\big)\, d\rho \approx 0 \tag{177}$$

Then $h_1(x,t)$ can be written as:

$$\begin{aligned} h_1(x,t) = {} & \frac{c_0}{2\pi}\frac{1}{t-x} + \frac{1}{2\pi}\int_0^F (N(0,\rho)-c_0)\sin\big(\rho(t-x)\big)\, d\rho \\ & + \frac{1}{2\pi}\int_F^\infty \left(\frac{c_2}{\rho^2}+\frac{c_4}{\rho^4}+\frac{c_6}{\rho^6}+\frac{c_8}{\rho^8}+\frac{c_{10}}{\rho^{10}}+\frac{c_{12}}{\rho^{12}}\right)\sin\big(\rho(t-x)\big)\, d\rho \\ & + \frac{1}{2\pi}\int_0^G M(0,\rho)\cos\big(\rho(t-x)\big)\, d\rho \\ & + \frac{1}{2\pi}\int_G^\infty \frac{b_1}{\rho}\cos\big(\rho(t-x)\big)\, d\rho \\ & + \frac{1}{2\pi}\int_G^\infty \left(\frac{b_3}{\rho^3}+\frac{b_5}{\rho^5}+\frac{b_7}{\rho^7}+\frac{b_9}{\rho^9}+\frac{b_{11}}{\rho^{11}}\right)\cos\big(\rho(t-x)\big)\, d\rho \end{aligned} \tag{178}$$

In (178) 2nd and 4th terms can be evaluated numerically using Gauss-Legendre Quadrature Method while 3rd and 5th terms will be evaluated using the closed form expressions [12] given in Appendix B.

$$\begin{aligned} h_1(x,t) \approx {} & \frac{c_0}{2\pi}\frac{1}{t-x} - \frac{b_1}{2\pi}\log|t-x| - \frac{b_1}{2\pi}\big(Ci\big(G(t-x)\big)-\log|t-x|\big) \\ & + \frac{1}{2\pi}\int_0^F (N(0,\rho)-c_0)\sin\big(\rho(t-x)\big)\, d\rho + \frac{1}{2\pi}\int_0^G M(0,\rho)\cos\big(\rho(t-x)\big)\, d\rho \\ & + \frac{1}{2\pi}\int_F^\infty \left(\frac{c_2}{\rho^2}+\frac{c_4}{\rho^4}+\frac{c_6}{\rho^6}+\frac{c_8}{\rho^8}+\frac{c_{10}}{\rho^{10}}+\frac{c_{12}}{\rho^{12}}\right)\sin\big(\rho(t-x)\big)\, d\rho \\ & + \frac{1}{2\pi}\int_G^\infty \left(\frac{b_3}{\rho^3}+\frac{b_5}{\rho^5}+\frac{b_7}{\rho^7}+\frac{b_9}{\rho^9}+\frac{b_{11}}{\rho^{11}}\right)\cos\big(\rho(t-x)\big)\, d\rho \end{aligned} \tag{179}$$

Now $h_1(x,t)$ can be used for numerical computation.

Singular behavior of unknown function $g(t)$ changes in the case of edge crack where $a=0$. $h_2(x,t)$ becomes unbounded as x and t simultaneously approach 0. Therefore, for small values of x and t, an asymptotic analysis is needed as $\alpha_n \to \infty$ to calculate the kernel $h_2(x,t)$ accurately.

$$\begin{aligned} h_2(x,t) = \lim_{y\to 0}\Big[\Big\{\sum_{n=1}^{\infty}[(3-\kappa)p_1(\alpha_n)q_1(\alpha_n)+(\kappa+1)\alpha_n]\hat{B}_{1n}(\alpha_n)e^{p_1 x} \\ +[(3-\kappa)p_2(\alpha_n)q_2(\alpha_n)+(\kappa+1)\alpha_n]\hat{B}_{2n}(\alpha_n)e^{p_2 x} \\ +[(3-\kappa)p_3(\alpha_n)q_3(\alpha_n)+(\kappa+1)\alpha_n]\hat{B}_{3n}(\alpha_n)e^{p_3 x} \\ +[(3-\kappa)p_4(\alpha_n)q_4(\alpha_n)+(\kappa+1)\alpha_n]\hat{B}_{4n}(\alpha_n)e^{p_4 x} \\ -K_2{}^{\infty}(x,t,\alpha_n)\Big\}\cos(\alpha_n y)+\sum_{n=1}^{\infty}K_2{}^{\infty}(x,t,\alpha_n)\cos(\alpha_n y)\Big] \end{aligned} \tag{180}$$

where

$$K_2{}^{\infty}(x,t,\alpha_n) \approx \left[a_2\alpha_n{}^2 + a_1\alpha_n + a_0 + \frac{a_{-1}}{\alpha_n}\right]e^{-\alpha_n(t+x)+\frac{\beta(t-x)}{2}} \tag{181}$$

Note that $K_2{}^{\infty}(x,t,\alpha_n)$ gives asymptotic behavior of $K_2(x,t,\alpha_n)$ as $\alpha_n \to \infty$.

Terms a_i have been found earlier to be used in [36]. Since the behavior of Kernels are the same as $\alpha_n \to \infty$, they can also be used in this study and are given in Appendix C.

First summation group of (180) can be calculated by taking the limit and then summing the series until the terms start to be negligible.

$$h_2(x,t) \approx \lim_{y\to 0}\Big\{\sum_{n=1}^{\infty}K_2{}^{\infty}(x,t,\alpha_n)\cos(\alpha_n y)\Big\} + \sum_{n=1}^{H}[K_2(x,t,\alpha_n) - K_2{}^{\infty}(x,t,\alpha_n)] \tag{182}$$

H is an integer large enough for convergence of series. First term of (182) can be calculated using following formulae:

$$S_{-1}(\theta,\eta) = \sum_{n=1}^{\infty}\frac{1}{n}e^{-n\theta}\cos(n\eta) = -\frac{1}{2}\ln(2\cosh(\theta) - 2\cosh(\eta)) - \frac{1}{2}\theta\ , \tag{183.a}$$

$$S_0(\theta,\eta) = \sum_{n=1}^{\infty}e^{-n\theta}\cos(n\eta) = \frac{\sinh(\theta)}{2\cosh(\theta)-2\cos(\eta)} - \frac{1}{2}\ , \tag{183.b}$$

$$S_1(\theta,\eta) = \sum_{n=1}^{\infty}ne^{-n\theta}\cos(n\eta) = \frac{\cosh(\theta)}{2\cosh(\theta)-2\cos(\eta)} + 2\left(\frac{\sinh(\theta)}{2\cosh(\theta)-2\cos(\eta)}\right)^2\ , \tag{183.c}$$

$$\begin{aligned} S_2(\theta,\eta) = \sum_{n=1}^{\infty}n^2e^{-n\theta}\cos(n\eta) = \frac{\sinh(\theta)}{2\cosh(\theta)-2\cos(\eta)} \\ -6\frac{\cosh(\theta)}{(2\cosh(\theta)-\cos(\eta))^2}\sinh(\theta) + \left(\frac{\sinh(\theta)}{2\cosh(\theta)-2\cos(\eta)}\right)^3\ . \end{aligned} \tag{183.d}$$

Using (183.a-d) $h_2(x,t)$ can be written as,

$$h_2(x,t) \approx \left[a_2\left(\frac{\pi}{c}\right)^2 S_2\left(\frac{\pi(t+x)}{c},0\right) + a_1\frac{\pi}{c}S_1\left(\frac{\pi(t+x)}{c},0\right) + a_0 S_0\left(\frac{\pi(t+x)}{c},0\right) + \frac{a_{-1}}{\pi/c}S_{-1}\left(\frac{\pi(t+x)}{c},0\right)\right] e^{\frac{\beta(t-x)}{2}} + \sum_{n=1}^{H}[K_2(x,t,\alpha_n) - K_2{}^{\infty}(x,t,\alpha_n)] \ . \tag{184}$$

By substituting $h_1(x,t)$ and $h_2(x,t)$ into (145), singular integral equation can be expressed as follows:

$$\frac{1}{\pi}\int_a^b g(t)\left\{\frac{1}{t-x} - \frac{b_1}{c_0}\log|t-x| - \frac{b_1}{c_0}\left(Ci\big(G(t-x)\big) - \log|t-x|\right) + \frac{1}{c_0}\int_F^{\infty}\left(\frac{c_2}{\rho^2}+\frac{c_4}{\rho^4}+\frac{c_6}{\rho^6}+\frac{c_8}{\rho^8}+\frac{c_{10}}{\rho^{10}}+\frac{c_{12}}{\rho^{12}}\right)\sin\big(\rho(t-x)\big)\,d\rho + \frac{1}{c_0}\int_G^{\infty}\left(\frac{b_3}{\rho^3}+\frac{b_5}{\rho^5}+\frac{b_7}{\rho^7}+\frac{b_9}{\rho^9}+\frac{b_{11}}{\rho^{11}}\right)\cos\big(\rho(t-x)\big)\,d\rho + \frac{1}{c_0}\int_0^F (N(0,\rho)-c_0)\sin\big(\rho(t-x)\big)\,d\rho + \frac{1}{c_0}\int_0^G M(0,\rho)\cos\big(\rho(t-x)\big)\,d\rho + \frac{2\pi}{c_0}e^{\frac{\beta(t-x)}{2}}\sum_{k=-1}^{2} a_k\left(\frac{\pi}{c}\right)^k S_k\left(\frac{\pi(t+x)}{c},0\right) + \frac{2\pi}{c_0}\sum_{n=1}^{H}[K_2(x,t,\alpha_n) - K_2{}^{\infty}(x,t,\alpha_n)]\right\}dt = -2\frac{p(x)(\kappa-1)}{c_0\mu(x)} \tag{185}$$

The interval $a < x < b$ can be normalized by defining:

$$x = \frac{b-a}{2}r + \frac{b+a}{2}\ , \quad \text{where } -1 \le r \le 1\ , \tag{186.a}$$

$$t = \frac{b-a}{2}s + \frac{b+a}{2}\ , \quad \text{where } -1 \le s \le 1\ . \tag{186.b}$$

Using (186.b),

$$dt = \frac{b-a}{2}ds \tag{187}$$

By using (186-187), the singular integral equation can be written as follows:

$$\frac{1}{\pi}\int_{-1}^{1} G(s)\left\{\frac{2}{b-a}\frac{1}{s-r} - \frac{b_1}{c_0}\log|s-r| - \frac{b_1}{c_0}\left(Ci\left(G\left(\frac{b-a}{2}(s-r)\right)\right) - \log|s-r|\right) + \frac{1}{c_0}\int_F^{\infty}\left(\frac{c_2}{\rho^2}+\frac{c_4}{\rho^4}+\frac{c_6}{\rho^6}+\frac{c_8}{\rho^8}+\frac{c_{10}}{\rho^{10}}+\frac{c_{12}}{\rho^{12}}\right)\sin\left(\rho\left(\frac{b-a}{2}(s-r)\right)\right)d\rho + \frac{1}{c_0}\int_G^{\infty}\left(\frac{b_3}{\rho^3}+\frac{b_5}{\rho^5}+\frac{b_7}{\rho^7}+\frac{b_9}{\rho^9}+\frac{b_{11}}{\rho^{11}}\right)\cos\left(\rho\left(\frac{b-a}{2}(s-r)\right)\right)d\rho + \frac{1}{c_0}\int_0^F (N(0,\rho)-c_0)\sin\left(\rho\left(\frac{b-a}{2}(s-r)\right)\right)d\rho + \frac{1}{c_0}\int_0^G M(0,\rho)\cos\left(\rho\left(\frac{b-a}{2}(s-r)\right)\right)d\rho + \frac{2\pi}{c_0}e^{\frac{\beta(\frac{b-a}{2}(s-r))}{2}}\sum_{k=-1}^{2} a_k\left(\frac{\pi}{c}\right)^k S_k\left(\frac{\pi\left(\frac{b-a}{2}(s+r)+a+b\right)}{c},0\right) + \frac{2\pi}{c_0}\sum_{n=1}^{H}[K_2(x(r),t(s),\alpha_n) - K_2{}^{\infty}(x(r),t(s),\alpha_n)]\right\}\frac{b-a}{2}ds \ = -2\frac{p(x(r))(\kappa-1)}{c_0\mu(x(r))} \tag{188}$$

where

$$G(s) = g(t(s))\ . \tag{189.a}$$

The expression of G(s) for an edge crack is written as

$$G(s) = \varphi(s)\frac{1}{\sqrt{1-s}} \tag{189.b}$$

where $\varphi(s)$ can be written in terms of an infinite series of Jacobi polynomials.

$$\varphi(s) = \sum_{n=0}^{\infty} C_n P_n^{(\alpha,\beta)}(s). \tag{189.c}$$

Instead of long terms in (188), one can define contractions such as

$$K(s,r) = K_1(s,r) + K_2(s,r) + K_3(s,r) + K_4(s,r) + K_5(s,r) + K_6(s,r) + K_7(s,r), \tag{190}$$

where

$$K_1(s,r) = -\left(\frac{b_1}{c_0}\right)\left(\frac{b-a}{2}\right)\left[Ci\left(G\left(\frac{b-a}{2}(s-r)\right)\right) - \log|s-r|\right], \tag{191}$$

$$K_2(s,r) = \left(\frac{1}{c_0}\right)\left(\frac{b-a}{2}\right)\int_F^{\infty}\left(\frac{c_2}{\rho^2} + \frac{c_4}{\rho^4} + \frac{c_6}{\rho^6} + \frac{c_8}{\rho^8} + \frac{c_{10}}{\rho^{10}} + \frac{c_{12}}{\rho^{12}}\right)\sin\left(\rho\left(\frac{b-a}{2}(s-r)\right)\right)d\rho, \tag{192}$$

$$K_3(s,r) = \left(\frac{1}{c_0}\right)\left(\frac{b-a}{2}\right)\int_G^{\infty}\left(\frac{b_3}{\rho^3} + \frac{b_5}{\rho^5} + \frac{b_7}{\rho^7} + \frac{b_9}{\rho^9} + \frac{b_{11}}{\rho^{11}}\right)\cos\left(\rho\left(\frac{b-a}{2}(s-r)\right)\right)d\rho\ , \tag{193}$$

$$K_4(s,r) = \left(\frac{1}{c_0}\right)\left(\frac{b-a}{2}\right)\int_0^F (N(0,\rho) - c_0)\sin\left(\rho\left(\frac{b-a}{2}(s-r)\right)\right)d\rho\ , \tag{194}$$

$$K_5(s,r) = \left(\frac{1}{c_0}\right)\left(\frac{b-a}{2}\right)\int_0^G M(0,\rho)\cos\left(\rho\left(\frac{b-a}{2}(s-r)\right)\right)d\rho\ , \tag{195}$$

$$K_6(s,r) = (b-a)\left(\frac{\pi}{c_0}\right)e^{\frac{\beta\left(\frac{b-a}{2}(s-r)\right)}{2}}\sum_{k=-1}^{2} a_k\left(\frac{\pi}{c}\right)^k S_k\left(\frac{\pi\left(\frac{b-a}{2}(s+r)+a+b\right)}{c}, 0\right), \tag{196}$$

$$K_7(s,r) = (b-a)\left(\frac{\pi}{c_0}\right)\sum_{n=1}^{H}[K_2(x(r),t(s),\alpha_n) - K_2{}^{\infty}(x(r),t(s),\alpha_n)]\ . \tag{197}$$

Using the definitions above and (171.a,b) the singular integral equation can be expressed in the following form:

$$\frac{1}{\pi}\int_{-1}^{1} G(s)\left\{\frac{2}{b-a}\frac{1}{s-r} - \frac{\beta}{2}\log|s-r| + K(s,r)\right\}ds = -\frac{p(x(r))(\kappa+1)}{4\mu(x(r))}\ . \tag{198}$$

Note that the zero displacement condition outside the crack should be enforced by adding $\frac{\pi}{c}$ to the Fredholm Kernel. The details and justification of this modification can be found in [36].

The definition of mode-I SIF for the edge crack is taken from [36] as

$$k(b) = \lim_{x\to b^+}\sqrt{2(x-b)}\sigma_{yy}(x,0) = -\frac{4\mu(+1)}{\kappa+1}\sqrt{b}\varphi(+1)\ . \tag{199}$$

2.5 Thermal Loading

In order to find thermal stress intensity factors, the stresses ($\sigma_{yy}(x)$) for an uncracked plate at the location of the would-be crack should be applied as crack surface tractions with the opposite sign. Hence one should first find the thermal stress distribution in the crack free plate. In [11], for an infinite (i.e. $-\infty < y, z < \infty, 0<x<h$) plate free of surface

tractions at $x=0$ and $x=h$, and subjected to a temperature distribution $T(x)$, the following conditions are given (plate is graded in x direction):
$\sigma_{xx}=0$, $\sigma_{xy}=0$, $\sigma_{yy}=\sigma_{zz}$. Also it is clear that $\sigma_{xz}=\sigma_{yz}=0$.

Furthermore it is stated that all non-zero field quantities are independent of y and z. Then the given stress field satisfies the equilibrium equations in the absence of body forces and the only compatibility condition that needs to be satisfied reduces to

$$\frac{d^2\varepsilon_{yy}}{dx^2} = 0 \ , \tag{200}$$

which gives

$$\varepsilon_{yy}(x) = Ax + B \ . \tag{201}$$

Then by using Hooke's law one can easily show that (see Appendix D)

$$\sigma_{yy}(x) = \frac{E(x)}{1-\nu}[Ax + B - \alpha(x)(T(x) - T_0)]. \tag{202}$$

If temperature is time dependent, then A and B and therefore σ_{yy} and ε_{yy} will also be time dependent.

A and B should be obtained from the boundary conditions at the far edges of the plate. Here we can identify three cases. The first case is a fully free plate. If the plate is unconstrained along its edges, one can use

$$\int_0^h \sigma_{yy}(x)dx = 0 \ , \tag{203}$$

$$\int_0^h x\sigma_{yy}(x)dx = 0 \ . \tag{204}$$

These equations mean that there is no net force and net moment acting on the edges, therefore under one dimensional heat flow in x direction, FGM plate can deform into a shallow spherical shell [11]. When subjected to a cooling thermal shock at x=0, plate can shrink and bend. This case is schematically shown in Fig. 2.5.

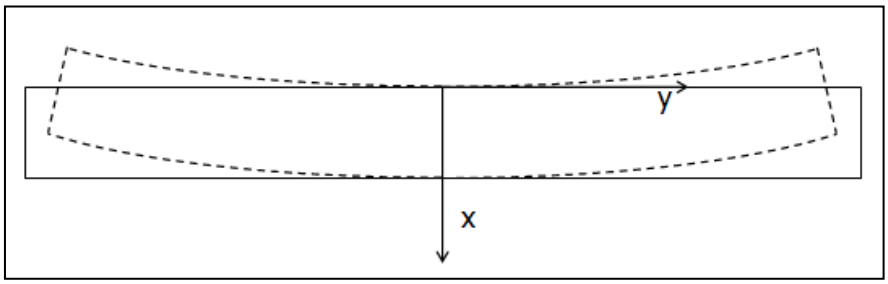

Figure 2.5 Plate whose ends are free

The second case is a fully constrained plate, where $\varepsilon_{yy} = 0$. Then it is clear that $A=0$ and $B=0$ [11]. Such a constraint can be schematically shown as in Fig. 2.6.

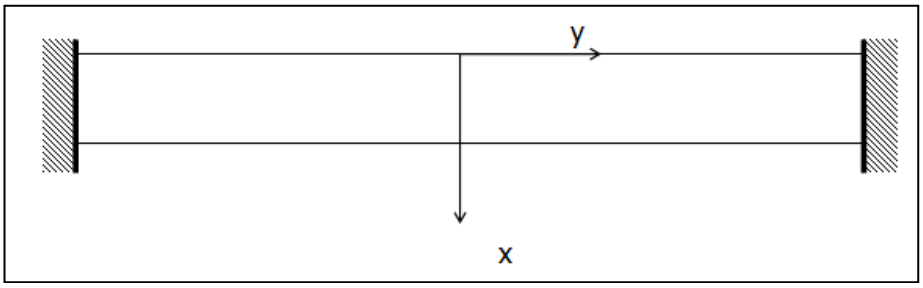

Figure 2.6 Plate whose ends are fixed

The third case which is utilized in this study is that of partial constraint. The edges are supported such that expansion or contraction of the plate is allowed but rotations of the edges are constrained. This case can be schematically shown as in Fig. 2.7. It is as if though the plate is attached to rigid blocks which can slide but are not allowed to turn.

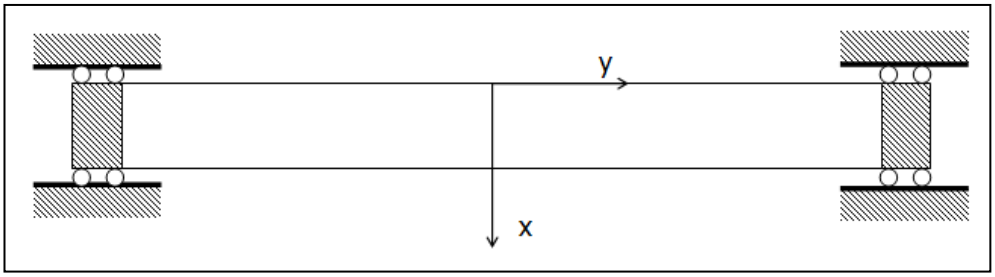

Figure 2.7 Plate under partial constraint

In this case a uniform ε_{yy} will develop, i.e. $A=0$ but $B\neq 0$. B can be found from Eq. (203) given above, whereas constraining moment M (per unit width) can be obtained from

$$\int_0^h x\sigma_{yy}(x)dx = M \ . \tag{205}$$

Note that because of this partial constraint, the plate would remain flat and a surface crack on the cooling side would be subjected to a more severe opening action compared to a crack in a fully free plate.

The thermal stress solution $\sigma_{yy}(x,t)$ along with uniform strain $\varepsilon_{yy}(t) = \varepsilon_{0t}$ (which is a function of time under transient loading) is readily given in [12] and used in thesis.

$$\sigma_{yy}(x,t) = \frac{E(x)}{1-\nu}\left(\varepsilon_{ot}(t) - \alpha(x)\theta(x,t)\right) \tag{206}$$

where

$$\varepsilon_{ot}(t) = \alpha_0(T_a - T_0)\left\{\frac{\beta(\beta-\delta-\beta e^{\delta h}+\delta e^{(\beta+\omega)h}+\omega-\omega e^{\delta h})}{(e^{\beta h}-1)(e^{\delta h}-1)(\beta+\omega)(\beta+\omega-\delta)}\right.$$

$$-\sum_{n=1}^{\infty}\frac{2n^2\pi^2\beta h\left(e^{\delta\frac{h}{2}}-e^{(\beta+\omega)h}\cos(n\pi)\right)e^{-\delta\frac{h}{2}}e^{-\left(n^2\pi^2+\frac{\delta^2h^2}{4}\right)\left(\frac{Dt}{h^2}\right)}}{\left(n^2\pi^2+\frac{\delta^2h^2}{4}\right)(e^{\beta h}-1)\left(\beta h^2(\beta-\delta)+n^2\pi^2+\frac{\delta^2h^2}{4}+\omega h^2(2\beta-\delta+\omega)\right)} \tag{207}$$

$k(x)$ is the coefficient of heat conduction and $\alpha(x)$ is the coefficient of thermal expansion and both are varying along x-axis as exponential functions. δ and ω are the nonhomogeneity constants for $k(x)$ and $\alpha(x)$ respectively.

$$k(x) = k_0 e^{\delta x} \ , \tag{208}$$

$$\alpha(x) = \alpha_0 e^{\omega x} \ . \tag{209}$$

D is the thermal diffusivity which is assumed as constant.

$$D = \frac{k(x)}{c(x)\rho(x)} \tag{210}$$

where $c(x)$ is the specific heat and $\rho(x)$ is the density.

Temperature distribution is determined by solving Fourier's equation of heat conduction

$$\frac{\partial}{\partial x}\left(k(x)\frac{\partial T(x,t)}{\partial x}\right) = \rho(x)c(x)\frac{\partial T(x,t)}{\partial t} \ , \tag{211}$$

and the solution is given in [12].

$\theta(x,t)$ is the transient temperature distribution which is defined as

$$\theta(x,t) = T(x,t) - T_0 \tag{212.a}$$

with the boundary conditions and initial conditions

$$\theta(0,t) = \theta_a = T_a - T_0 \ , \tag{212.b}$$

$$\theta(h,t) = 0 \ , \tag{212.c}$$

$$\theta(x,0) = 0 \ . \tag{212.d}$$

Using the boundary and initial conditions, $\theta(x,t)$ is expressed as [12]

$$\theta(x,t) = \theta_a\left[\frac{e^{-\delta x} - e^{-\delta h}}{1-e^{-\delta h}} - \sum_{n=1}^{\infty}\frac{8n\pi}{\delta^2 h^2 + 4n^2\pi^2}\sin\left(\frac{n\pi x}{h}\right)e^{-\frac{\delta}{2}x}e^{-\left(n^2\pi^2+\frac{\delta^2 h^2}{4}\right)\left(\frac{Dt}{h^2}\right)}\right] . \tag{212.e}$$

As $t \to \infty$, the solutions above are valid for steady state heat conduction problem. Steady state thermal stress solution, $\sigma_{yy}(x)$ can also be written independent of time [12] as:

$$\sigma_{yy}(x) = \frac{E(x)}{1-\nu}(\varepsilon_{os} - \alpha(x)(T(x) - T(0)) \tag{213}$$

where

$$\varepsilon_{OS} = \frac{\alpha_0(T_1 - T_0)\beta(\beta - \delta - \beta e^{\delta h} + \delta e^{(\beta+\omega)h} + \omega - \omega e^{\delta h})}{(e^{\beta h}-1)(e^{\delta h}-1)(\beta+\omega)(\beta+\omega-\delta)} \ , \tag{214}$$

$$T(x) = \frac{e^{\delta h}T(h) - T(0)}{e^{\delta h}-1} + \frac{(T(0)-T(h))e^{\delta(h-x)}}{e^{\delta h}-1} \ . \tag{215}$$

2.6 Numerical Solution and Stress Intensity Factors

The singular integral equation (198) is solved by using a series expansion collocation method, an example of which can be found in [38]. According to this method, the unknown function is expressed in terms of an infinite series of Jacobi polynomials as given by (189.a-c). The singular integral equation is converted to a linear system of equations. After determining $G(s)$, the mode-I SIFs can be readily obtained from (199). An existing program in FORTRAN, which has been used for [36] is modified to solve the integral equation derived in this study. This modification amounts to replacing the kernel $K_7(s,r)$ and adding the thermal stress solutions.

CHAPTER 3

NUMERICAL RESULTS

In this chapter, the SIFs which are calculated for different values of nonhomogeneity parameters and for different loadings are presented. An edge crack in the FGM strip is considered.

The SIFs are determined for uniform crack surface traction, fixed grip (constant strain) loading, transient heat conduction and steady state heat conduction.

Since all the results are presented in non-dimensional form through appropriate normalizations the strip thickness, h, is taken as unity in all calculations for simplicity.

In order to verify the results by comparing them with the earlier results in literature, the following loading cases are considered:

a) Uniform crack surface traction,
b) Fixed grip loading,
c) Thermal loading.

These are explained and relevant results are presented below.

3.1 Uniform Crack Surface Traction

Uniform surface traction is assumed on the crack surface and it is expressed as

$$\sigma_{yy}(x,0) = -\sigma_0 \ , \qquad 0 < x < b. \tag{216}$$

SIFs are normalized as follows:

$$k^*(b) = \frac{k(b)}{\sigma_0\sqrt{b}} \ . \tag{217}$$

3.1.1 Stress Intensity Factors (Tables)

Table 3.1 Normalized SIFs under uniform crack surface traction in a homogeneous material, κ=1.8

	βh=0 (homogeneous material)								
	b/2c=0.1			b/2c=0.5			b/2c=1.0		
b/h	**k*(b)**	**k*(b) [39]**	**Diff. %**	**k*(b)**	**k*(b) [39]**	**Diff. %**	**k*(b)**	**k*(b) [39]**	**Diff. %**
0.1	1.0390	1.0390	0	0.5581	0.5581	0	0.3987	0.3987	0
0.3	1.1403	1.1402	0.01	0.5581	0.5581	0	0.3987	0.3987	0
0.5	1.3474	1.3473	0.01	0.5609	0.5609	0	0.3987	0.3987	0

Table 3.2 Normalized SIFs under uniform crack surface traction, κ=2.0

	βb=-1.0			βb=0.0			βb=1.0		
b/h	**c/b=0.5**	**c/b=1.0**	**c/b=2.0**	**c/b=0.5**	**c/b=1.0**	**c/b=2.0**	**c/b=0.5**	**c/b=1.0**	**c/b=2.0**
0.60	0.3819	0.5094	0.6702	0.3992	0.5660	0.8344	0.4183	0.6493	1.0548
0.55	0.3817	0.5090	0.6728	0.3988	0.5634	0.8321	0.4177	0.6396	1.0215
0.50	0.3817	0.5084	0.6745	0.3987	0.5609	0.8263	0.4176	0.6321	0.9849
0.45		0.5080	0.6752	0.3987	0.5592	0.8182	0.4175	0.6277	0.9495
0.40		0.5078	0.6752		0.5584	0.8094	0.4175	0.6258	0.9193
0.35		0.5077	0.6747		0.5582	0.8017		0.6252	0.8976
0.30		0.5077	0.6742		0.5581	0.7965		0.6251	0.8855
0.25			0.6740		0.5581	0.7941		0.6251	0.8810
0.20			0.6739			0.7935			0.8801
0.15			0.6739			0.7934			0.8801
0.10						0.7934			
0.00 [36]	**0.3817**	**0.5077**	**0.6739**	**0.3987**	**0.5581**	**0.7934**	**0.4175**	**0.6251**	**0.8801**

Table 3.3 Influence of the crack period on the normalized SIFs under uniform crack surface traction, βh=0.375, κ=1.68

	βh=0.375 (E_1/E_0=1.455)			
	b/h=0.1	**b/h=0.2**	**b/h=0.4**	**b/h=0.5**
c/b=0.5	0.3993	0.4000	0.4014	0.4021
c/b=0.5 [41]	0.3989	0.3996	0.4010	0.4017
diff. %	0.09	0.10	0.11	0.11
c/b=1	0.5603	0.5626	0.5676	0.5730
c/b=1 [41]	0.5594	0.5617	0.5667	0.5721
diff. %	0.15	0.16	0.16	0.16
c/b=2	0.7975	0.8016	0.8292	0.8579
c/b=2 [41]	0.7980	0.8021	0.8297	0.8584
diff. %	0.07	0.07	0.06	0.06
c/b=5	1.0362	1.0605	1.2559	1.3906
c/b=5 [41]	1.0334	1.0576	1.2524	1.3868
diff. %	0.28	0.27	0.28	0.28
c/b=10	1.1006	1.1800	1.5443	1.8193
c/b=10 [41]	1.0799	1.1577	1.5151	1.7848
diff. %	1.92	1.93	1.93	1.93
c/b=20	1.1352	1.2512	1.7524	2.1721
c/b=20 [41]	1.1014	1.2139	1.7001	2.1071
diff. %	3.07	3.07	3.08	3.08
c/b=40	1.1534	1.2903	1.8814	2.4125
c/b=60	1.1596	1.3040	1.9292	2.5061
single crack [12]	**1.1732**	**1.3339**	**2.0402**	**2.7371**

Table 3.4 Influence of the crack period on the normalized SIFs under uniform crack surface traction, βh=1.609, κ=1.68

	βh=1.609 (E_1/E_0=5)			
	b/h=0.1	**b/h=0.2**	**b/h=0.4**	**b/h=0.5**
c/b=0.5	0.4016	0.4045	0.4105	0.4137
c/b=0.5 [41]	0.4012	0.4041	0.4101	0.4133
diff. %	0.11	0.10	0.09	0.10
c/b=1	0.5679	0.5781	0.6003	0.6170
c/b=1 [41]	0.5670	0.5772	0.5994	0.6161
diff. %	0.16	0.15	0.16	0.15
c/b=2	0.8105	0.8265	0.8868	0.9569
c/b=2 [41]	0.8111	0.8271	0.8874	0.9575
diff. %	0.07	0.07	0.07	0.06
c/b=5	1.0274	1.0441	1.2725	1.4871
c/b=5 [41]	1.0245	1.0412	1.2690	1.4830
diff. %	0.28	0.28	0.28	0.28
c/b=10	1.0746	1.1301	1.4907	1.8340
c/b=10 [41]	1.0543	1.1088	1.4626	1.7993
diff. %	1.93	1.92	1.92	1.93
c/b=20	1.0985	1.1788	1.6311	2.0788
c/b=20 [41]	1.0658	1.1437	1.5825	2.0168
diff. %	3.07	3.07	3.07	3.07
c/b=40	1.1110	1.2047	1.7119	2.2287
c/b=60	1.1152	1.2137	1.7388	2.2662
single crack [12]	**1.1252**	**1.2348**	**1.8123**	**2.4261**

Table 3.5 Influence of the crack period on the normalized SIFs under uniform crack surface traction, βh=2.079, κ=1.68

	βh=2.079 (E_1/E_0=8)			
	b/h=0.1	**b/h=0.2**	**b/h=0.4**	**b/h=0.5**
c/b=0.5	0.4024	0.4062	0.4142	0.4184
c/b=0.5 [41]	0.4020	0.4058	0.4138	0.4180
diff. %	0.10	0.09	0.10	0.11
c/b=1	0.5708	0.5843	0.6135	0.6350
c/b=1 [41]	0.5700	0.5834	0.6126	0.6340
diff. %	0.15	0.15	0.15	0.16
c/b=2	0.8153	0.8353	0.9051	0.9898
c/b=2 [41]	0.8158	0.8358	0.9057	0.9904
diff. %	0.06	0.07	0.06	0.07
c/b=5	1.0242	1.0378	1.2687	1.5044
c/b=5 [41]	1.0214	1.0349	1.2652	1.5003
diff. %	0.27	0.28	0.28	0.27
c/b=10	1.0661	1.1129	1.4623	1.8173
c/b=10 [41]	1.0460	1.0920	1.4347	1.7830
diff. %	1.92	1.92	1.93	1.92
c/b=20	1.0867	1.1548	1.5824	2.0277
c/b=20 [41]	1.0544	1.1204	1.5354	1.9673
diff. %	3.07	3.07	3.06	3.07
c/b=40	1.0974	1.1769	1.6499	2.1527
c/b=60	1.1010	1.1845	1.6687	2.1644
single crack [12]	**1.1099**	**1.2031**	**1.7360**	**2.3190**

Table 3.6 Influence of the crack period on the normalized SIFs under uniform crack surface traction, βh=-1.609, κ=1.68

	βh=-1.609 (E_1/E_0=0.2)			
	b/h=0.1	**b/h=0.2**	**b/h=0.4**	**b/h=0.5**
c/b=0.5	0.3958	0.3930	0.3876	0.3849
c/b=0.5 [41]	0.3954	0.3927	0.3872	0.3845
diff. %	0.09	0.09	0.11	0.10
c/b=1	0.5487	0.5398	0.5236	0.5171
c/b=1 [41]	0.5478	0.5389	0.5228	0.5163
diff. %	0.16	0.16	0.15	0.16
c/b=2	0.7753	0.7563	0.7208	0.7001
c/b=2 [41]	0.7758	0.7568	0.7213	0.7006
diff. %	0.06	0.06	0.07	0.07
c/b=5	1.0506	1.0758	1.1334	1.1169
c/b=5 [41]	1.0477	1.0728	1.1304	1.1139
diff. %	0.28	0.28	0.27	0.27
c/b=10	1.1525	1.2633	1.5135	1.5770
c/b=10 [41]	1.1307	1.2394	1.4849	1.5472
diff. %	1.93	1.93	1.93	1.93
c/b=20	1.2106	1.3888	1.8658	2.0921
c/b=20 [41]	1.1745	1.3473	1.8101	2.0299
diff. %	3.08	3.08	3.07	3.06
c/b=40	1.2420	1.4627	2.1295	2.5498
c/b=60	1.2528	1.4892	2.2425	2.8127

3.1.2 Stress Intensity Factors (Figures)

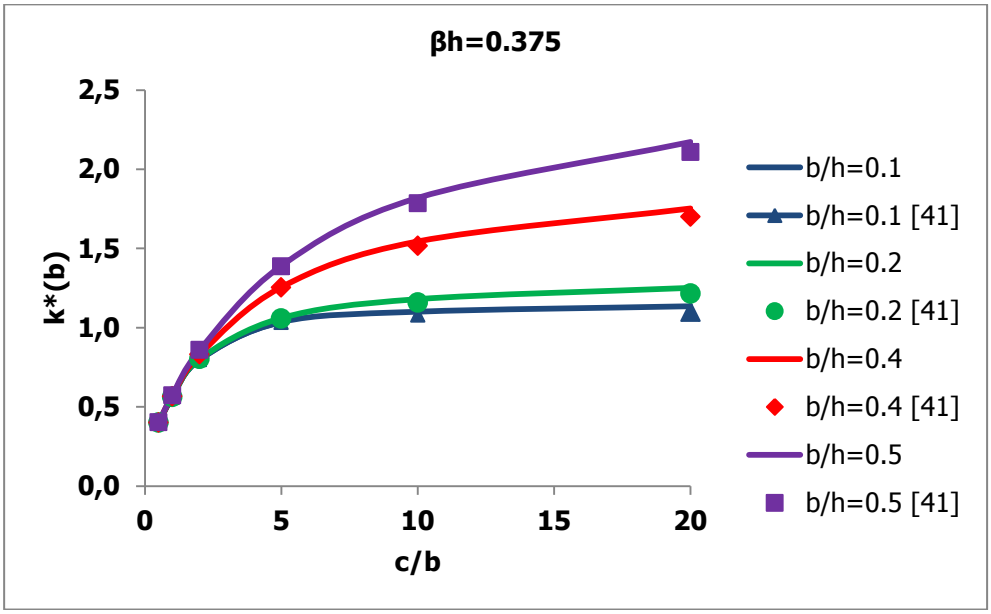

Figure 3.1 Influence of the crack period on the normalized SIFs under uniform crack surface traction, βh= 0.375, κ=1.68

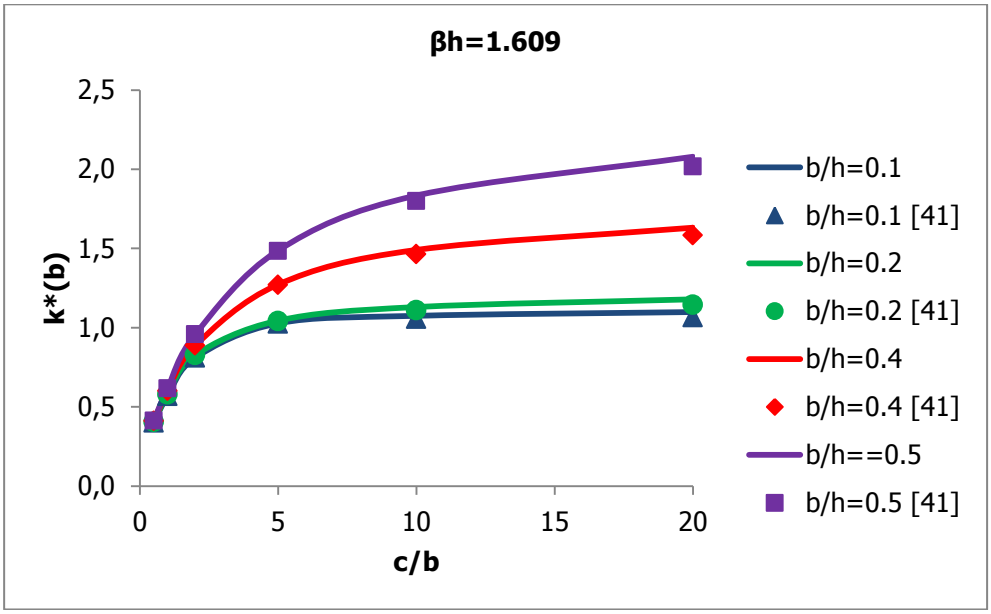

Figure 3.2 Influence of the crack period on the normalized SIFs under uniform crack surface traction, βh= 1.609, κ=1.68

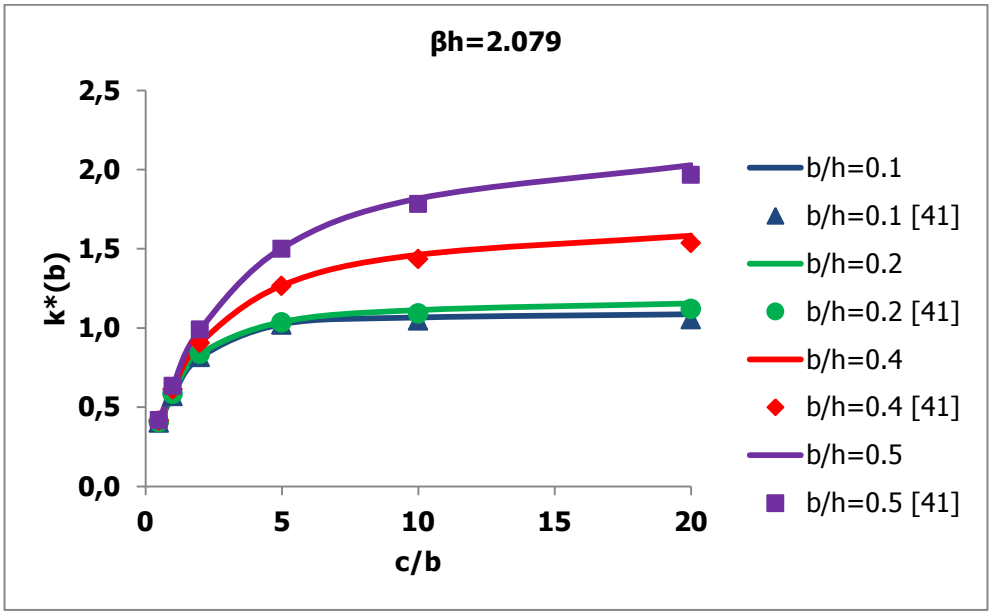

Figure 3.3 Influence of the crack period on the normalized SIFs under uniform crack surface traction, βh= 2.079, κ=1.68

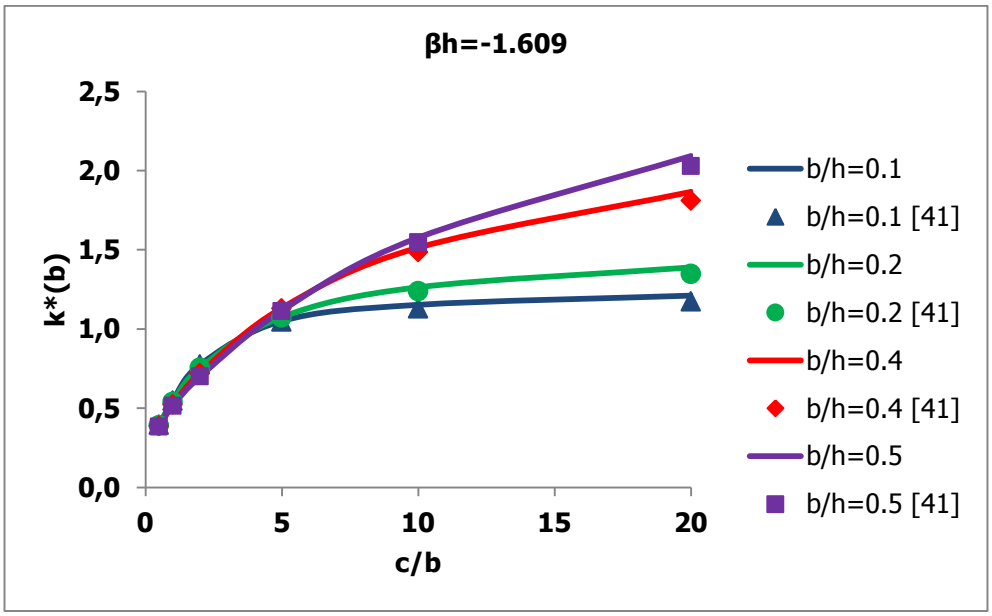

Figure 3.4 Influence of the crack period on the normalized SIFs under uniform crack surface traction, βh= -1.609, κ=1.68

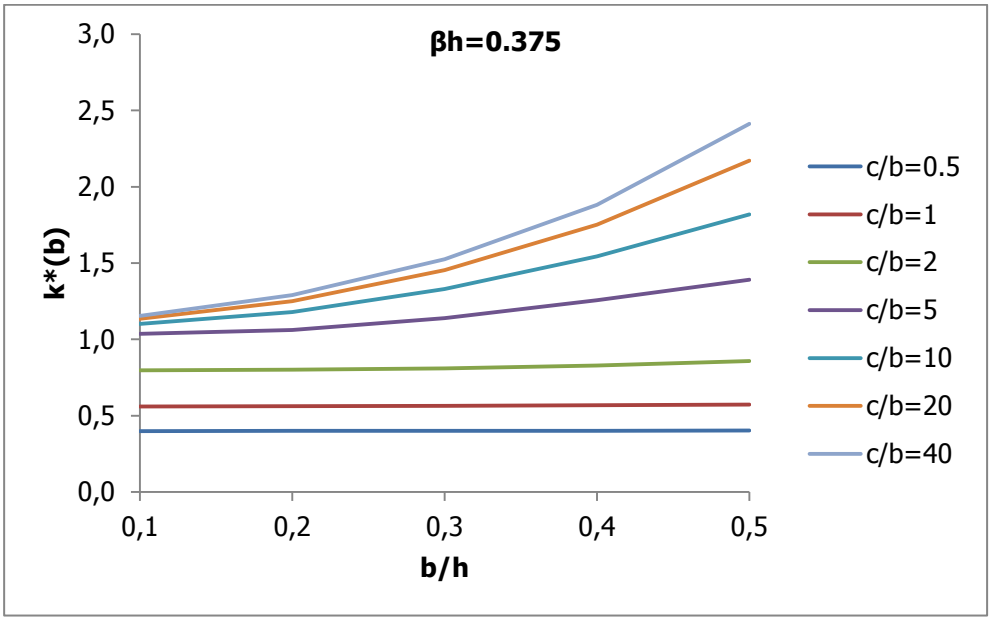

Figure 3.5 Variation of the normalized SIFs under uniform crack surface traction, with respect to b/h for different c/b's, κ=1.68

3.2 Fixed Grip Loading

In this loading type the strip is subjected to a constant strain. The crack surface traction is given by

$$\sigma_{yy}(x,0) = -\frac{E(x)\varepsilon_0}{1-v^2} \tag{218}$$

where

$$E(x) = E_0 e^{\beta x} \tag{219}$$

and

$$E_0 = 2\mu_0(1+v). \tag{220}$$

SIFs are normalized as follows:

$$k^*(b) = k(b)/\left[\frac{E_0\varepsilon_0}{1-v^2}\sqrt{b}\right]. \tag{221}$$

3.2.1 Stress Intensity Factors (Tables)

Table 3.7 Influence of the crack period on the normalized SIFs under fixed grip loading, βh=1.609, κ=1.8

	βh=1.609			
c/b	**b/h=0.1**	**b/h=0.2**	**b/h=0.3**	**b/h=0.4**
0.5	0.4650	0.5423	0.6325	0.7377
1	0.6475	0.7511	0.8711	1.0107
2	0.9066	1.0346	1.1853	1.3855
5	1.1379	1.2824	1.5268	1.8875
10	1.1882	1.3805	1.6961	2.1714
20	1.2137	1.4360	1.7976	2.3539
40	1.2270	1.4656	1.8536	2.4591
60	1.2316	1.4758	1.8731	2.4990
single crack [10]	**1.29**	**1.55**	**1.90**	**2.58**

Table 3.8 Influence of the crack period on the normalized SIFs under fixed grip loading, βh=0 (homogeneous), κ=1.8

	βh=0 (homogeneous)			
c/b	**b/h=0.1**	**b/h=0.2**	**b/h=0.3**	**b/h=0.4**
0.5	0.3987	0.3987	0.3987	0.3987
1	0.5581	0.5581	0.5581	0.5584
2	0.7935	0.7935	0.7965	0.8094
5	1.0390	1.0650	1.1403	1.2419
10	1.1096	1.1960	1.3474	1.5516
20	1.1480	1.2756	1.4861	1.7845
40	1.1682	1.3198	1.5679	1.9331
60	1.1752	1.3353	1.5973	1.9888
single crack [10]	**1.19**	**1.39**	**1.65**	**2.13**

Table 3.9 Influence of the crack period on the normalized SIFs under fixed grip loading, βh=-1.609, κ=1.8

	βh=-1.609			
c/b	**b/h=0.1**	**b/h=0.2**	**b/h=0.3**	**b/h=0.4**
0.5	0.3418	0.2931	0.2513	0.2155
1	0.4809	0.4143	0.3568	0.3074
2	0.6933	0.6046	0.5272	0.4603
5	0.9516	0.8866	0.8405	0.7855
10	1.0471	1.0520	1.0759	1.0856
20	1.1015	1.1628	1.2594	1.3638
40	1.1310	1.2279	1.3793	1.5718
60	1.1411	1.2513	1.4248	1.6527
single crack [10]	**1.19**	**1.29**	**1.52**	**1.87**

3.2.2 Stress Intensity Factors (Figures)

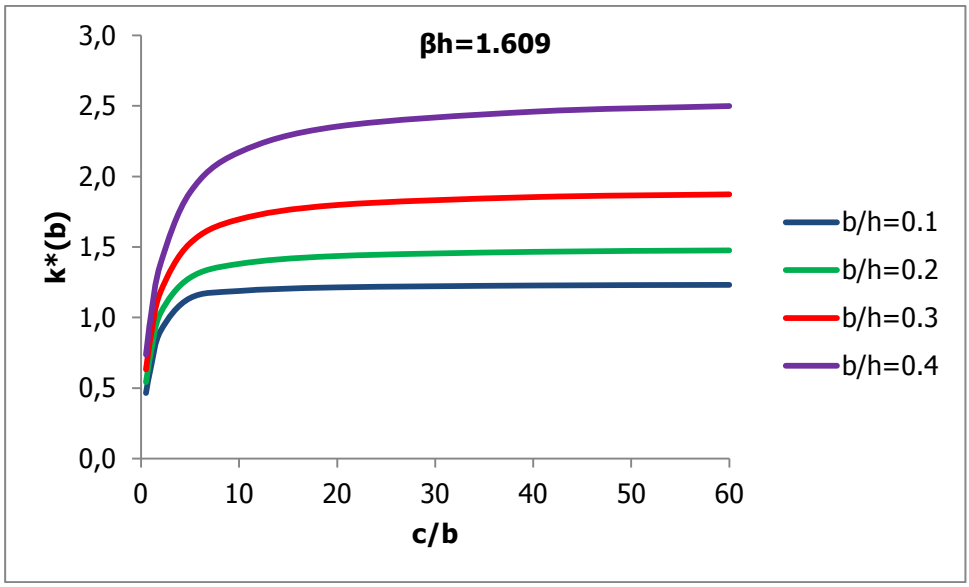

Figure 3.6 Influence of the crack period on the normalized SIFs under fixed grip loading, βh=1.609, κ=1.8

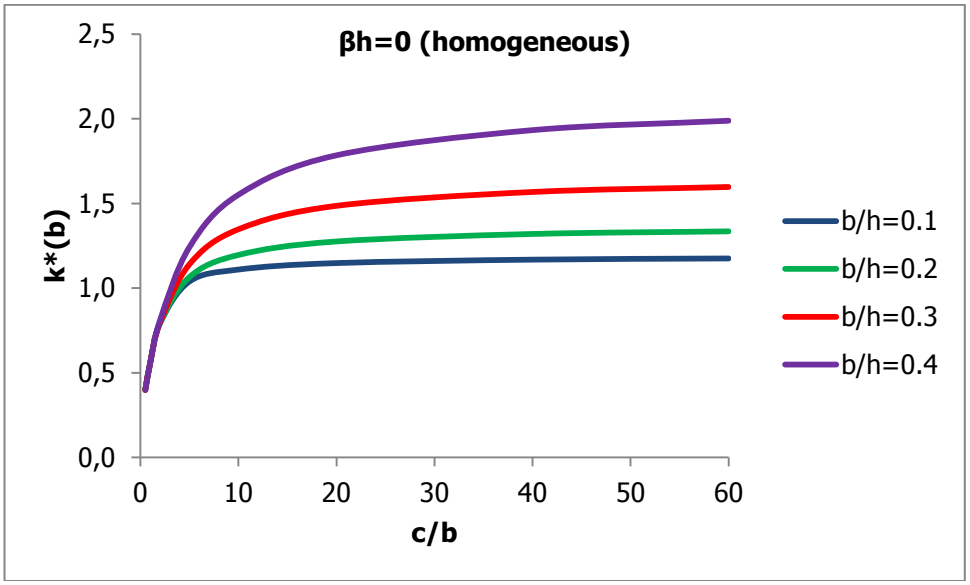

Figure 3.7 Influence of the crack period on the normalized SIFs under fixed grip loading, βh=0 (homogeneous) , κ=1.8

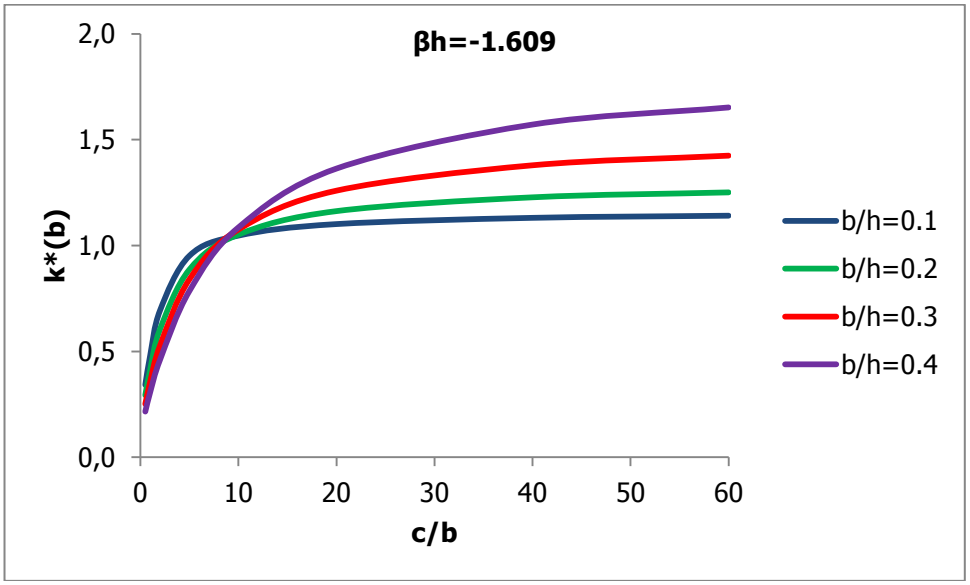

Figure 3.8 Influence of the crack period on the normalized SIFs under fixed grip loading, βh=-1.609, κ=1.8

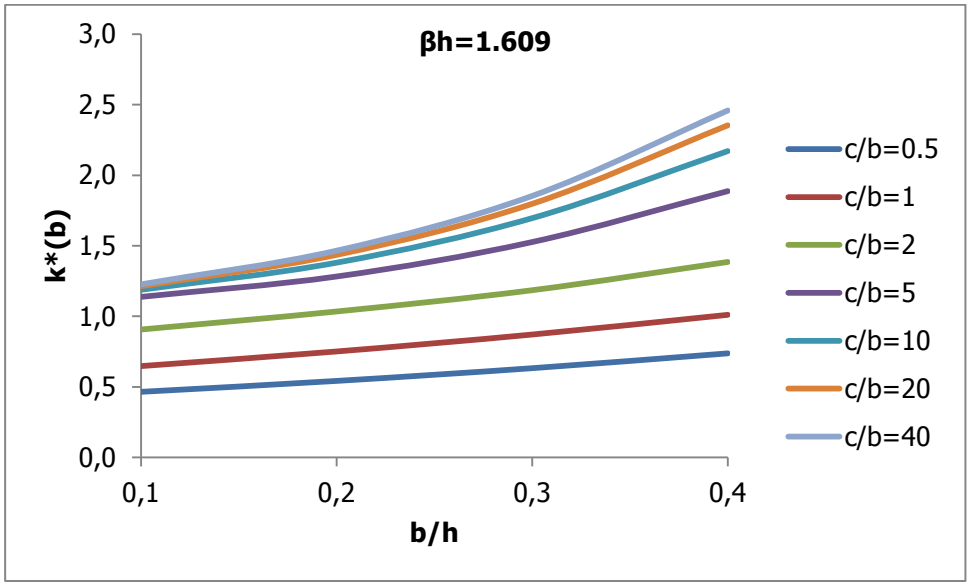

Figure 3.9 Variation of the normalized SIFs under fixed grip loading, with respect to b/h for different c/b's, κ=1.8

3.3 Thermal Loading

a) Transient Heat Conduction

For transient heat conduction problem the strip is assumed to be at uniform temperature T_0, then suddenly the surface at $x=0$ is brought to a temperature T_a and kept at this temperature while the surface at $x=h$ is kept at T_0. In the tables and figures T_t^* denotes T_a/T_0.

To facilitate comparison, numerical results are given for the same materials used in [12]. Properties are given in the table below.

Table 3.10 Material properties

	E (GPa)	ν	α (K^{-1})	K (Cal/mm.s.K)
Material-1= Zirconia	151	0.33	10^{-5}	0.05
Material-2= Rene 41	219.7	0.33	$1.67*10^{-5}$	0.61

Using the values given in Table 3.10, nonhomogeneity parameters can be calculated as: $\beta h = 0.3750059006$, $\omega h = 0.5128236264$and $\delta h = 2.501435952$.

The thermal stress given by Eq. (206) is used for this case. The SIFs are normalized by σ_0 where

$$\sigma_0 = \frac{E_0 \alpha_0 T_0}{1-\nu}. \tag{222}$$

b) Steady State Heat Conduction

The thermal stress given by Eq. (213) is used for this case. The SIFs are normalized by σ_0 given in Eq. (222).

T_s^* denotes T_1/T_0 where T_1 is the temperature at $x=0$ and T_0 is the temperature of stress free state.

In the following section, temperature ($\Theta(x,\tau)$) and thermal stress ($\sigma_{yy}(x,\tau)$) distributions are given for different τ (nondimensional time) values.

$$\tau = \frac{Dt}{b^2}. \tag{223}$$

$\Theta_{ss}(x)$ and $\sigma_{yyss}(x)$ denote steady state temperature and thermal stress distribution respectively.

<u>Temperature and Thermal Stresses Distribution</u>

In Figs. 3.10 and 3.12 transient and steady state temperature distribution in a Zirconia-Rene 41 strip are plotted for cooling and heating thermal shock respectively. Similarly, transient and steady state thermal stress distributions are plotted in Figs. 3.11 and 3.13. Plots are same with the plots given in [12].

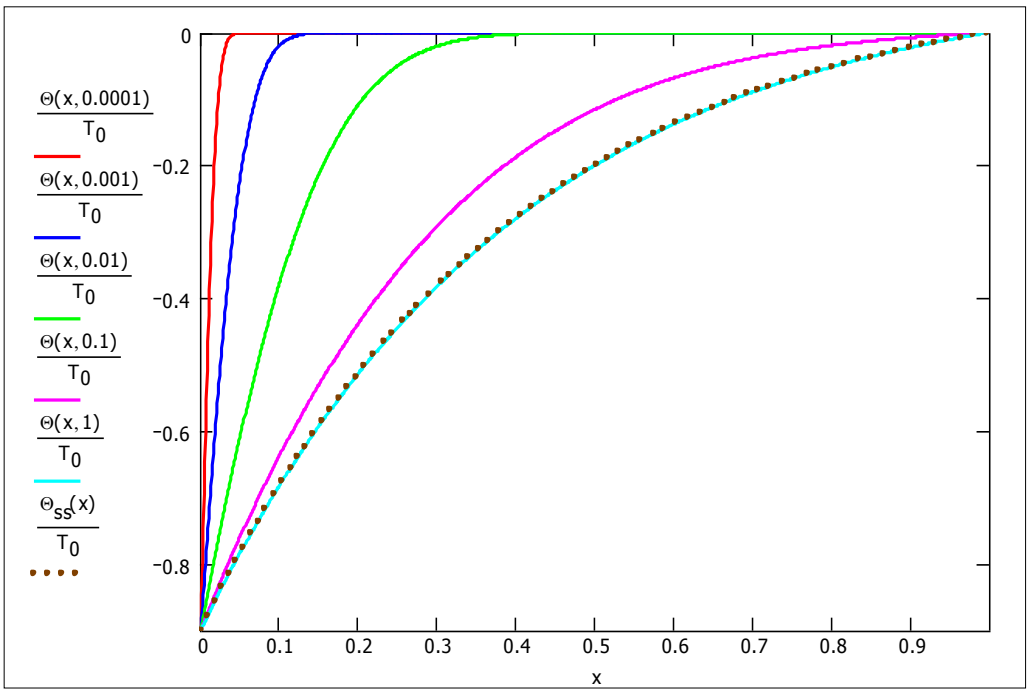

Figure 3.10 Transient and steady state temperature distribution in a Zirconia-Rene 41 strip, T_t^*=0.1 (cooling thermal shock)

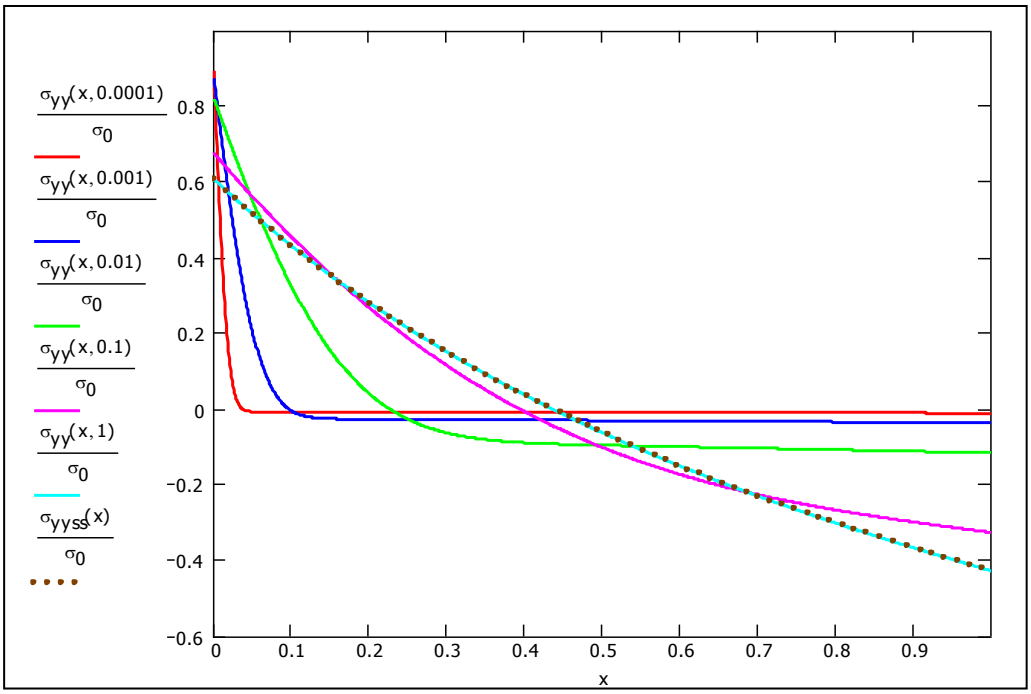

Figure 3.11 Transient and steady state thermal stress distribution in a Zirconia-Rene 41 strip, T_t*=0.1

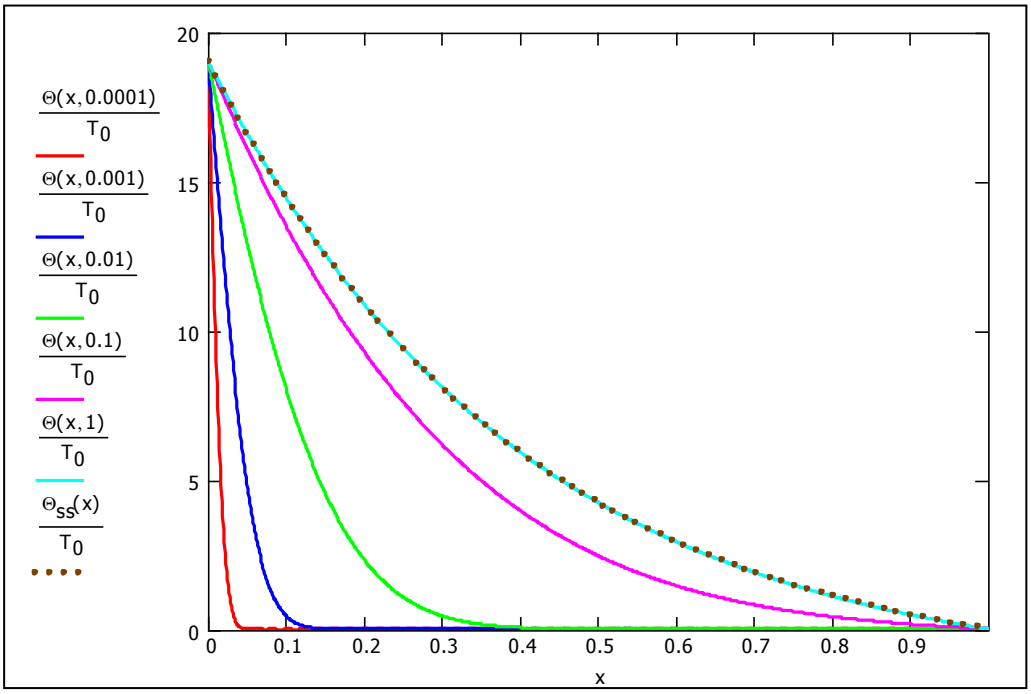

Figure 3.12 Transient and steady state temperature distribution in a Zirconia-Rene 41 strip, T_t*=20 (heating thermal shock)

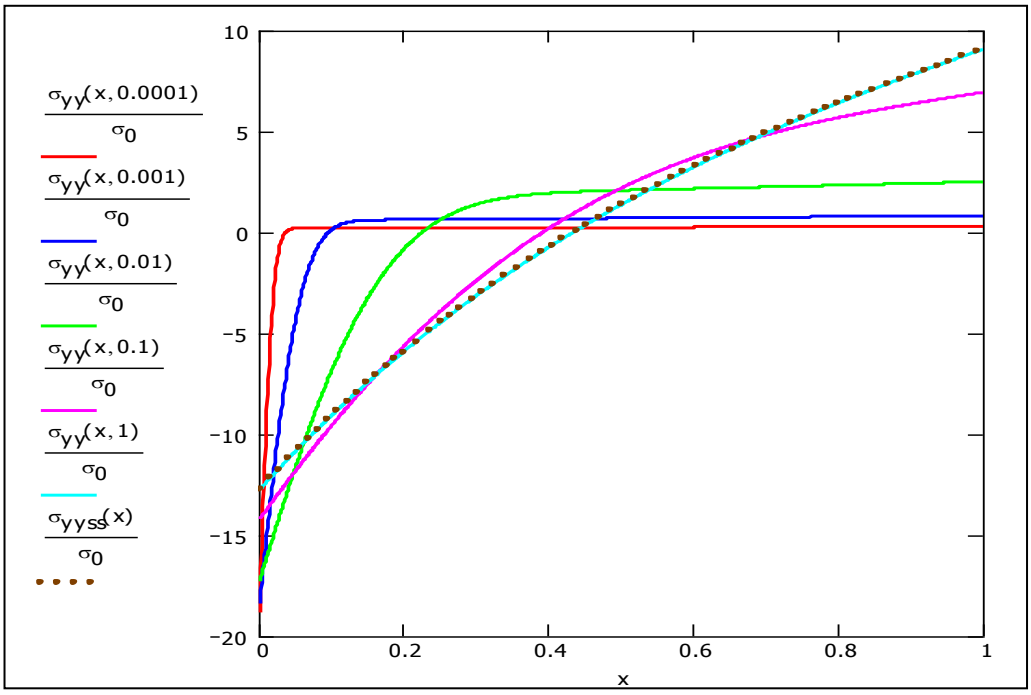

Figure 3.13 Transient and steady state thermal stress distribution in a Zirconia-Rene 41 strip, T_t*=20

SIFs given in following tables and figures are calculated for cooling thermal shock case.

3.3.1 Stress Intensity Factors (Tables)

Table 3.11 Influence of b/h on the normalized SIFs in a Zirconia-Rene 41 strip under transient thermal stress, with respect to nondimensional time τ , c/b=5, κ=1.68

τ	b/h=0.025	b/h=0.075	b/h=0.100	b/h=0.150	b/h=0.200	b/h=0.250	b/h=0.300	b/h=0.350	b/h=0.400	b/h=0.450	b/h=0.500
0	0	0	0	0	0	0	0	0	0	0	0
0.0025	0.7241	0.4421	0.3399	0.2090	0.1444	0.1117	0.0932	0.0816	0.0736	0.0676	0.0623
0.005	0.7531	0.5329	0.4408	0.3001	0.2127	0.1619	0.1323	0.1143	0.1023	0.0937	0.0866
0.01	0.7621	0.5954	0.5202	0.3929	0.2993	0.2345	0.1910	0.1621	0.1427	0.1288	0.1180
0.015	0.7588	0.6176	0.5524	0.4380	0.3490	0.2825	0.2339	0.1991	0.1741	0.1557	0.1412
0.02	0.7526	0.6270	0.5683	0.4637	0.3800	0.3152	0.2655	0.2279	0.1996	0.1779	0.1604
0.03	0.7386	0.6317	0.5811	0.4898	0.4151	0.3552	0.3070	0.2684	0.2374	0.2122	0.1908
0.04	0.7249	0.6290	0.5835	0.5008	0.4326	0.3772	0.3317	0.2941	0.2628	0.2363	0.2130
0.05	0.7122	0.6238	0.5817	0.5050	0.4417	0.3900	0.3471	0.3110	0.2803	0.2535	0.2294
0.1	0.6645	0.5938	0.5601	0.4986	0.4481	0.4069	0.3722	0.3423	0.3158	0.2913	0.2678
0.15	0.6367	0.5733	0.5429	0.4877	0.4427	0.4063	0.3757	0.3492	0.3254	0.3031	0.2810
0.2	0.6209	0.5612	0.5326	0.4807	0.4386	0.4047	0.3764	0.3518	0.3296	0.3085	0.2873
0.3	0.6070	0.5505	0.5234	0.4744	0.4348	0.4031	0.3767	0.3537	0.3329	0.3130	0.2927
0.4	0.6025	0.5470	0.5205	0.4724	0.4336	0.4025	0.3767	0.3543	0.3340	0.3144	0.2944
0.5	0.6011	0.5469	0.5196	0.4717	0.4332	0.4024	0.3768	0.3545	0.3343	0.3149	0.2949

Table 3.12 Influence of c/b on the normalized SIFs in a Zirconia-Rene 41 strip under transient thermal stress, with respect to nondimensional time τ , b/h=0.025, κ=1.68

τ	c/b=0.5	c/b=1	c/b=2	c/b=5	c/b=10	c/b=20	c/b=40
0	0	0	0	0	0	0	0
0.0025	0.2487	0.3624	0.5402	0.7241	0.7684	0.7803	0.7839
0.005	0.2679	0.3854	0.5662	0.7531	0.7980	0.8102	0.8138
0.010	0.2771	0.3956	0.5758	0.7621	0.8070	0.8191	0.8227
0.015	0.2784	0.3962	0.5745	0.7588	0.8031	0.8151	0.8187
0.020	0.2776	0.3943	0.5705	0.7526	0.7965	0.8083	0.8119
0.030	0.2740	0.3884	0.5606	0.7386	0.7815	0.7930	0.7965
0.040	0.2698	0.3820	0.5506	0.7249	0.7669	0.7782	0.7816
0.050	0.2656	0.3758	0.5412	0.7122	0.7534	0.7645	0.7678
0.100	0.2489	0.3516	0.5055	0.6645	0.7028	0.7131	0.7162
0.150	0.2389	0.3373	0.4846	0.6367	0.6734	0.6833	0.6862
0.200	0.2331	0.3291	0.4726	0.6209	0.6567	0.6663	0.6692
0.300	0.2281	0.3219	0.4621	0.6070	0.6419	0.6513	0.6541
0.400	0.2265	0.3196	0.4587	0.6025	0.6372	0.6465	0.6493
0.500	0.2259	0.3188	0.4577	0.6011	0.6357	0.6450	0.6478

Table 3.13 Influence of c/b on the normalized SIFs in a Zirconia-Rene 41 strip under transient thermal stress, with respect to nondimensional time τ , b/h=0.075, κ=1.68

τ	c/b=0.5	c/b=1	c/b=2	c/b=5	c/b=10	c/b=20	c/b=40
0	0	0	0	0	0	0	0
0.0025	0.1003	0.1719	0.3056	0.4421	0.4748	0.4895	0.4973
0.005	0.1493	0.2348	0.3825	0.5329	0.5691	0.5853	0.5939
0.010	0.1864	0.2810	0.4369	0.5954	0.6335	0.6506	0.6597
0.015	0.2014	0.2992	0.4571	0.6176	0.6563	0.6735	0.6827
0.020	0.2090	0.3080	0.4662	0.6270	0.6658	0.6831	0.6923
0.030	0.2156	0.3151	0.4721	0.6317	0.6701	0.6873	0.6964
0.040	0.2174	0.3164	0.4714	0.6290	0.6670	0.6840	0.6930
0.050	0.2174	0.3153	0.4684	0.6238	0.6613	0.6780	0.6869
0.100	0.2104	0.3035	0.4476	0.5938	0.6291	0.6449	0.6533
0.150	0.2044	0.2942	0.4326	0.5733	0.6072	0.6223	0.6304
0.200	0.2007	0.2886	0.4238	0.5612	0.5943	0.6091	0.6170
0.300	0.1974	0.2835	0.4160	0.5505	0.5829	0.5974	0.6051
0.400	0.1963	0.2819	0.4135	0.5470	0.5792	0.5936	0.6013
0.500	0.1960	0.2814	0.4127	0.5459	0.5781	0.5924	0.6001

Table 3.14 Influence of c/b on the normalized SIFs in a Zirconia-Rene 41 strip under transient thermal stress, with respect to nondimensional time τ , b/h=0.100, κ=1.68

τ	c/b=0.5	c/b=1	c/b=2	c/b=5	c/b=10	c/b=20	c/b=40
0	0	0	0	0	0	0	0
0.0025	0.0520	0.1074	0.2228	0.3399	0.3713	0.3882	0.3970
0.005	0.1020	0.1736	0.3064	0.4408	0.4769	0.4963	0.5065
0.010	0.1463	0.2301	0.3744	0.5202	0.5595	0.5805	0.5916
0.015	0.1663	0.2547	0.4028	0.5524	0.5926	0.6142	0.6256
0.020	0.1772	0.2680	0.4175	0.5683	0.6090	0.6308	0.6423
0.030	0.1881	0.2805	0.4302	0.5811	0.6218	0.6436	0.6551
0.040	0.1927	0.2852	0.4337	0.5835	0.6239	0.6455	0.6569
0.050	0.1944	0.2866	0.4335	0.5817	0.6216	0.6431	0.6544
0.100	0.1921	0.2805	0.4197	0.5601	0.5979	0.6182	0.6289
0.150	0.1879	0.2735	0.4077	0.5429	0.5794	0.5989	0.6093
0.200	0.1852	0.2691	0.4004	0.5326	0.5683	0.5874	0.5975
0.300	0.1827	0.2652	0.3938	0.5234	0.5584	0.5771	0.5870
0.400	0.1819	0.2639	0.3917	0.5205	0.5552	0.5738	0.5837
0.500	0.1817	0.2635	0.3910	0.5196	0.5542	0.5728	0.5826

Table 3.15 Influence of c/b on the normalized SIFs in a Zirconia-Rene 41 strip under transient thermal stress, with respect to nondimensional time τ , b/h=0.200, κ=1.68

τ	c/b=0.5	c/b=1	c/b=2	c/b=5	c/b=10	c/b=20	c/b=40
0	0	0	0	0	0	0	0
0.0025	-0.0164	0.0025	0.0700	0.1444	0.1787	0.1991	0.2104
0.005	-0.0019	0.0306	0.1174	0.2127	0.2565	0.2827	0.2971
0.010	0.0318	0.0798	0.1846	0.2993	0.3522	0.3837	0.4010
0.015	0.0559	0.1121	0.2253	0.3490	0.4059	0.4399	0.4586
0.020	0.0725	0.1336	0.2515	0.3800	0.4393	0.4746	0.4941
0.030	0.0932	0.1597	0.2819	0.4151	0.4765	0.5131	0.5332
0.040	0.1050	0.1741	0.2978	0.4326	0.4947	0.5318	0.5522
0.050	0.1123	0.1826	0.3067	0.4417	0.5040	0.5411	0.5616
0.100	0.1246	0.1956	0.3165	0.4481	0.5087	0.5449	0.5648
0.150	0.1269	0.1968	0.3146	0.4427	0.5018	0.5370	0.5564
0.200	0.1277	0.1968	0.3127	0.4386	0.4967	0.5314	0.5504
0.300	0.1282	0.1967	0.3108	0.4348	0.4920	0.5261	0.5449
0.400	0.1283	0.1966	0.3101	0.4336	0.4905	0.5244	0.5431
0.500	0.1284	0.1966	0.3099	0.4332	0.4900	0.5239	0.5425

Table 3.16 Influence of c/b on the normalized SIFs in a Zirconia-Rene 41 strip under transient thermal stress, with respect to nondimensional time τ , b/h=0.400, κ=1.68

τ	c/b=0.5	c/b=1	c/b=2	c/b=5	c/b=10	c/b=20	c/b=40
0	0	0	0	0	0	0	0
0.0025	-0.0231	-0.0211	0.0137	0.0736	0.1143	0.1437	0.1620
0.005	-0.0305	-0.0253	0.0217	0.1023	0.1570	0.1966	0.2211
0.010	-0.0363	-0.0244	0.0374	0.1427	0.2141	0.2657	0.2977
0.015	-0.0350	-0.0175	0.0536	0.1741	0.2557	0.3148	0.3514
0.020	-0.0307	-0.0087	0.0688	0.1996	0.2883	0.3523	0.3921
0.030	-0.0201	0.0084	0.0938	0.2374	0.3347	0.4050	0.4486
0.040	-0.0104	0.0223	0.1122	0.2628	0.3649	0.4386	0.4843
0.050	0.0000	0.0330	0.1255	0.2803	0.3851	0.4608	0.5077
0.100	0.0190	0.0601	0.1560	0.3158	0.4239	0.5020	0.5504
0.150	0.0280	0.0707	0.1664	0.3254	0.4331	0.5108	0.5590
0.200	0.0327	0.0760	0.1713	0.3296	0.4367	0.5140	0.5620
0.300	0.0367	0.0806	0.1755	0.3329	0.4395	0.5164	0.5642
0.400	0.0380	0.0821	0.1768	0.3340	0.4404	0.5172	0.5648
0.500	0.0384	0.0825	0.1772	0.3343	0.4407	0.5174	0.5651

Table 3.17 Variation of the normalized SIFs in a Zirconia-Rene 41 strip under steady state thermal stress with respect to b/h for different c/b's, κ=1.68

c/b	b/h= 0.05	b/h= 0.10	b/h= 0.15	b/h= 0.20	b/h= 0.25	b/h= 0.35	b/h= 0.40	b/h= 0.45	b/h= 0.50
0.5	0.2106	0.1815	0.1542	0.1284	0.1041	0.0593	0.0386	0.0189	0.0002
1	0.2996	0.2633	0.2290	0.1966	0.1659	0.1090	0.0827	0.0579	0.0344
2	0.4344	0.3907	0.3492	0.3099	0.2727	0.2065	0.1774	0.1501	0.1237
5	0.5726	0.5191	0.4714	0.4340	0.4023	0.3546	0.3345	0.3151	0.2952
10	0.6052	0.5537	0.5167	0.4898	0.4703	0.4470	0.4408	0.4368	0.4338
20	0.6155	0.5723	0.5429	0.5236	0.5125	0.5100	0.5175	0.5303	0.5479
40	0.6208	0.5821	0.5569	0.5422	0.5362	0.5477	0.5651	0.5908	0.6257

3.3.2 Stress Intensity Factors (Figures)

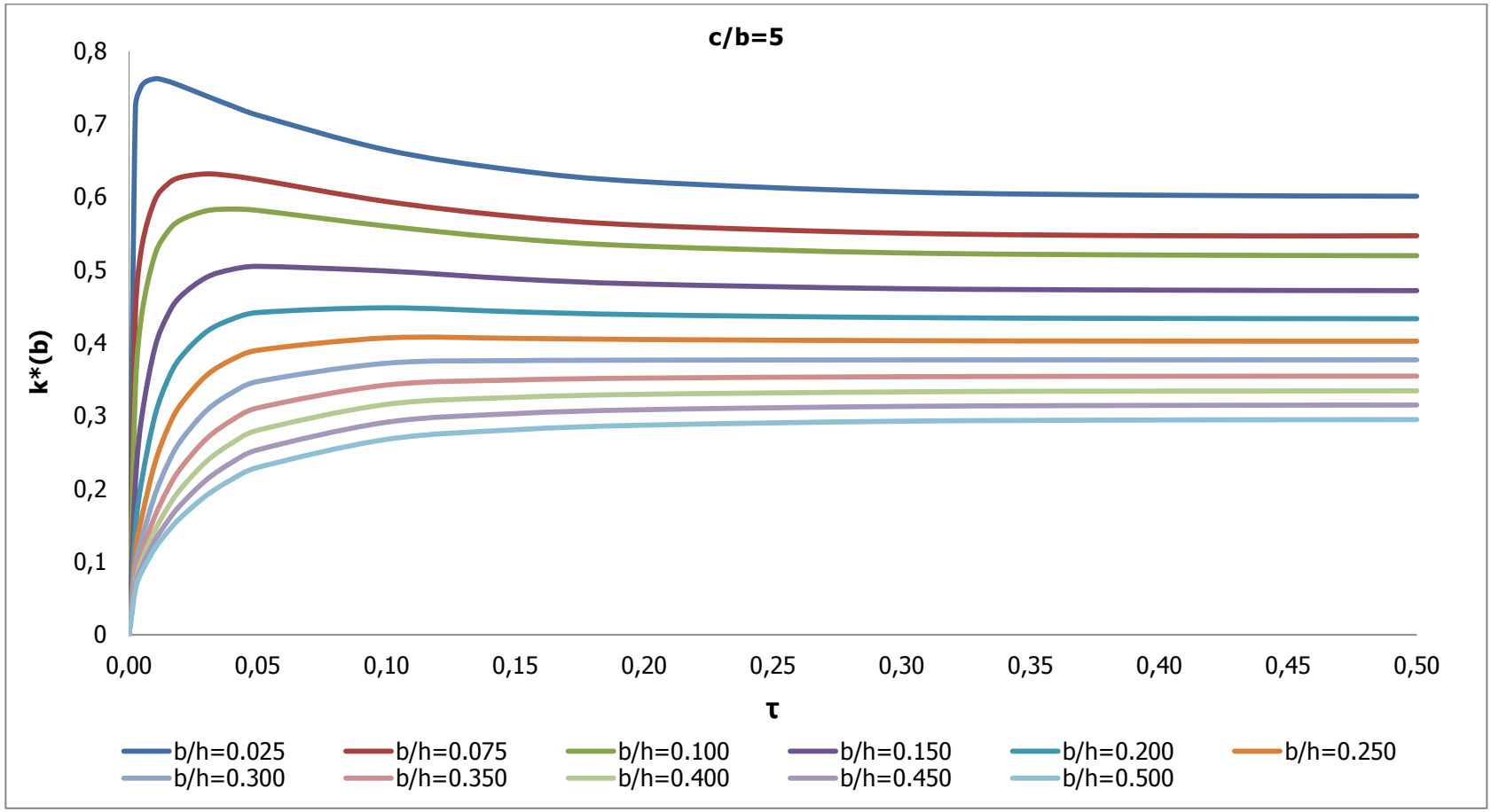

Figure 3.14 Influence of b/h on the normalized SIFs in a Zirconia-Rene 41 strip under transient thermal stress, with respect to nondimensional time τ , c/b=5, κ=1.68

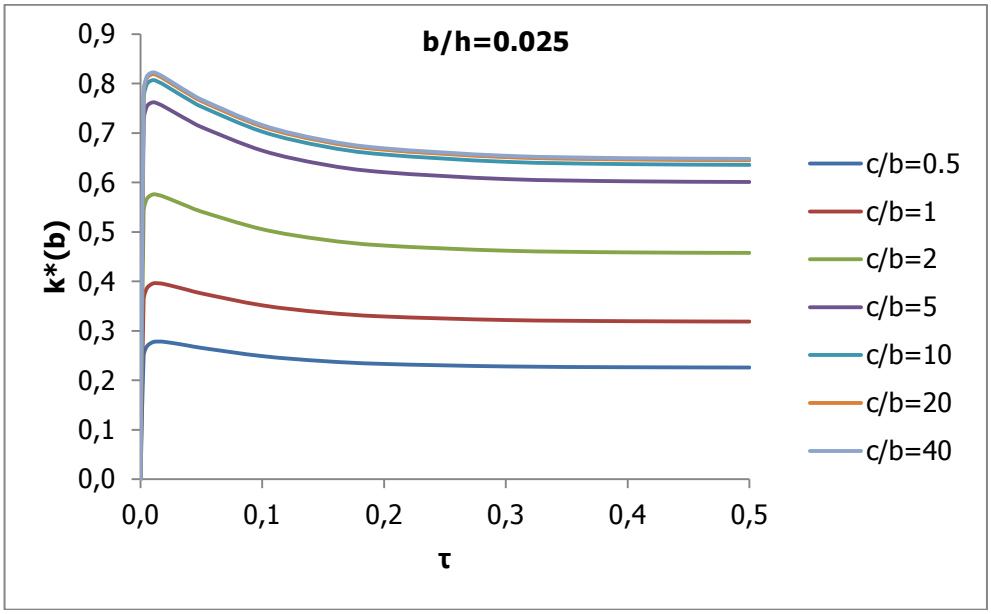

Figure 3.15 Influence of c/b on the normalized SIFs in a Zirconia-Rene 41 strip under transient thermal stress, with respect to nondimensional time τ , b/h=0.025, κ=1.68

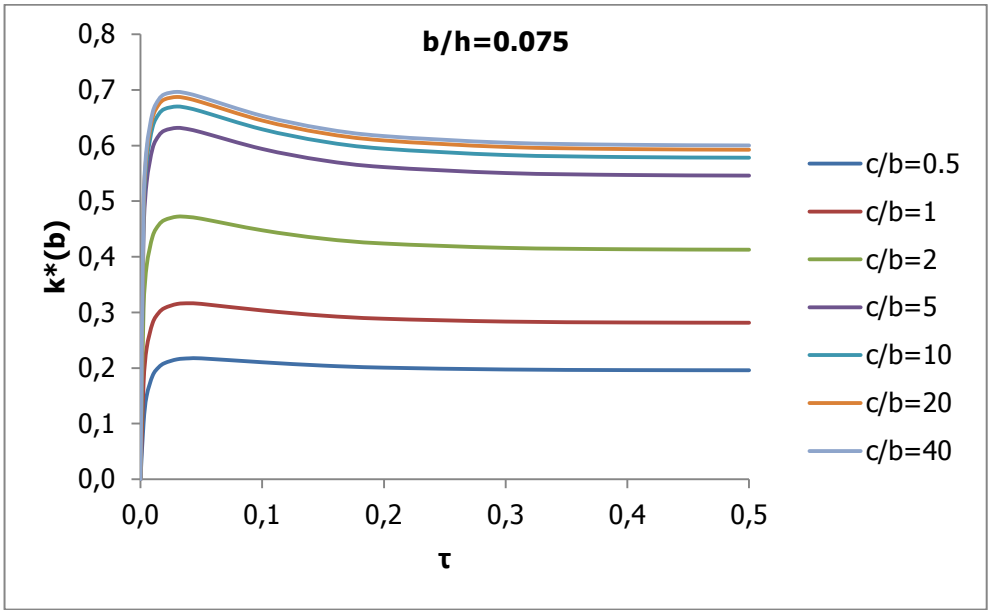

Figure 3.16 Influence of c/b on the normalized SIFs in a Zirconia-Rene 41 strip under transient thermal stress, with respect to nondimensional time τ , b/h=0.075, κ=1.68

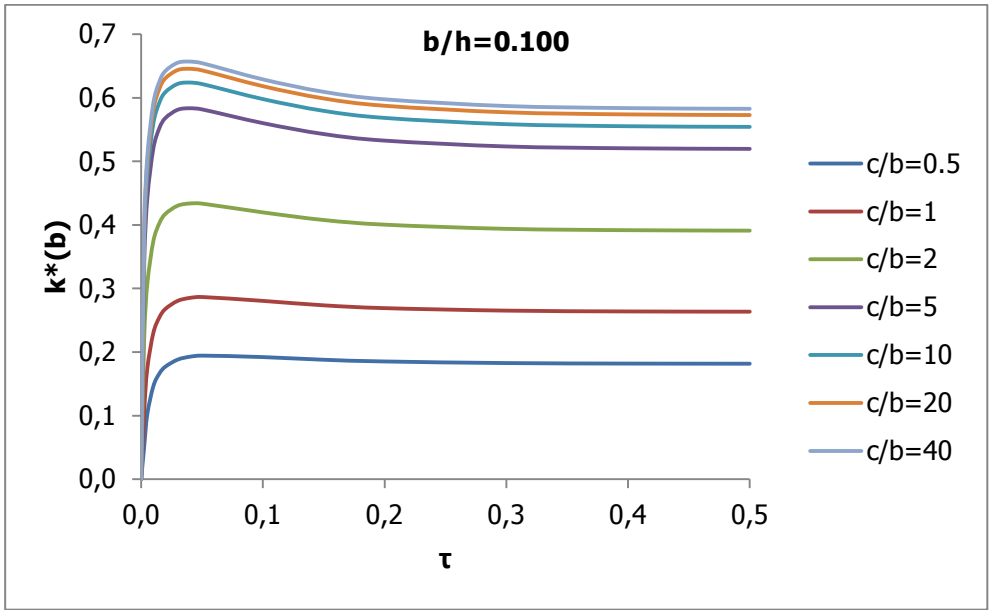

Figure 3.17 Influence of c/b on the normalized SIFs in a Zirconia-Rene 41 strip under transient thermal stress, with respect to nondimensional time τ , b/h=0.100, κ=1.68

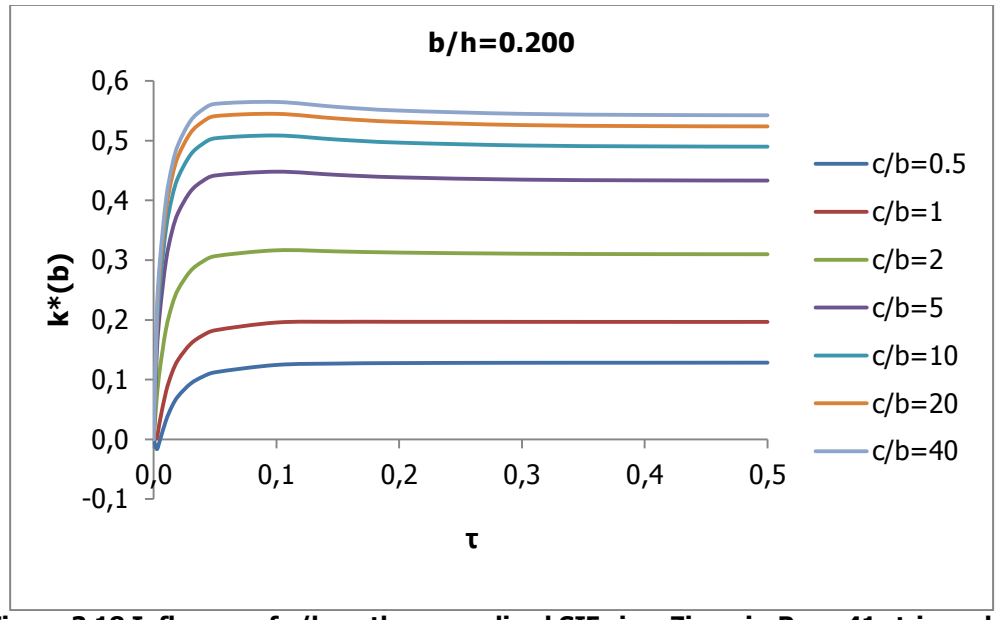

Figure 3.18 Influence of c/b on the normalized SIFs in a Zirconia-Rene 41 strip under transient thermal stress, with respect to nondimensional time τ , b/h=0.200, κ=1.68

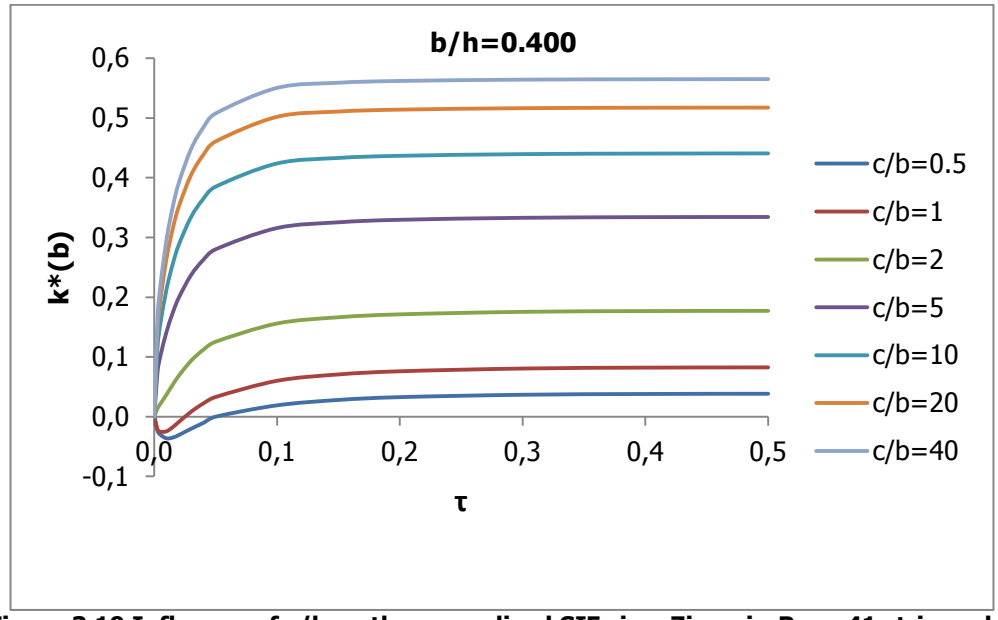

Figure 3.19 Influence of c/b on the normalized SIFs in a Zirconia-Rene 41 strip under transient thermal stress, with respect to nondimensional time τ , b/h=0.400, κ=1.68

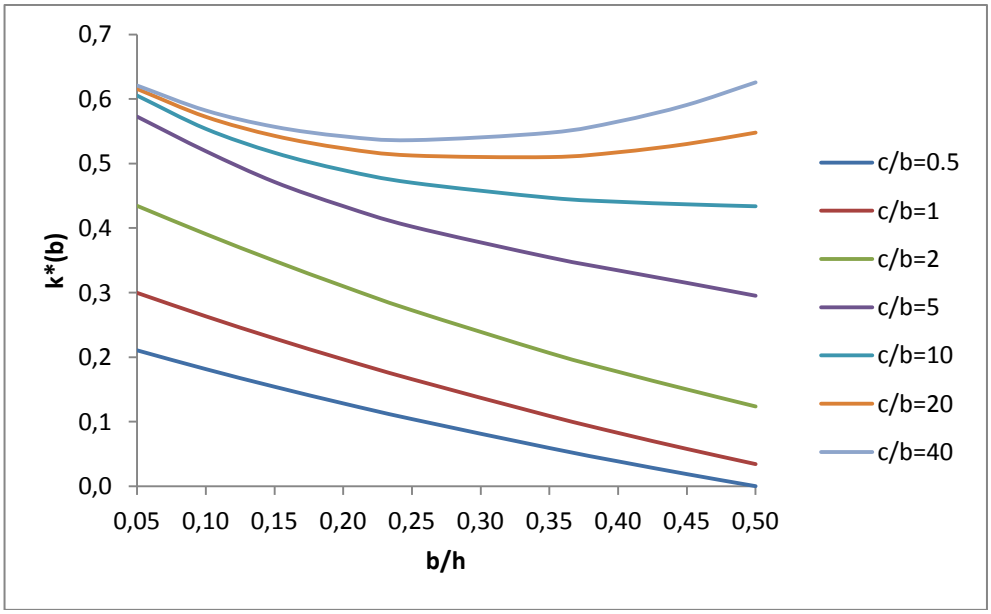

Figure 3.20 Variation of the normalized SIFs in a Zirconia-Rene 41 strip under steady state thermal stress with respect to b/h for different c/b's, κ=1.68

CHAPTER 4

DISCUSSION, CONCLUSION AND FUTURE STUDIES

4.1 Discussion

In this study, stress intensity factors (SIFs) are calculated for periodic edge cracks in an FGM strip. Uniform crack surface traction, fixed grip, transient heat conduction and steady state heat conduction are the applied load types. Results are given in tables and figures in Chapter 3. The crack problem is formulated and the computer program which is suitable for the problem studied in [36] is modified. SIFs calculated under uniform crack surface traction are compared with [12], [36], [39] and the FEM results provided by Dr. B. Yıldırım. SIFs calculated under fixed grip loading are compared with the results given in [10]. A good agreement is observed in all these comparisons.

Table 3.1 shows that for smaller crack spacing, the effect of crack length on SIF is smaller. For homogeneous materials, as b/h increases the normalized SIF increases.

Table 3.2 shows the comparison of the results with [36] in which periodic crack in a half plane is examined. As the strip thickness increases or b/h decreases, SIFs decrease and approach to the results of [36]. For smaller crack spacing this approach is faster. The SIFs of edge crack in half plane provide the lower bound for SIFs obtained in this study.

The results for uniform crack surface traction are given in Tables 3.3 – 3.6 and Figs. 3.1 – 3.4 and compared with the FEM results [41]. The SIFs of single edge crack studied in [12] are observed to be the upper bound for SIFs found in this study. For small crack period, SIF increases as E_1/E_0 increases. Same behavior is obtained in [36]. However, when the crack space is larger SIF decreases as E_1/E_0 increases. This result is consistent with [12].

In Fig. 3.5 we plot the normalized stress intensity factors for stiffening strip with respect to crack length for various crack spacings. The increase in SIFs at large crack spacing is more significant with increasing crack length.

The results for fixed grip loading are given in Tables 3.7 – 3.9 and Figs. 3.6 – 3.9. The SIFs of single edge crack studied in [10] provide the upper bound for SIFs obtained in this study. As for uniform crack surface traction, Fig. 3.9 shows that the increase in SIFs at large crack spacing is more significant with increasing crack length.

Thermal SIFs for periodic cracks are quantified for a particular material pair Zirconia-Rene 41.

The temperature distribution and thermal stresses are shown in Fig. 3.10 and Fig. 3.11 for $T_t^*=0.1$, in Fig. 3.12 and Fig. 3.13 for $T_t^*=20$. It can be easily seen that as the nondimensional time, τ, approaches to 1, the temperature distribution approaches to steady state.

From Fig. 3.11 and Fig. 3.13, it can be said that the side of the strip where the cracks exist is under tension for T_t*=0.1 (cooling thermal shock) and under compression for T_t*=20 (heating thermal shock). Moreover, it is understood that maximum of the thermal stresses occurs at the surface subjected to the thermal shock for all time.
In Fig. 3.14 SIF vs. nondimensional time τ in a Zirconia-Rene 41 strip is plotted for different crack lengths. The crack spacing is kept constant. The variations of the SIFs with respect to τ are similar to [12]. For smaller crack length, SIFs reach a peak and then decrease and approach a steady state value. However, for longer cracks, SIFs asymptotically approach the steady state value which happens to be the maximum value for SIFs.

In Figs. 3.15- 3.19 the normalized stress intensity factors with respect to τ are given for various crack spacings and crack lengths. At very beginning of the thermal shock negative SIFs are obtained for larger crack length. This is an expectable result because Fig. 3.11 shows that σ_{yy} changes sign after some x value. Therefore, the region where the crack tip exist is under compression. Negative SIF means that the crack is closed up to a point close to the surface that is subjected to the thermal shock.

In Fig. 3.20 the normalized stress intensity factors under steady state thermal stress are plotted with respect to b/h for different crack spacing values. For smaller crack spacings, SIF decreases as crack length increases. However, for large crack spacing, although thermal stress decreases with increasing of x, SIFs increase as b/h increases after some value of crack length. This is because, the crack length has a more dominant influence on SIF for large crack spacing as shown in Fig. 3.5.

4.2 Conclusion

In this thesis, periodic edge cracks in a functionally graded strip was examined. Normalized stress intensity factors (mode I) were computed under three loading types: uniform crack surface traction, fixed grip loading and thermal loading.

The following concluding remarks can be stated:

- Under uniform crack surface traction and fixed grip loading, SIFs increase as crack length increases and this increase is more significant at large crack spacing.
- Periodic cracking is more effective in relieving stresses for all three loading types so single crack SIFs provide an upper bound. Crack arrest is more likely in the case of periodic cracks.
- For transient thermal conduction problem, SIFs go to a peak and then tend to their relatively lower steady state value for smaller crack lengths. However, they increase and reach a steady state value for larger crack lengths.
- Under transient thermal loading, for very large crack length, crack closure (crack face contact) may happen because the region where the crack tip exist could be subjected to compression.

4.3 Future Studies

As a future study, periodic imbedded crack in an FGM strip can be investigated. This requires a minor modification in the program to implement single valuedness condition. Periodic crack in an FGM cylinder can be studied. This can be done by introducing an elastic foundation at $x=h$ boundary as in [12]. Then the SIF solutions approximate those of periodic circumferential cracks in a thin walled FGM cylinder. Finally, by eliminating constant diffusivity assumption, a more realistic temperature distribution and thereby thermal stress solutions can be used. More realistic temperature distributions have been readily given in [34] and [35] for small τ values.

REFERENCES

[1] ASGHARI, M. and GHAFOORI, E., 'A Three-Dimensional Elasticity Solution for Functionally Graded Rotating Disks', Composite Structures, Vol. 92, pp.1092-1099, 2010.

[2] AFSAR, A. M. and SOHAG, F. A., 'Effect of FGM Coating on Thermoelastic Characteristics of a Rotating Circular Disk', The International Conference on Marine Technology, Buet, Dhaha, Bangladesh, 11-12 December 2010.

[3] RUYS, A. and SUN, D., 'Functionally Graded Materials (FGM) and Their Production Methods', 2002.
Retrieved from: http://www.azom.com/article.aspx?ArticleID=1592# 22.01.2013

[4] SLADEK J., SLADEK V. and ZHANG C., 'Stress Analysis in Anisotropic Functionally Graded Materials by the MLPG Method', Engineering Analysis with Boundary Elements, Vol. 29, pp. 597-609, 2005.

[5] KIEBACK, B., NEUBRAND, A. and RIEDEL, H., 'Processing Techniques for Functionally Graded Materials', Materials Science and Engineering, Vol. A362, pp. 81-105, 2003.

[6] KIM, J. I., KIM, W.-J., CHOI, D. J. and PARK, J. Y., 'Deposition of Compositionally Graded SiC/C Layers on C-C Composites by Low Pressure Chemical Vapor Deposition', Journal of Nuclear Materials, Vol. 307-311, pp. 1084-1087, 2002.

[7] KAWASAKI, A. and WATANABE, R., 'Concept and P/M Fabrication of Functionally Gradient Materials', Ceramics International, Vol. 23, pp. 73-83, 1997.

[8] RODRÍGUEZ-CASTRO, R., WETHERHOLD, R. C. and KELESTEMUR, M. H., 'Microstructure and Mechanical Behavior of Functionally Graded Al A359/SiC_p Composite', Materials Science and Engineering, Vol.A323, pp. 445-456, 2002.

[9] MOON, J., CABALLERO, A. C., HOZER, L., CHIANG, Y.-M. and CIMA, M. J., 'Fabrication of Functionally Graded Reaction Infiltrated SiC-Si Composite by Three-Dimensional Printing (3DPTM) Process', Materials Science and Engineering, Vol. A298, pp. 110-119, 2001.

[10] ERDOGAN, F. and WU, B. H., 'Analysis of FGM Specimens for Fracture Toughness Testing', The American Ceramic Society, Vol. 34, pp. 39-46, 1993.

[11] ERDOGAN, F. and WU, B. H., 'Crack Problems in FGM Layers Under Thermal Stresses', J Therm Stresses, Vol. 19, pp. 237-265, 1996.

[12] DAĞ, S., 'Crack Problems in a Functionally Graded Layer Under Thermal Stresses', M.Sc. Thesis, METU, Ankara, 1997.

[13] KADIOĞLU, S., DAĞ, S. and YAHŞİ, O. S., 'Crack Problem for a Functionally Graded Layer on an Elastic Foundation', International Journal of Fracture, Vol. 94, pp. 63-77, 1998.

[14] DAĞ, S., KADIOĞLU, S. and YAHŞİ, O. S., 'Circumferential Crack Problem for an FGM Cylinder Under Thermal Stresses', Journal of Thermal Stresses, Vol. 22, pp. 659-687, 1999.

[15] LEE, Y.-D. and ERDOGAN, F., "Interface Cracking of FGM Coatings Under Steady – State Heat Flow", Engineering Fracture Mechanics, Vol. 59, pp. 361-380, 1998.

[16] JIN, Z.-H. and PAULINO, G.H., "Transient Thermal Stress Analysis of an Edge Crack in a Functionally Graded Material", International Journal of Fracture, Vol. 107, pp. 73-98, 2001.

[17] GUO, L. C. and NODA, N., 'Fracture Mechanics Analysis of Functionally Graded Layered Structures With a Crack Crossing The Interface', Mechanics of Material, Vol. 40, pp. 81-99, 2008.

[18] GUO, L. C., WANG, Z. H. and ZHANG, L., 'A Fracture Mechanics Problem of a Functionally Graded Layered Structure With an Arbitrarily Oriented Crack Crossing The Interface', Mechanics of Material, Vol. 46, pp. 69-82, 2012.

[19] SHABANA, Y. M. and NODA, N., "Geometry Effects of Substrate and Coating Layers on the Thermal Stress Response of FGM Structure", Acta Mechanica, Vol. 159, pp.143-156, 2002.

[20] CHI, S.-H. and CHUNG, Y.-L., "Cracking in Coating – Substrate Composites with Multi - Layered and FGM Coatings", Engineering Fracture Mechanics, Vol. 70, pp. 1227-1243, 2003.

[21] YILDIRIM, B., DAG, S. and ERDOGAN, F., 'Three Dimensional Fracture Analysis of FGM Coatings Under Thermomechanical Loading', International Journal of Fracture, Vol. 132, pp. 369-395, 2005.

[22] NAMI, M. R. and ESKANDARI, H., 'Three-Dimensional Investigations of Stress Intensity Factors in a Thermo-Mechanically Loaded Cracked FGM Hollow Cylinder', International Journal of Pressure Vessels and Piping, Vol. 89, pp. 222-229, 2012.

[23] AFSAR, A. M. and ANISUZZAMAN, M., 'Stress Intensity Factors of Two Diametrically Opposed Edge Cracks in a Thick-Walled Functionally Graded Material Cylinder', Engineering Fracture Mechanics, Vol.74, pp. 1617-1636, 2007.

[24] AFSAR, A. M. and SONG, J. I., 'Effect of FGM Coating Thickness on Apparent Fracture Toughness of a Thick-Walled Cylinder', Engineering Fracture Mechanics, Vol.77, pp. 2919-2926, 2010.

[25] BABAEI, M. H. and CHEN, Z. T., 'Hyperbolic Heat Conduction in a Functionally Graded Hollow Sphere', International Journal of Thermophysics, Vol. 29, pp. 1457-1469, 2008.

[26] BABAEI, M. H. and CHEN, Z. T., 'Transient Hyperbolic Heat Conduction in a Functionally Graded Hollow Cylinder', Journal of Thermophysics and Heat Transfer, Vol. 24, No. 2, 2010.

[27] KELES, I. and CONKER, C., 'Transient Hyperbolic Heat Conduction in Thick-Walled FGM Cylinders and Spheres With Exponentially-Varying Properties', European Journal of Mechanics A/Solids, Vol. 30, pp. 449-455, 2011.

[28] HU, K. and CHEN, Z., 'Thermoelastic Analysis of o Partially Insulated Crack in a Strip Under Thermal Impact Loading Using The Hyperbolic Heat Conduction Theory', International Journal of Engineering Science, Vol. 51, pp. 144-160, 2012.

[29] CHANG, D. M. and WANG, B. L., 'Transient Thermal Fracture and Crack Growth Behavior in Brittle Media Based on Non-Fourier Heat Conduction', Engineering Fracture Mechanics, Vol. 94, pp. 29-36, 2012.

[30] ERDOGAN, F. and ÖZTÜRK, M., 'Periodic Cracking of Functionally Graded coatings, International Journal Engineering Science, Vol.33, pp.2179–2195, 1995.

[31] WANG, B. L. and MAI, Y. –W., 'A Periodic Array of Cracks in Functionally Graded Materials Subjected to Thermo-Mechanical Loading', International Journal of Engineering Science, Vol. 43, pp. 432–446, 2005.

[32] WANG, B. L. and MAI, Y. –W., 'A Periodic Array of Cracks in Functionally Graded Materials Subjected to Transient Loading', International Journal of Engineering Science, Vol. 44, pp. 351–364, 2006.

[33] DING, S. –H. and LI, X., 'Anti-Plane Problem of Periodic Interface Cracks in a Functionally Graded Coating-Substrate Structure', International Journal of Fracture, Vol.153, pp. 53-62, 2008.

[34] JIN, Z. –H. and FENG, Y. Z., 'Thermal Fracture Resistance of a Functionally Graded Coating with Periodic Edge Cracks', Surface & Coatings Technology, Vol. 202, pp. 4189–4197, 2008.

[35] JIN, Z. –H. and FENG, Y. Z., 'Thermal Fracture of Functionally Graded Plate with Parallel Surface Cracks', Acta Mechanica Solida Sinica, Vol. 22, pp. 453-464, 2009.

[36] YILDIRIM, B., KUTLU, Ö. and KADIOĞLU, S., 'Periodic Crack Problem for a Functionally Graded Half-Plane an Analytic Solution', International Journal of Solids and Structures, Vol. 48, pp. 3020–3031, 2011.

[37] SCHULZE, G. W. and ERDOGAN, F., 'Periodic Cracking of Elastic Coatings', International Journal of Solids and Structures, Vol. 35, pp. 3615-3634, 1998.

[38] DAĞ, S. and ERDOGAN, F., 'A Surface Crack in a Graded Medium Loaded by a Sliding Rigid Stamp', Engineering Fracture Mechanics, Vol. 69, Issues 14-16, pp. 1729-1751, 2002.

[39] SCHULZE, G., 'Infinite Homogeneous Strip with Periodic Array of Edge Cracks', Ph.D. Dissertation, Lehigh University, 1995.

[40] ÇETİN, S., 'Analytical Solution of a Crack Problem in a Radially Graded FGM', M.Sc. Thesis, METU, Ankara, 2007.

[41] Private communication with Dr. B. Yıldırım from Hacettepe University Mechanical Engineering Department.

APPENDIX-A

CALCULATION OF I_1, I_2, I_3 AND I_4

Following calculations are done by Maple to evaluate integral using Residue Theorem.

```
> assign(rho1=-beta*I/2-I/2*sqrt(beta^2+4*alpha^2-4*I*alpha*beta*sqrt((3-
kappa)/(kappa+1))));
> assign(rho2=-beta*I/2+I/2*sqrt(beta^2+4*alpha^2-4*I*alpha*beta*sqrt((3-
kappa)/(kappa+1))));
> assign(rho3=-beta*I/2-I/2*sqrt(beta^2+4*alpha^2+4*I*alpha*beta*sqrt((3-
kappa)/(kappa+1))));
> assign(rho4=-beta*I/2+I/2*sqrt(beta^2+4*alpha^2+4*I*alpha*beta*sqrt((3-
kappa)/(kappa+1))));
> assign(denominator=rho^4+2*I*rho^3*beta-rho^2*beta^2+alpha^2*(beta^2*(3-
kappa)/(kappa+1)+alpha^2+2*rho^2+2*I*beta*rho));
> assign(F1=exp(I*t*rho)*rho/denominator);
> simplify(residue(F1,rho=rho2));
```

$$\frac{\frac{1}{4} I\, \mathbf{e}^{\left(\frac{t\left(-\sqrt{\beta^2+4\alpha^2-4 I \alpha \beta \sqrt{-\frac{\kappa-3}{\kappa+1}}}+\beta\right)}{2}\right)}\left(-\sqrt{\beta^2+4\alpha^2-4 I \alpha \beta \sqrt{-\frac{\kappa-3}{\kappa+1}}}+\beta\right)}{\sqrt{\beta^2+4\alpha^2-4 I \alpha \beta \sqrt{-\frac{\kappa-3}{\kappa+1}}}\ \alpha \beta \sqrt{-\frac{\kappa-3}{\kappa+1}}}$$

Substituting λ_j's;

$$Res\ F_1(\rho_2) = \frac{i\lambda_4\,(-\lambda_2+\beta)}{\lambda_1\lambda_2}$$

```
> simplify(residue(F1,rho=rho4));
```

$$\frac{\frac{-1}{4} I\, \mathbf{e}^{\left(\frac{t\left(-\sqrt{\beta^2+4\alpha^2+4 I \alpha \beta \sqrt{-\frac{\kappa-3}{\kappa+1}}}+\beta\right)}{2}\right)}\left(-\sqrt{\beta^2+4\alpha^2+4 I \alpha \beta \sqrt{-\frac{\kappa-3}{\kappa+1}}}+\beta\right)}{\sqrt{\beta^2+4\alpha^2+4 I \alpha \beta \sqrt{-\frac{\kappa-3}{\kappa+1}}}\ \alpha \beta \sqrt{-\frac{\kappa-3}{\kappa+1}}}$$

Substituting λ_j's;

$$Res\ F_1(\rho_4) = -\frac{i\lambda_5\,(-\lambda_3+\beta)}{\lambda_1\lambda_3}$$

$$Res\ F_1(\rho_2) + Res\ F_1(\rho_4) = \frac{i\lambda_4\,(-\lambda_2+\beta)}{\lambda_1\lambda_2} - \frac{i\lambda_5\,(-\lambda_3+\beta)}{\lambda_1\lambda_3}$$

Simplifying;

$$Res\ F_1(\rho_2) + Res\ F_1(\rho_4) = \frac{i}{\lambda_1}\left[\lambda_4\left(-1+\frac{\beta}{\lambda_2}\right) - \lambda_5\left(-1+\frac{\beta}{\lambda_3}\right)\right]$$

Since $I_1(t) = 2\pi i\big(Res\ F_1(\rho_2) + Res\ F_1(\rho_4)\big)$

$$I_1(t) = 2\pi i\left\{\frac{i}{\lambda_1}\left[\lambda_4\left(-1+\frac{\beta}{\lambda_2}\right) - \lambda_5\left(-1+\frac{\beta}{\lambda_3}\right)\right]\right\}$$

$$I_1(t) = \frac{2\pi}{\lambda_1}\left[\lambda_4\left(1-\frac{\beta}{\lambda_2}\right) - \lambda_5\left(1-\frac{\beta}{\lambda_3}\right)\right]$$

```
> assign(F2=exp(I*(t-h)*rho)*rho/denominator);
> simplify(residue(F2,rho=rho1));
```

$$\frac{\frac{-1}{4} I\, \mathbf{e}^{\left(-\frac{\left(\sqrt{\beta^2+4\alpha^2-4 I \alpha \beta \sqrt{-\frac{\kappa-3}{\kappa+1}}}+\beta\right)(-t+h)}{2}\right)}\left(\sqrt{\beta^2+4\alpha^2-4 I \alpha \beta \sqrt{-\frac{\kappa-3}{\kappa+1}}}+\beta\right)}{\sqrt{\beta^2+4\alpha^2-4 I \alpha \beta \sqrt{-\frac{\kappa-3}{\kappa+1}}}\ \alpha \beta \sqrt{-\frac{\kappa-3}{\kappa+1}}}$$

Substituting λ_j's;

$$Res\ F_2(\rho_1) = -\frac{i\lambda_6(\lambda_2+\beta)}{\lambda_1\lambda_2}$$

```
> simplify(residue(F2,rho=rho3));
```

$$\frac{\frac{1}{4} I\, \mathbf{e}^{\left(-\frac{\left(\sqrt{\beta^2+4\alpha^2+4 I \alpha \beta \sqrt{-\frac{\kappa-3}{\kappa+1}}}+\beta\right)(-t+h)}{2}\right)}\left(\sqrt{\beta^2+4\alpha^2+4 I \alpha \beta \sqrt{-\frac{\kappa-3}{\kappa+1}}}+\beta\right)}{\sqrt{\beta^2+4\alpha^2+4 I \alpha \beta \sqrt{-\frac{\kappa-3}{\kappa+1}}}\ \alpha \beta \sqrt{-\frac{\kappa-3}{\kappa+1}}}$$

Substituting λ_j's;

$$Res\ F_2(\rho_3) = \frac{i\lambda_7(\lambda_3+\beta)}{\lambda_1\lambda_3}$$

$$Res\ F_2(\rho_1) + Res\ F_2(\rho_3) = -\frac{i\lambda_6(\lambda_2+\beta)}{\lambda_1\lambda_2} + \frac{i\lambda_7(\lambda_3+\beta)}{\lambda_1\lambda_3}$$

Simplifying;

$$Res\ F_2(\rho_1) + Res\ F_2(\rho_3) = \frac{i}{\lambda_1}\left[-\lambda_6\left(1+\frac{\beta}{\lambda_2}\right) + \lambda_7\left(1+\frac{\beta}{\lambda_3}\right)\right]$$

Since $I_2(t) = -2\pi i\big(Res\ F_2(\rho_1) + Res\ F_2(\rho_3)\big)$

$$I_2(t) = -2\pi i\left\{\frac{i}{\lambda_1}\left[-\lambda_6\left(1+\frac{\beta}{\lambda_2}\right)+\lambda_7\left(1+\frac{\beta}{\lambda_3}\right)\right]\right\}$$

$$I_2(t) = \frac{2\pi}{\lambda_1}\left[-\lambda_6\left(1+\frac{\beta}{\lambda_2}\right)+\lambda_7\left(1+\frac{\beta}{\lambda_3}\right)\right]$$

```
> assign(F3=exp(I*t*rho)*(beta-I*rho)*rho/denominator);
> simplify(residue(F3,rho=rho2));
```

$$-\frac{1}{2}\frac{e^{\left(\frac{t\left(-\sqrt{\beta^2+4\alpha^2-4I\alpha\beta\sqrt{-\frac{\kappa-3}{\kappa+1}}}+\beta\right)}{2}\right)}\left(\beta\sqrt{-\frac{\kappa-3}{\kappa+1}}+\alpha I\right)}{\sqrt{\beta^2+4\alpha^2-4I\alpha\beta\sqrt{-\frac{\kappa-3}{\kappa+1}}}\;\beta\sqrt{-\frac{\kappa-3}{\kappa+1}}}$$

Substituting λ_j's;

$$Res\ F_3(\rho_2) = -\frac{1}{2}\frac{\lambda_4(\beta\sqrt{\frac{3-\kappa}{\kappa+1}}+\alpha i)}{\lambda_2\beta\sqrt{\frac{3-\kappa}{\kappa+1}}}$$

Multiplying by 4α both the numerator and the denominator;

$$Res\ F_3(\rho_2) = -\frac{1}{2}\frac{\lambda_4(\lambda_1+4i\alpha^2)}{\lambda_1\lambda_2}$$

```
> simplify(residue(F3,rho=rho4));
```

$$\frac{1}{2}\frac{e^{\left(\frac{t\left(-\sqrt{\beta^2+4\alpha^2+4I\alpha\beta\sqrt{-\frac{\kappa-3}{\kappa+1}}}+\beta\right)}{2}\right)}\left(-\beta\sqrt{-\frac{\kappa-3}{\kappa+1}}+\alpha I\right)}{\sqrt{\beta^2+4\alpha^2+4I\alpha\beta\sqrt{-\frac{\kappa-3}{\kappa+1}}}\;\beta\sqrt{-\frac{\kappa-3}{\kappa+1}}}$$

Substituting λ_j's;

$$Res\ F_3(\rho_4) = \frac{1}{2}\frac{\lambda_5(-\beta\sqrt{\frac{3-\kappa}{\kappa+1}}+\alpha i)}{\lambda_3\beta\sqrt{\frac{3-\kappa}{\kappa+1}}}$$

Multiplying by 4α both the numerator and the denominator;

$$Res\ F_3(\rho_4) = \frac{1}{2}\frac{\lambda_5(-\lambda_1+4i\alpha^2)}{\lambda_1\lambda_3}$$

$$Res\ F_3(\rho_2) + Res\ F_3(\rho_4) = -\frac{1}{2}\frac{\lambda_4(\lambda_1+4i\alpha^2)}{\lambda_1\lambda_2}+\frac{1}{2}\frac{\lambda_5(-\lambda_1+4i\alpha^2)}{\lambda_1\lambda_3}$$

Simplifying;

$$Res\ F_3(\rho_2) + Res\ F_3(\rho_4) = \frac{1}{2\lambda_1}\left[-\frac{\lambda_4}{\lambda_2}(\lambda_1 + 4i\alpha^2) + \frac{\lambda_5}{\lambda_3}(-\lambda_1 + 4i\alpha^2)\right]$$

Since $I_3(t) = 2\pi i\big(Res\ F_3(\rho_2) + Res\ F_3(\rho_4)\big)$

$$I_3(t) = 2\pi i\left\{\frac{1}{2\lambda_1}\left[-\frac{\lambda_4}{\lambda_2}(\lambda_1 + 4i\alpha^2) + \frac{\lambda_5}{\lambda_3}(-\lambda_1 + 4i\alpha^2)\right]\right\}$$

$$I_3(t) = \frac{\pi i}{\lambda_1}\left[-\frac{\lambda_4}{\lambda_2}(\lambda_1 + 4i\alpha^2) + \frac{\lambda_5}{\lambda_3}(-\lambda_1 + 4i\alpha^2)\right]$$

```
> assign(F4=exp(I*(t-h)*rho)*(beta-I*rho)*rho/denominator);
> simplify(residue(F4,rho=rho1));
```

$$\frac{1}{2}\frac{e^{\left(-\frac{\left(\sqrt{\beta^2+4\alpha^2-4I\alpha\beta\sqrt{-\frac{\kappa-3}{\kappa+1}}}+\beta\right)(-t+h)}{2}\right)}\left(\beta\sqrt{-\frac{\kappa-3}{\kappa+1}}+\alpha I\right)}{\sqrt{\beta^2+4\alpha^2-4I\alpha\beta\sqrt{-\frac{\kappa-3}{\kappa+1}}}\ \beta\sqrt{-\frac{\kappa-3}{\kappa+1}}}$$

Substituting λ_j's;

$$Res\ F_4(\rho_1) = \frac{1}{2}\frac{\lambda_6(\beta\sqrt{\frac{3-\kappa}{\kappa+1}} + \alpha i)}{\lambda_2\beta\sqrt{\frac{3-\kappa}{\kappa+1}}}$$

Multiplying by 4α both the numerator and the denominator;

$$Res\ F_4(\rho_1) = \frac{1}{2}\frac{\lambda_6(\lambda_1 + 4i\alpha^2)}{\lambda_1\lambda_2}$$

```
> simplify(residue(F4,rho=rho3));
```

$$-\frac{1}{2}\frac{e^{\left(-\frac{\left(\sqrt{\beta^2+4\alpha^2+4I\alpha\beta\sqrt{-\frac{\kappa-3}{\kappa+1}}}+\beta\right)(-t+h)}{2}\right)}\left(-\beta\sqrt{-\frac{\kappa-3}{\kappa+1}}+\alpha I\right)}{\sqrt{\beta^2+4\alpha^2+4I\alpha\beta\sqrt{-\frac{\kappa-3}{\kappa+1}}}\ \beta\sqrt{-\frac{\kappa-3}{\kappa+1}}}$$

Substituting λ_j's;

$$Res\ F_4(\rho_3) = -\frac{1}{2}\frac{\lambda_7(-\beta\sqrt{\frac{3-\kappa}{\kappa+1}} + \alpha i)}{\lambda_3\beta\sqrt{\frac{3-\kappa}{\kappa+1}}}$$

Multiplying by 4α both the numerator and the denominator;

$$Res\ F_4(\rho_3) = -\frac{1}{2}\frac{\lambda_7(-\lambda_1 + 4i\alpha^2)}{\lambda_1\lambda_3}$$

$$Res\ F_4(\rho_1) + Res\ F_4(\rho_3) = \frac{1}{2}\frac{\lambda_6(\lambda_1 + 4i\alpha^2)}{\lambda_1\lambda_2} - \frac{1}{2}\frac{\lambda_7(-\lambda_1 + 4i\alpha^2)}{\lambda_1\lambda_3}$$

Simplifying;

$$Res\ F_4(\rho_1) + Res\ F_4(\rho_3) = \frac{1}{2\lambda_1}\left[\frac{\lambda_6}{\lambda_2}(\lambda_1 + 4i\alpha^2) - \frac{\lambda_7}{\lambda_3}(-\lambda_1 + 4i\alpha^2)\right]$$

Since $I_4(t) = -2\pi i\big(Res\ F_4(\rho_1) + Res\ F_4(\rho_3)\big)$

$$I_4(t) = -2\pi i\left\{\frac{1}{2\lambda_1}\left[\frac{\lambda_6}{\lambda_2}(\lambda_1 + 4i\alpha^2) - \frac{\lambda_7}{\lambda_3}(-\lambda_1 + 4i\alpha^2)\right]\right\}$$

$$I_4(t) = \frac{\pi i}{\lambda_1}\left[-\frac{\lambda_6}{\lambda_2}(\lambda_1 + 4i\alpha^2) + \frac{\lambda_7}{\lambda_3}(-\lambda_1 + 4i\alpha^2)\right]$$

APPENDIX-B

INTEGRALS

Following expression is used to evaluate 2nd and 4th terms of Eqn. (172) and it is taken from [40].

$$\int_A^\infty \frac{\sin(\lambda(s-r)\rho)d\rho}{\rho^{2n}} = \cos(A\lambda(s-r)) \sum_{j=1}^{n-1} \frac{(-1)^{j+1}\left(\lambda(s-r)\right)^{2j-1}(2n-2j-1)!}{(2n-1)!A^{2n-2j}} + \sin(A\lambda(s-r)) \sum_{j=1}^{n} \frac{(-1)^{j+1}\left(\lambda(s-r)\right)^{2j-1}(2n-2j)!}{(2n-1)!A^{2n-2j+1}} + (-1)^n \frac{\left(\lambda(s-r)\right)^{2n-1}}{(2n-1)!} Ci(A\lambda(s-r))$$

This identity is valid for every positive integer value of n but is used for $n=2,4,6,8,10,12$.

Ci is the cosine integral and it is given below.

$$Ci\big(A\lambda(s-r)\big) = \gamma_0 + \log|A\lambda(s-r)| + \int_0^{|A\lambda(s-r)|} \frac{\cos\alpha - 1}{\alpha} d\alpha$$

$$\int_A^\infty \frac{\cos(\lambda(s-r)\rho)d\rho}{\rho^{2n-1}} = \cos(A\lambda(s-r)) \sum_{j=1}^{n-1} \frac{(-1)^{j+1}\left(\lambda(s-r)\right)^{2(j-1)}(2n-2j-1)!}{(2n-2)!A^{2n-2j}} + \sin(A\lambda(s-r)) \sum_{j=1}^{n-1} \frac{(-1)^{j}\left(\lambda(s-r)\right)^{2j-1}(2n-2j-2)!}{(2n-2)!A^{2n-2j-1}} + (-1)^n \frac{\left(\lambda(s-r)\right)^{2n-2}}{(2n-2)!} Ci(A\lambda(s-r))$$

This identity is valid for every positive integer value of n but is used for $n=3,5,7,9,11$.

$$\int_C^\infty \frac{e^{-(t+x)\alpha}}{\alpha} d\alpha = -Ei(-(t+x)C)$$

$$\int_C^\infty \frac{e^{-(t+x)\alpha}}{\alpha^{n+1}} d\alpha = (-1)^{n+1} \frac{(t+x)^n Ei(-(t+x)C)}{n!} + \frac{e^{-(t+x)C}}{C^n} \sum_{k=0}^{n-1} \frac{(-1)^k (t+x)^k C^k}{n(n-1)\ldots(n-k)}$$

n is any positive integer and the function Ei is the exponential integral function which is defined as follows,

$$Ei(x) = \int_{-x}^\infty \frac{e^{-t}}{t} dt \qquad x < 0$$

$$Ei(x) = -\lim_{\varepsilon \to +0} \left[\int_{-x}^{-\varepsilon} \frac{e^{-t}}{t} dt + \int_\varepsilon^\infty \frac{e^{-t}}{t} dt\right] \qquad x > 0$$

APPENDIX-C

ASYMPTOTIC EXPANSIONS

Following expressions, ($c_0, c_2,..., c_{12}$) and ($b_1, b_3,...,b_{11}$) are for the infinite integrals and they are the same as those given in [12]. Instead of β and κ symbols, bb and K are used.

```
c0=(8.*(-1.+K))/(1.+K)
c2=(2.*bb**2*(-1.+K)**2)/((1.+K)**2)
c4=-(bb**4*(-1.+K)*(-5.+2.*K+K**2))/(2.*(1.+K)**3)
c6=(bb**6*(-1.+K)*(-39.-7.*K+13.*K**2+K**3))/(8.*(1.+K)**4)
c8=(bb**8*(-3.+K)*(-1.+K)*(-18.+27.*K+49.*K**2+15.*K**3+K**4))/
        (32.*(1.+K)**5)
c10=-(bb**10*(-3.+K)*(-1.+K)*(-178.-
        10.*K+276.*K**2+204.*K**3+102.*K**4+
        51.*K**5+14.*K**6+K**7))/(128.*(1.+K)**6)
c12=(bb**12*(-3.+K)*(-1.+K)*(-1260.-
        619.*K+1875.*K**2+2078.*K**3+1050.*K**4+
        382.*K**5+90.*K**6+38.*K**7+36.*K**8+13.*K**9+
        K**10))/(512.*(1.+K)**7)
b1=4.*bb*(K-1.)/(K+1.)
b3=-((bb**3*(-1.+K)**2)/((1.+K)**2))
b5=(bb**5*(-1.+K)*(-13.+6.*K+K**2))/(4.*(1.+K)**3)
b7=(bb**7*(-3.+K)*(-1.+K)*(-9.+2.*K+K**2))/(16.*(1.+K)**4)
b9=-(bb**9*(-3.+K)*(-1.+K)*
        (-67.+38.*K+94.*K**2+52.*K**3+14.*K**4+K**5))/
        (64.*(1.+K)**5)
b11=(bb**11*(-3.+K)*(-1.+K)*(-491.+76.*K+
        664.*K**2+406.*K**3+127.*K**4+
        51.*K**5+37.*K**6+13.*K**7+K**8))/(256.*(1.+K)**6)
```

Following expressions, (a_2, a_1, a_0, a_{-1}) are taken from [36]. sBB denotes the sign of β. Instead of a_2, a_1, a_0 and a_{-1}, ca2, ca1, ca0, cam1 are used. DBLE() extracts real part of its argument in double precision. DIMAG() extracts imaginary part of its argument in double precision.

```
zp1=-1
zp0=-BB/2.-(0,1/2.)*Sqrt(BB**2*(3-K)/(1+K))*sBB
zpm1=-BB**2/(2*(1+K))
zpm2=(0,3/4.)*BB**2*Sqrt(BB**2*(3-K)/(1+K))*sBB/((3-K)*(1+K))-
(0,1/4.)*BB**2*K*Sqrt(BB**2*(3-K)/(1+K))*sBB/((3-K)*(1+K))
zpm3=BB**4/(2*(1+K)**2)-BB**4*K/(8*(1+K)**2)
zpm4=(0,-3/8.)*BB**4*Sqrt(BB**2*(3-K)/(1+K))*sBB/(1+K)**2+
        (0,1/16.)*BB**4*K*Sqrt(BB**2*(3-K)/(1+K))*sBB/(1+K)**2
zq0=1
zqm1=-BB+BB*K/2.-(0,1/2.)*K*Sqrt(BB**2*(3-K)/(1+K))*sBB
zqm2=BB**2-BB**2*K+BB**2*K**2/4.-BB**2/(8*(1+K))-
        BB**2*K/(2*(1+K))+BB**2*K**2/(8*(1+K))+
        (0,1/2.)*BB*Sqrt(BB**2*(3-K)/(1+K))*sBB+
        (0,1/4.)*BB*K*Sqrt(BB**2*(3-K)/(1+K))*sBB-
```

```
        (0,1/4.)*BB*K**2*Sqrt(BB**2*(3-K)/(1+K))*sBB-
        3*BB**2*sBB**2/(8*(1+K))-BB**2*K*sBB**2/(4*(1+K))+
        BB**2*K**2*sBB**2/(8*(1+K))
zqm3=-BB**3+3*BB**3*K/2.-3*BB**3*K**2/4.+BB**3*K**3/8.+
        5*BB**3/(8*(1+K))+3*BB**3*K/(16*(1+K))-
        3*BB**3*K**2/(8*(1+K))+BB**3*K**3/(16*(1+K))-
        (0,1)*BB**2*Sqrt(BB**2*(3-K)/(1+K))*sBB+
        (0,1/2.)*BB**2*K*Sqrt(BB**2*(3-K)/(1+K))*sBB+
        (0,1/4.)*BB**2*K**2*Sqrt(BB**2*(3-K)/(1+K))*sBB-
        (0,1/8.)*BB**2*K**3*Sqrt(BB**2*(3-K)/(1+K))*sBB+
        (0,1/16.)*BB**2*Sqrt(BB**2*(3-K)/(1+K))*sBB/(1+K)+
        (0,3/4.)*BB**2*Sqrt(BB**2*(3-K)/(1+K))*sBB/((3-K)*(1+K))+
        (0,1/2.)*BB**2*K*Sqrt(BB**2*(3-K)/(1+K))*sBB/(1+K)-
        (0,1/4.)*BB**2*K*Sqrt(BB**2*(3-K)/(1+K))*sBB/((3-K)*(1+K))-
        (0,1/16.)*BB**2*K**2*Sqrt(BB**2*(3-K)/(1+K))*sBB/(1+K)+
        9*BB**3*sBB**2/(8*(1+K))+3*BB**3*K*sBB**2/(16*(1+K))-
        3*BB**3*K**2*sBB**2/(4*(1+K))+3*BB**3*K**3*sBB**2/(16*(1+K))+
        (0,3/16.)*BB**2*Sqrt(BB**2*(3-K)/(1+K))*sBB**3/(1+K)+
        (0,1/8.)*BB**2*K*Sqrt(BB**2*(3-K)/(1+K))*sBB**3/(1+K)-
        (0,1/16.)*BB**2*K**2*Sqrt(BB**2*(3-K)/(1+K))*sBB**3/(1+K)
xp1=dble(zp1)
xp0=dble(zp0)
xpm1=dble(zpm1)
xpm2=dble(zpm2)
xpm3=dble(zpm3)
xpm4=dble(zpm4)
yp1=dimag(zp1)
yp0=dimag(zp0)
ypm1=dimag(zpm1)
ypm2=dimag(zpm2)
ypm3=dimag(zpm3)
ypm4=dimag(zpm4)
xq0=dble(zq0)
xqm1=dble(zqm1)
xqm2=dble(zqm2)
xqm3=dble(zqm3)
yq0=dimag(zq0)
yqm1=dimag(zqm1)
yqm2=dimag(zqm2)
yqm3=dimag(zqm3)
zS1=xp1 - xq0 + (0,1)*yp1 - (0,1)*yq0
zS0=xp0 - xqm1 + (0,1)*yp0 - (0,1)*yqm1
zSm1=xpm1 - xqm2 + (0,1)*ypm1 - (0,1)*yqm2
zSm2=xpm2 - xqm3 + (0,1)*ypm2 - (0,1)*yqm3
zSm3=xpm3 + (0,1)*ypm3
zSm4=xpm4 + (0,1)*ypm4

zM1=3 - K + xp1*xq0 + K*xp1*xq0 + (0,1)*xq0*yp1 +(0,1)*K*xq0*yp1+
        (0,1)*xp1*yq0 + (0,1)*K*xp1*yq0 - yp1*yq0 - K*yp1*yq0
zM0=xp1*xqm1 + K*xp1*xqm1 + xp0*xq0 + K*xp0*xq0 + (0,1)*xq0*yp0 +
        (0,1)*K*xq0*yp0 + (0,1)*xqm1*yp1 + (0,1)*K*xqm1*yp1 +
        (0,1)*xp1*yqm1 + (0,1)*K*xp1*yqm1 - yp1*yqm1 - K*yp1*yqm1 +
        (0,1)*xp0*yq0 + (0,1)*K*xp0*yq0 - yp0*yq0 - K*yp0*yq0
zMm1=xp0*xqm1 + K*xp0*xqm1 + xp1*xqm2 + K*xp1*xqm2 + xpm1*xq0 +
        K*xpm1*xq0 + (0,1)*xq0*ypm1 + (0,1)*K*xq0*ypm1 +
```

```
        (0,1)*xqm1*yp0 + (0,1)*K*xqm1*yp0 + (0,1)*xqm2*yp1 +
        (0,1)*K*xqm2*yp1+(0,1)*xp0*yqm1 + (0,1)*K*xp0*yqm1- yp0*yqm1 –
        K*yp0*yqm1+(0,1)*xp1*yqm2 + (0,1)*K*xp1*yqm2 - yp1*yqm2 –
        K*yp1*yqm2 +(0,1)*xpm1*yq0 + (0,1)*K*xpm1*yq0 –ypm1*yq0 –
        K*ypm1*yq0
zMm2=xpm1*xqm1 + K*xpm1*xqm1 + xp0*xqm2 + K*xp0*xqm2 +
        xp1*xqm3 + K*xp1*xqm3 + xpm2*xq0 + K*xpm2*xq0 +
        (0,1)*xqm1*ypm1 + (0,1)*K*xqm1*ypm1 + (0,1)*xq0*ypm2 +
        (0,1)*K*xq0*ypm2 +(0,1)*xqm2*yp0 + (0,1)*K*xqm2*yp0 +
        (0,1)*xqm3*yp1 +(0,1)*K*xqm3*yp1 + (0,1)*xpm1*yqm1 +
        (0,1)*K*xpm1*yqm1 - ypm1*yqm1 - K*ypm1*yqm1 +
        (0,1)*xp0*yqm2 + (0,1)*K*xp0*yqm2 - yp0*yqm2 –
        K*yp0*yqm2 + (0,1)*xp1*yqm3 + (0,1)*K*xp1*yqm3 –
        yp1*yqm3 - K*yp1*yqm3 + (0,1)*xpm2*yq0 + (0,1)*K*xpm2*yq0 –
        ypm2*yq0 - K*ypm2*yq0
zMm3=xpm2*xqm1 + K*xpm2*xqm1 + xpm1*xqm2 + K*xpm1*xqm2 +
        xp0*xqm3 + K*xp0*xqm3 + xpm3*xq0 + K*xpm3*xq0 +
        (0,1)*xqm2*ypm1 +  (0,1)*K*xqm2*ypm1 + (0,1)*xqm1*ypm2 +
        (0,1)*K*xqm1*ypm2 +  (0,1)*xq0*ypm3 + (0,1)*K*xq0*ypm3 +
        (0,1)*xqm3*yp0 + (0,1)*K*xqm3*yp0 + (0,1)*xpm2*yqm1 +
        (0,1)*K*xpm2*yqm1 - ypm2*yqm1 – K*ypm2*yqm1 +
        (0,1)*xpm1*yqm2 + (0,1)*K*xpm1*yqm2 - ypm1*yqm2 –
        K*ypm1*yqm2 + (0,1)*xp0*yqm3 + (0,1)*K*xp0*yqm3 - yp0*yqm3 -
        K*yp0*yqm3 + (0,1)*xpm3*yq0 + (0,1)*K*xpm3*yq0 - ypm3*yq0 -
        K*ypm3*yq0
zMm4=xpm3*xqm1 + K*xpm3*xqm1 + xpm2*xqm2 +K*xpm2*xqm2 +
         xpm1*xqm3 +K*xpm1*xqm3 + xpm4*xq0 + K*xpm4*xq0 +
        (0,1)*xqm3*ypm1 + (0,1)*K*xqm3*ypm1 + (0,1)*xqm2*ypm2 +
        (0,1)*K*xqm2*ypm2 + (0,1)*xqm1*ypm3 + (0,1)*K*xqm1*ypm3 +
        (0,1)*xq0*ypm4 +(0,1)*K*xq0*ypm4 + (0,1)*xpm3*yqm1 +
        (0,1)*K*xpm3*yqm1 -ypm3*yqm1 - K*ypm3*yqm1+
        (0,1)*xpm2*yqm2 +(0,1)*K*xpm2*yqm2 - ypm2*yqm2 –
        K*ypm2*yqm2+(0,1)*xpm1*yqm3 + (0,1)*K*xpm1*yqm3 –
        ypm1*yqm3 - K*ypm1*yqm3 +(0,1)*xpm4*yq0 +
        (0,1)*K*xpm4*yq0 - ypm4*yq0 - K*ypm4*yq0
xS1 =DBLE(zS1)
xS0 =DBLE(zS0)
xSm1=DBLE(zSm1)
xSm2=DBLE(zSm2)
xSm3=DBLE(zSm3)
xSm4=DBLE(zSm4)
xM1 =DBLE(zM1)
xM0 =DBLE(zM0)
xMm1=DBLE(zMm1)
xMm2=DBLE(zMm2)
xMm3=DBLE(zMm3)
xMm4=DBLE(zMm4)
yS1 =DIMAG(zS1)
yS0 =DIMAG(zS0)
ySm1=DIMAG(zSm1)
ySm2=DIMAG(zSm2)
ySm3=DIMAG(zSm3)
ySm4=DIMAG(zSm4)
yM1 =DIMAG(zM1)
yM0 =DIMAG(zM0)
```

```
yMm1=DIMAG(zMm1)
yMm2=DIMAG(zMm2)
yMm3=DIMAG(zMm3)
yMm4=DIMAG(zMm4)
vvss=Sqrt((3*BB**2-BB**2*K)/(1+K))*sBB/2.
zF1m1=Pi/(2*BB*Sqrt((3-K)/(1+K)))
zF1m2=-Pi/(4*Sqrt((3-K)/(1+K)))
zF1m3=(0,-1/8.)*Sqrt(BB**2*(3-K)/(1+K))*Pi*sBB/Sqrt((3-K)/(1+K))
zF1m4=BB**2*Pi*(2+3*sBB**2-K*sBB**2)/ (16*Sqrt((3-K)/(1+K))*(1+K))
zF30=Pi/(2*BB*Sqrt((3-K)/(1+K)))
zF3m1=(0,-1)*Pi*(BB*Sqrt((3-K)/(1+K))/2.-
        Sqrt(BB**2*(3-K)/(1+K))*sBB/4.)/(BB*Sqrt((3-K)/(1+K)))
zF3m2=(0,-1)*Pi*((0,1/4.)*BB*Sqrt((3-K)/(1+K))*
        Sqrt(BB**2*(3-K)/(1+K))*sBB+(0,1/8.)*BB**2*
        (-2-3*sBB**2+K*sBB**2)/(1+K))/(BB*Sqrt((3-K)/(1+K)))
zF3m3=(0,-1)*Pi*(BB**3*Sqrt((3-K)/(1+K))*(-2-3*sBB**2+K*sBB**2)/
        (8*(1+K))+(0,1/2.)*((0,1/4.)*BB**4*(-3+K)*sBB/
        (Sqrt(BB**2*(3-K)/(1+K))*(1+K)**2)-
        (0,1/4.)*BB**2*Sqrt(BB**2*(3-K)/(1+K))*sBB/(1+K)+
        (0,1/8.)*BB**2*Sqrt(BB**2*(3-K)/(1+K))*sBB*
        (-2-3*sBB**2+K*sBB**2)/(1+K)))/ (BB*Sqrt((3-K)/(1+K)))

xF1m1=DBLE(zF1m1)
xF1m2=DBLE(zF1m2)
xF1m3=DBLE(zF1m3)
xF1m4=DBLE(zF1m4)
yF1m1=DIMAG(zF1m1)
yF1m2=DIMAG(zF1m2)
yF1m3=DIMAG(zF1m3)
yF1m4=DIMAG(zF1m4)
xF30 =DBLE(zF30)
xF3m1=DBLE(zF3m1)
xF3m2=DBLE(zF3m2)
xF3m3=DBLE(zF3m3)
yF30 =DIMAG(zF30)
yF3m1=DIMAG(zF3m1)
yF3m2=DIMAG(zF3m2)
yF3m3=DIMAG(zF3m3)

zNR12=(0,4)*xF30*(xM1 - (0,1)*yM1) - 4*yF30*(xM1 - (0,1)*yM1) +
        (0,4)*(-xF1m1 - (0,1)*yF1m1)*(xS1 - (0,1)*yS1) +
        (0,4)*K*(xF1m1 + (0,1)*yF1m1)*(xS1 - (0,1)*yS1)
zNR11=(0,4)*xF30*xM0 + (0,4)*xS0*(-xF1m1 - (0,1)*yF1m1) +
        (0,4)*K*xS0*(xF1m1 + (0,1)*yF1m1) - 4*xM0*yF30 + 4*xF30*yM0 +
        (0,4)*yF30*yM0 + (0,4)*(xF3m1 + (0,1)*yF3m1)*(xM1 - (0,1)*yM1) +
        4*(-xF1m1 - (0,1)*yF1m1)*yS0 + 4*K*(xF1m1 + (0,1)*yF1m1)*yS0 –
        (0,4)*(xF1m2 + (0,1)*yF1m2)*(xS1 - (0,1)*yS1) +
        (0,4)*K*(xF1m2 + (0,1)*yF1m2)*(xS1 - (0,1)*yS1)
zNR10=(0,-4)*xS0*(xF1m2 + (0,1)*yF1m2) +
        (0,4)*K*xS0*(xF1m2 + (0,1)*yF1m2) +
        (0,4)*xM0*(xF3m1+ (0,1)*yF3m1)+ (0,4)*xF30*(xMm1 -(0,1)*yMm1) -
        4*yF30*(xMm1 - (0,1)*yMm1) + 4*(xF3m1 + (0,1)*yF3m1)*yM0 +
        (0,4)*(xF3m2 + (0,1)*yF3m2)*(xM1 - (0,1)*yM1) +
        (0,4)*(-xF1m1 - (0,1)*yF1m1)*(xSm1 - (0,1)*ySm1) +
        (0,4)*K*(xF1m1 + (0,1)*yF1m1)*(xSm1 - (0,1)*ySm1) –
```

```
        4*(xF1m2 + (0,1)*yF1m2)*yS0 + 4*K*(xF1m2 + (0,1)*yF1m2)*yS0 –
        (0,4)*(xF1m3 + (0,1)*yF1m3)*(xS1 - (0,1)*yS1) +
        (0,4)*K*(xF1m3 + (0,1)*yF1m3)*(xS1 - (0,1)*yS1)
zNR1m1=(0,-4)*xS0*(xF1m3 + (0,1)*yF1m3) +
        (0,4)*K*xS0*(xF1m3 + (0,1)*yF1m3) +
        (0,4)*xM0*(xF3m2 + (0,1)*yF3m2) +
        (0,4)*(xF3m1 + (0,1)*yF3m1)*(xMm1 - (0,1)*yMm1) +
        (0,4)*xF30*(xMm2 - (0,1)*yMm2) - 4*yF30*(xMm2 - (0,1)*yMm2) +
        4*(xF3m2 + (0,1)*yF3m2)*yM0 +
        (0,4)*(xF3m3 + (0,1)*yF3m3)*(xM1 - (0,1)*yM1) –
        (0,4)*(xF1m2 + (0,1)*yF1m2)*(xSm1 - (0,1)*ySm1) +
        (0,4)*K*(xF1m2 + (0,1)*yF1m2)*(xSm1 - (0,1)*ySm1) +
        (0,4)*(-xF1m1 - (0,1)*yF1m1)*(xSm2 - (0,1)*ySm2) +
        (0,4)*K*(xF1m1 + (0,1)*yF1m1)*(xSm2 - (0,1)*ySm2) –
        4*(xF1m3 + (0,1)*yF1m3)*yS0 + 4*K*(xF1m3 + (0,1)*yF1m3)*yS0 –
        (0,4)*(xF1m4 + (0,1)*yF1m4)*(xS1 - (0,1)*yS1) +
        (0,4)*K*(xF1m4 + (0,1)*yF1m4)*(xS1 - (0,1)*yS1)
zNR22=(0,-4)*xF30*(xM1 - (0,1)*yM1) - 4*yF30*(xM1 - (0,1)*yM1) +
        (0,4)*(xF1m1 - (0,1)*yF1m1)*(xS1 - (0,1)*yS1) –
        (0,4)*K*(xF1m1 - (0,1)*yF1m1)*(xS1 - (0,1)*yS1)
zNR21=(0,-4)*xF30*xM0 + (0,4)*xS0*(xF1m1 - (0,1)*yF1m1) –
        (0,4)*K*xS0*(xF1m1 - (0,1)*yF1m1) - 4*xM0*yF30 - 4*xF30*yM0 +
        (0,4)*yF30*yM0 - (0,4)*(xF3m1 - (0,1)*yF3m1)*(xM1 - (0,1)*yM1) +
        4*(xF1m1 - (0,1)*yF1m1)*yS0 - 4*K*(xF1m1 - (0,1)*yF1m1)*yS0 +
        (0,4)*(xF1m2 - (0,1)*yF1m2)*(xS1 - (0,1)*yS1) –
        (0,4)*K*(xF1m2 - (0,1)*yF1m2)*(xS1 - (0,1)*yS1)
zNR20=(0,4)*xS0*(xF1m2 - (0,1)*yF1m2) –
        (0,4)*K*xS0*(xF1m2 - (0,1)*yF1m2) –
        (0,4)*xM0*(xF3m1 - (0,1)*yF3m1) - (0,4)*xF30*(xMm1 -(0,1)*yMm1) -
        4*yF30*(xMm1 - (0,1)*yMm1) - 4*(xF3m1 - (0,1)*yF3m1)*yM0 -
        (0,4)*(xF3m2 - (0,1)*yF3m2)*(xM1 - (0,1)*yM1) +
        (0,4)*(xF1m1 - (0,1)*yF1m1)*(xSm1 - (0,1)*ySm1) –
        (0,4)*K*(xF1m1 - (0,1)*yF1m1)*(xSm1 - (0,1)*ySm1) +
        4*(xF1m2 - (0,1)*yF1m2)*yS0 - 4*K*(xF1m2 - (0,1)*yF1m2)*yS0 +
        (0,4)*(xF1m3 - (0,1)*yF1m3)*(xS1 - (0,1)*yS1) -
        (0,4)*K*(xF1m3 - (0,1)*yF1m3)*(xS1 - (0,1)*yS1)
zNR2m1=(0,4)*xS0*(xF1m3 - (0,1)*yF1m3) –
        (0,4)*K*xS0*(xF1m3 - (0,1)*yF1m3) -
        (0,4)*xM0*(xF3m2 - (0,1)*yF3m2) -
        (0,4)*(xF3m1 - (0,1)*yF3m1)*(xMm1 - (0,1)*yMm1) -
        (0,4)*xF30*(xMm2 - (0,1)*yMm2) - 4*yF30*(xMm2 - (0,1)*yMm2) -
        4*(xF3m2 - (0,1)*yF3m2)*yM0 -
        (0,4)*(xF3m3 - (0,1)*yF3m3)*(xM1 - (0,1)*yM1) +
        (0,4)*(xF1m2 - (0,1)*yF1m2)*(xSm1 - (0,1)*ySm1) -
        (0,4)*K*(xF1m2 - (0,1)*yF1m2)*(xSm1 - (0,1)*ySm1) +
        (0,4)*(xF1m1 - (0,1)*yF1m1)*(xSm2 - (0,1)*ySm2) -
        (0,4)*K*(xF1m1 - (0,1)*yF1m1)*(xSm2 - (0,1)*ySm2) +
        4*(xF1m3 - (0,1)*yF1m3)*yS0 - 4*K*(xF1m3 - (0,1)*yF1m3)*yS0 +
        (0,4)*(xF1m4 - (0,1)*yF1m4)*(xS1 - (0,1)*yS1) -
        (0,4)*K*(xF1m4 - (0,1)*yF1m4)*(xS1 - (0,1)*yS1)
zDR2=c*Pi*(xM1 + (0,1)*yM1)*(xS1 - (0,1)*yS1)/2. +
        c*K*Pi*(xM1 + (0,1)*yM1)*(xS1 - (0,1)*yS1)/2. -
        c*Pi*(xM1 - (0,1)*yM1)*(xS1 + (0,1)*yS1)/2. -
        c*K*Pi*(xM1 - (0,1)*yM1)*(xS1 + (0,1)*yS1)/2.
zDR1=-(c*Pi*xS0*(xM1 - (0,1)*yM1))/2. - c*K*Pi*xS0*(xM1 -
```

```
        (0,1)*yM1)/2. + c*Pi*xS0*(xM1 + (0,1)*yM1)/2.+
        c*K*Pi*xS0*(xM1 + (0,1)*yM1)/2. - (0,0.5)*c*Pi*(xM1 –
        (0,1)*yM1)*yS0 - (0,0.5)*c*K*Pi*(xM1 - (0,1)*yM1)*yS0 –
        (0,0.5)*c*Pi*(xM1 + (0,1)*yM1)*yS0 –
        (0,0.5)*c*K*Pi*(xM1 + (0,1)*yM1)*yS0 +
        c*Pi*xM0*(xS1 - (0,1)*yS1)/2. + c*K*Pi*xM0*(xS1 - (0,1)*yS1)/2. +
         (0,0.5)*c*Pi*yM0*(xS1 - (0,1)*yS1) +
        (0,0.5)*c*K*Pi*yM0*(xS1 - (0,1)*yS1) -
        c*Pi*xM0*(xS1 + (0,1)*yS1)/2. - c*K*Pi*xM0*(xS1 + (0,1)*yS1)/2. +
        (0,0.5)*c*Pi*yM0*(xS1 + (0,1)*yS1) +
        (0,0.5)*c*K*Pi*yM0*(xS1 + (0,1)*yS1)
zDR0=(0,1)*c*Pi*xS0*yM0 + (0,1)*c*K*Pi*xS0*yM0 +
        c*Pi*(xM1 + (0,1)*yM1)*(xSm1 - (0,1)*ySm1)/2. +
        c*K*Pi*(xM1 + (0,1)*yM1)*(xSm1 - (0,1)*ySm1)/2. -
        c*Pi*(xM1 - (0,1)*yM1)*(xSm1 + (0,1)*ySm1)/2. -
        c*K*Pi*(xM1 - (0,1)*yM1)*(xSm1 + (0,1)*ySm1)/2. -
        (0,1)*c*Pi*xM0*yS0 - (0,1)*c*K*Pi*xM0*yS0 +
        c*Pi*(xMm1 + (0,1)*yMm1)*(xS1 - (0,1)*yS1)/2. +
        c*K*Pi*(xMm1 + (0,1)*yMm1)*(xS1 - (0,1)*yS1)/2. -
        c*Pi*(xMm1 - (0,1)*yMm1)*(xS1 + (0,1)*yS1)/2. -
        c*K*Pi*(xMm1 - (0,1)*yMm1)*(xS1 + (0,1)*yS1)/2.
zDRm1=-(c*Pi*xS0*(xMm1 - (0,1)*yMm1))/2. -
        c*K*Pi*xS0*(xMm1 - (0,1)*yMm1)/2. +
        c*Pi*xS0*(xMm1 + (0,1)*yMm1)/2. +
        c*K*Pi*xS0*(xMm1 + (0,1)*yMm1)/2. +
        c*Pi*xM0*(xSm1 - (0,1)*ySm1)/2. +
        c*K*Pi*xM0*(xSm1 - (0,1)*ySm1)/2. +
        (0,0.5)*c*Pi*yM0*(xSm1 - (0,1)*ySm1) +
        (0,0.5)*c*K*Pi*yM0*(xSm1 - (0,1)*ySm1) -
        c*Pi*xM0*(xSm1 + (0,1)*ySm1)/2. - c*K*Pi*xM0*
        (xSm1 + (0,1)*ySm1)/2. +
        (0,0.5)*c*Pi*yM0*(xSm1 + (0,1)*ySm1) +
        (0,0.5)*c*K*Pi*yM0*(xSm1 + (0,1)*ySm1) +
        c*Pi*(xM1 + (0,1)*yM1)*(xSm2 - (0,1)*ySm2)/2. +
        c*K*Pi*(xM1 + (0,1)*yM1)*(xSm2 - (0,1)*ySm2)/2. -
        c*Pi*(xM1 - (0,1)*yM1)*(xSm2 + (0,1)*ySm2)/2. -
        c*K*Pi*(xM1 - (0,1)*yM1)*(xSm2 + (0,1)*ySm2)/2. -
        (0,0.5)*c*Pi*(xMm1 - (0,1)*yMm1)*yS0 -
        (0,0.5)*c*K*Pi*(xMm1 - (0,1)*yMm1)*yS0 -
        (0,0.5)*c*Pi*(xMm1 + (0,1)*yMm1)*yS0 -
        (0,0.5)*c*K*Pi*(xMm1 + (0,1)*yMm1)*yS0 +
        c*Pi*(xMm2 + (0,1)*yMm2)*(xS1 - (0,1)*yS1)/2. +
        c*K*Pi*(xMm2 + (0,1)*yMm2)*(xS1 - (0,1)*yS1)/2. -
        c*Pi*(xMm2 - (0,1)*yMm2)*(xS1 + (0,1)*yS1)/2. -
        c*K*Pi*(xMm2 - (0,1)*yMm2)*(xS1 + (0,1)*yS1)/2.
zDRm2=-(c*Pi*xS0*(xMm2 - (0,1)*yMm2))/2. -
        c*K*Pi*xS0*(xMm2 - (0,1)*yMm2)/2. +
        c*Pi*xS0*(xMm2 + (0,1)*yMm2)/2. +
        c*K*Pi*xS0*(xMm2 + (0,1)*yMm2)/2. +
        c*Pi*(xMm1 + (0,1)*yMm1)*(xSm1 - (0,1)*ySm1)/2. +
        c*K*Pi*(xMm1 + (0,1)*yMm1)*(xSm1 - (0,1)*ySm1)/2. -
        c*Pi*(xMm1 - (0,1)*yMm1)*(xSm1 + (0,1)*ySm1)/2. -
        c*K*Pi*(xMm1 - (0,1)*yMm1)*(xSm1 + (0,1)*ySm1)/2. +
        c*Pi*xM0*(xSm2 - (0,1)*ySm2)/2. + c*K*Pi*xM0*(xSm2 -
        (0,1)*ySm2)/2. + (0,0.5)*c*Pi*yM0*(xSm2 - (0,1)*ySm2) +
```

```
        (0,0.5)*c*K*Pi*yM0*(xSm2 - (0,1)*ySm2) -
        c*Pi*xM0*(xSm2 + (0,1)*ySm2)/2. - c*K*Pi*xM0*(xSm2 +
        (0,1)*ySm2)/2. + (0,0.5)*c*Pi*yM0*(xSm2 + (0,1)*ySm2) +
        (0,0.5)*c*K*Pi*yM0*(xSm2 + (0,1)*ySm2) +
        c*Pi*(xM1 + (0,1)*yM1)*(xSm3 - (0,1)*ySm3)/2. +
        c*K*Pi*(xM1 + (0,1)*yM1)*(xSm3 - (0,1)*ySm3)/2. -
        c*Pi*(xM1 - (0,1)*yM1)*(xSm3 + (0,1)*ySm3)/2. -
        c*K*Pi*(xM1 - (0,1)*yM1)*(xSm3 + (0,1)*ySm3)/2. -
        (0,0.5)*c*Pi*(xMm2 - (0,1)*yMm2)*yS0 -
        (0,0.5)*c*K*Pi*(xMm2 - (0,1)*yMm2)*yS0 -
        (0,0.5)*c*Pi*(xMm2 + (0,1)*yMm2)*yS0 -
        (0,0.5)*c*K*Pi*(xMm2 + (0,1)*yMm2)*yS0 +
        c*Pi*(xMm3 + (0,1)*yMm3)*(xS1 - (0,1)*yS1)/2. +
        c*K*Pi*(xMm3 + (0,1)*yMm3)*(xS1 - (0,1)*yS1)/2. -
        c*Pi*(xMm3 - (0,1)*yMm3)*(xS1 + (0,1)*yS1)/2. -
        c*K*Pi*(xMm3 - (0,1)*yMm3)*(xS1 + (0,1)*yS1)/2.
zR11=zNR12/zDR1
zR10=zNR11/zDR1 - zDR0*zNR12/zDR1**2
zR1m1=zNR10/zDR1 - zDR0*zNR11/zDR1**2 + zDR0**2*zNR12/zDR1**3 -
        zDRm1*zNR12/zDR1**2
zR1m2=zNR1m1/zDR1 - zDR0*zNR10/zDR1**2 + zDR0**2*zNR11/zDR1**3 -
        zDRm1*zNR11/zDR1**2 - zDR0**3*zNR12/zDR1**4 +
        2*zDRm1*zDR0*zNR12/zDR1**3 - zDRm2*zNR12/zDR1**2
zR21=zNR22/zDR1
zR20=zNR21/zDR1 - zDR0*zNR22/zDR1**2
zR2m1=zNR20/zDR1 - zDR0*zNR21/zDR1**2 + zDR0**2*zNR22/zDR1**3 -
        zDRm1*zNR22/zDR1**2
zR2m2=zNR2m1/zDR1 - zDR0*zNR20/zDR1**2 + zDR0**2*zNR21/zDR1**3 -
        zDRm1*zNR21/zDR1**2 - zDR0**3*zNR22/zDR1**4 +
        2*zDRm1*zDR0*zNR22/zDR1**3 - zDRm2*zNR22/zDR1**2
zZ1R5s2=(1 + K + (3 - K)*(xp1 + (0,1)*yp1)*(xq0 + (0,1)*yq0))*
        ((zR11 + zR21)*Cos(vvss*t) +(0,1)*(zR11 - zR21)*Sin(vvss*t))
zZ1R5s1=(1 + K + (3 - K)*(xp1 + (0,1)*yp1)*(xq0 + (0,1)*yq0))*
        ((zR10 + zR20)*Cos(vvss*t) + (0,1)*(zR10 - zR20)*Sin(vvss*t)) +
        (3 - K)*((xp1 + (0,1)*yp1)*(xqm1 + (0,1)*yqm1) +
        (xp0 + (0,1)*yp0)*(xq0 + (0,1)*yq0))*
        ((zR11 + zR21)*Cos(vvss*t) + (0,1)*(zR11 - zR21)*Sin(vvss*t))
zZ1R5s0=(1 + K + (3 - K)*(xp1 + (0,1)*yp1)*(xq0 + (0,1)*yq0))*
        ((zR1m1 + zR2m1)*Cos(vvss*t) +  (0,1)*(zR1m1 - zR2m1)*
        Sin(vvss*t)) + (3 - K)*((xp1 + (0,1)*yp1)*(xqm1 + (0,1)*yqm1) +
        (xp0 + (0,1)*yp0)*(xq0 + (0,1)*yq0))* ((zR10 + zR20)*Cos(vvss*t) +
        (0,1)*(zR10 - zR20)*Sin(vvss*t)) +
        (3 - K)*((xp0 + (0,1)*yp0)*(xqm1 + (0,1)*yqm1) +
        (xp1 + (0,1)*yp1)*(xqm2 + (0,1)*yqm2) +
        (xpm1 + (0,1)*ypm1)*(xq0 + (0,1)*yq0))*
        ((zR11 + zR21)*Cos(vvss*t) + (0,1)*(zR11 - zR21)*Sin(vvss*t))
zZ1R5sm1=(3 - K)*((xp1 + (0,1)*yp1)*(xqm1 + (0,1)*yqm1) +
        (xp0 + (0,1)*yp0)*(xq0 + (0,1)*yq0))*
        ((zR1m1 + zR2m1)*Cos(vvss*t) + (0,1)*(zR1m1 - zR2m1)*
        Sin(vvss*t))+(1 + K + (3 - K)*(xp1 + (0,1)*yp1)*(xq0 + (0,1)*yq0))*
        ((zR1m2 + zR2m2)*Cos(vvss*t) +  (0,1)*(zR1m2 - zR2m2)*
        Sin(vvss*t)) + (3 - K)*((xp0 + (0,1)*yp0)*(xqm1 + (0,1)*yqm1) +
        (xp1 + (0,1)*yp1)*(xqm2 + (0,1)*yqm2) +
        (xpm1 + (0,1)*ypm1)*(xq0 + (0,1)*yq0))*
        ((zR10 + zR20)*Cos(vvss*t) + (0,1)*(zR10 - zR20)* Sin(vvss*t)) +
```

```
        (3 - K)*((xpm1 + (0,1)*ypm1)*(xqm1 + (0,1)*yqm1) +
        (xp0 + (0,1)*yp0)*(xqm2 + (0,1)*yqm2) +
        (xp1 + (0,1)*yp1)*(xqm3 + (0,1)*yqm3) +
        (xpm2 + (0,1)*ypm2)*(xq0 + (0,1)*yq0))*
        ((zR11 + zR21)*Cos(vvss*t) + (0,1)*(zR11 - zR21)*Sin(vvss*t))
xZ1R5s2 =DBLE(zZ1R5s2)
xZ1R5s1 =DBLE(zZ1R5s1)
xZ1R5s0 =DBLE(zZ1R5s0)
xZ1R5sm1=DBLE(zZ1R5sm1)
yZ1R5s2 =DIMAG(zZ1R5s2)
yZ1R5s1 =DIMAG(zZ1R5s1)
yZ1R5s0 =DIMAG(zZ1R5s0)
yZ1R5sm1=DIMAG(zZ1R5sm1)
ca2 =2*xZ1R5s2*Cos(sBB*Sqrt((3*BB**2 - BB**2*K)/(1 + K))*xx/2.) +
        2*yZ1R5s2*Sin(sBB*Sqrt((3*BB**2 - BB**2*K)/(1 + K))*xx/2.)
ca1 =2*xZ1R5s1*Cos(sBB*Sqrt((3*BB**2 - BB**2*K)/(1 + K))*xx/2.) +
        2*yZ1R5s1*Sin(sBB*Sqrt((3*BB**2 - BB**2*K)/(1 + K))*xx/2.)
ca0 =2*xZ1R5s0*Cos(sBB*Sqrt((3*BB**2 - BB**2*K)/(1 + K))*xx/2.) +
        2*yZ1R5s0*Sin(sBB*Sqrt((3*BB**2 - BB**2*K)/(1 + K))*xx/2.)
cam1=2*xZ1R5sm1*Cos(sBB*Sqrt((3*BB**2 - BB**2*K)/(1 + K))*xx/2.) +
        2*yZ1R5sm1*Sin(sBB*Sqrt((3*BB**2 - BB**2*K)/(1 + K))*xx/2.)
```

APPENDIX-D

IMPLEMENTATION OF COMPATIBILITY EQUATION FOR THE THERMAL STRESS PROBLEM

$\varepsilon_{yy} = \frac{1}{E}\left[\sigma_{yy} - v\sigma_{xx} - v\sigma_{zz}\right] + \alpha\Delta T$

Substituting $\sigma_{xx} = 0$ and $\sigma_{yy} = \sigma_{zz}$ Hooke's law reduces to

$\varepsilon_{yy} = \frac{1-v}{E}\sigma_{yy} + \alpha\Delta T$.

Solving σ_{yy}, one obtains

$\sigma_{yy} = \frac{E}{1-v}\left[\varepsilon_{yy} - \alpha\Delta T\right]$.

Now substituting $\varepsilon_{yy}(x) = Ax + B$ into equation above, for an FGM plate one obtains

$\sigma_{yy}(x) = \frac{E(x)}{1-v(x)}\left[Ax + B - \alpha(x)(T(x) - T_0)\right]$.